Slot-Exchange Mechanisms and Weather-Based Rerouting within an Airspace Planning and Collaborative Decision-Making Model

Michael V. McCrea
Lieutenant Colonel, United States Army

Dissertation submitted to the Faculty of the
Virginia Polytechnic Institute and State University
in partial fulfillment of the requirements for the degree of

Doctor of Philosophy

in

Industrial and Systems Engineering

Hanif D. Sherali, Chairman
Ebru K. Bish
C. Patrick Koelling
Raymond W. Staats
Antonio A. Trani

April 14, 2006

Blacksburg, Virginia

Keywords: Mixed-Integer Programming, Air Traffic Control, Air Traffic Management, Collaborative Decision-Making, Ground Delay Program, National Airspace, Slot Exchanges, Airline Equity, Slot Offer Network, Trade Restrictions, Probability-Nets.

Slot-Exchange Mechanisms and Weather-Based Rerouting within an Airspace Planning and Collaborative Decision-Making Model

Michael V. McCrea

ABSTRACT

We develop and evaluate two significant modeling concepts within the context of a large-scale Airspace Planning and Collaborative Decision-Making Model (APCDM) and, thereby, enhance its current functionality in support of both strategic and tactical level flight assessments. The first major concept is a new severe weather-modeling paradigm that can be used to assess existing tactical en route flight plan strategies such as the Flight Management System (FMS) as well as to provide rerouting strategies. The second major concept concerns modeling the mediated bartering of slot exchanges involving airline trade offers for arrival/departure slots at an arrival airport that is affected by the Ground Delay Program (GDP), while simultaneously considering issues related to sector workloads, airspace conflicts, as well as overall equity concerns among the airlines. This research effort is part of an $11.5B, 10-year, Federal Aviation Administration (FAA)-sponsored program to increase the U.S. National Airspace (NAS) capacity by 30 percent by the year 2010.

Our innovative contributions of this research with respect to the severe weather rerouting include (a) the concept of "Probability-Nets" and the development of discretized representations of various weather phenomena that affect aviation operations; (b) the integration of readily accessible severe weather probabilities from existing weather forecast data provided by the National Weather Service (NWS); (c) the generation of flight plans that circumvent severe weather phenomena with specified probability levels, and (d) a probabilistic delay assessment methodology for evaluating planned flight routes that might encounter potentially disruptive weather along its trajectory. Given a fixed set of reporting stations from the CONUS Model Output Statistics (MOS), we begin by constructing weather-specific probability-nets that are dynamic with respect to time and space. Essential to the construction of the probability-nets are the point-by-point forecast probabilities associated with MOS reporting sites throughout the United States. Connections between the MOS reporting sites form the strands within the probability-nets, and are constructed based upon a user-defined adjacency threshold, which is defined as the maximum allowable great circle distance between any such pair of sites. When a

flight plan traverses through a probability-net, we extract probability data corresponding to the points where the flight plan and the probability-net strand(s) intersect. The ability to quickly extract this trajectory-related probability data is critical to our weather-based rerouting concepts and the derived expected delay and related cost computations in support of the decision-making process.

Next, we consider the superimposition of a flight-trajectory-grid network upon the probability-nets. Using the U.S. Navigational Aids (Navaids) as the network nodes, we develop an approach to generate flight plans that can circumvent severe weather phenomena with specified probability levels based on determining restricted, time-dependent shortest paths between the origin and destination airports. By generating alternative flight plans pertaining to specified threshold strand probabilities, we prescribe a methodology for computing appropriate expected weather delays and related disruption factors for inclusion within the APCDM model.

We conclude our severe weather-modeling research by conducting an economic benefit analysis using a *k*-means clustering mechanism in concert with our delay assessment methodology in order to evaluate delay costs and system disruptions associated with variations in probability-net refinement-based information. As a flight passes through the probability-net(s), we can generate a probability-footprint that acts as a record of the strand intersections and the associated probabilities from origin to destination. A flight plan's probability-footprint will differ for each level of data refinement, from whence we construct route-dependent scenarios and, subsequently, compute expected weather delay costs for each scenario for comparative purposes.

Our second major contribution is the development of a novel slot-exchange modeling concept within the APCDM model that incorporates various practical issues pertaining to the Ground Delay Program (GDP), a principal feature in the FAA's adoption of the Collaborative Decision-Making (CDM) paradigm. The key ideas introduced here include innovative model formulations and several new equity concepts that examine the impact of "at-least, at-most" trade offers on the entire mix of resulting flight plans from respective origins to destinations, while focusing on achieving defined measures of "fairness" with respect to the selected slot exchanges. The idea is to permit airlines to barter assigned slots at airports affected by the Ground Delay Program to their mutual advantage, with the FAA acting as a mediator, while being cognizant of the overall effect of the resulting mix of flight plans on air traffic control sector workloads, collision risk and safety, and equity considerations.

We start by developing two separate slot-exchange approaches. The first consists of an external approach in which we formulate a model for generating a set of package-deals, where each package-deal represents a potential slot-exchange solution. These package-deals are then embedded within the APCDM model. We further tighten the model representation using maximal clique cover-based cuts that relate to the joint compatibility among the individual package-deals. The second approach significantly improves the overall model efficiency by automatically generating package-deals as required within the APCDM model itself. The model output prescribes a set of equitable flight plans based on admissible trades and exchanges of assigned slots, which are in addition conformant with sector workload capabilities and conflict risk restrictions. The net reduction in passenger-minutes of delay for each airline is the primary metric used to assess and compare model solutions. Appropriate constraints are included in the model to ensure that the generated slot exchanges induce nonnegative values of this realized net reduction for each airline.

In keeping with the spirit of the FAA's CDM initiative, we next propose four alternative equity methods that are predicated on different specified performance ratios and related efficiency functions. These four methods respectively address equity with respect to slot-exchange-related measures such as total average delay, net delay savings, proportion of acceptable moves, and suitable value function realizations.

For our computational experiments, we constructed several scenarios using real data obtained from the FAA based on the Enhanced Traffic Management System (ETMS) flight information pertaining to the Miami and Jacksonville Air Route Traffic Control Centers (ARTCC). Through our experimentation, we provide insights into the effect of the different proposed modeling concepts and study the sensitivity with respect to certain key parameters. In particular, we compare the alternative proposed equity formulations by evaluating their corresponding slot-exchange solutions with respect to the net reduction in passenger-minutes of delay for each airline. Additionally, we evaluate and compare the computational-effort performance, under both time limits and optimality thresholds, for each equity method in order to assess the efficiency of the model. The four slot-exchange-based equity formulations, in conjunction with the internal slot-exchange mechanisms, demonstrate significant net savings in computational effort ranging from 25% to 86% over the original APCDM model equity formulation.

The model has been implemented using Microsoft Visual C++ and evaluated using a C++ interface with CPLEX 9.0. The overall results indicate that the proposed modeling concepts offer viable tools that can be used by the FAA in a timely fashion for both tactical purposes, as well as for exploring various strategic issues such as air traffic control policy evaluations; dynamic airspace resectorization strategies as a function of severe weather probabilities; and flight plan generation in response to various disruption scenarios.

Acknowledgements

I would like to express my sincere thanks to Dr. Hanif Sherali for granting me the honor to serve as a member of his research team. Rarely in life does a person come across an individual like Dr. Sherali who not only possesses the intellect and passion directed towards the advancement of theoretical and applied concepts within his profession, but is also genuinely committed to motivating others to follow in his footsteps. He has had a significant influence on my approach to problem solving and I truly appreciate the time he spent with me throughout my education process. While I will take away many memories from my three years at Virginia Tech, my most vivid memories will be of those related to my research experience under the guidance and mentorship of Dr. Sherali.

I would also like to acknowledge and thank my other committee members. Specifically, I wish to thank Dr. Raymond W. Staats for allowing me the opportunity to develop the proposed enhancements to his previous work and for his quick responses to my questions regarding model execution. I would also like to thank him for his friendship and wish him and his family the best of luck in their next assignment. I would like to thank Dr. C. Patrick Koelling for his heartfelt kindness and advice, especially during the pressure-packed moments of my research. I wish to thank Dr. Ebru Bish for the way she inspires others to succeed through her energetic approach to education. I would like to thank Dr. Antonio Trani for sharing his insights into the critical components of aviation operations and air-traffic-flow management.

I wish to thank Colonel Darrall Henderson, Ph.D. and Dr. Pat Driscoll at the United States Military Academy (West Point, New York) for insisting that the Grado Department of Industrial and Systems Engineering at Virginia Tech should be at the top of my list of graduate programs when I was researching schools back in June 2002. They were both instrumental later on when I sought advice regarding the composition of my committee.

Finally, I would like to thank my wife, Lisa, and my sons, Sean and Jake. Words cannot express the mental, emotional, and physical challenges I faced during the course of my research. Through it all, they stood by me with unwavering support and constantly motivated me to achieve a goal that at times appeared insurmountable. I look forward to our future together as a family knowing that I will have more time to be a husband and a father. Thank you.

Dedication

I dedicate this work to Lisa, Sean, and Jake.

Table of Contents

Chapter 1: Introduction……1

1.1. Motivation……..1

1.2. Scope of Research……..3

1.3. Summary of Contributions……4

1.4. Organization of the Dissertation……....6

Chapter 2: Literature Review……8

2.1. Weather Forecasting Tools and Methodologies……9

2.1.1. Evolution of Weather Forecasting……....9

2.1.2. Weather Advisories……..11

2.1.3. Weather Forecasts……...12

2.1.4. Weather Forecasting Errors……14

2.1.5. Regional Forecasting Models and Systems……15

2.1.6. Local Forecasting Models……18

2.2. Incorporating Weather Effects in Air Traffic Management……23

2.2.1. Europe's Air Traffic Flow Management Problem (TFMP)……23

2.2.2. Trajectory-based Air Traffic Management under Weather Uncertainty……26

2.2.3. Hub Closures and Schedule Recovery……28

2.3. Enhancements to the Ground Delay Program……29

2.4. Slot Trading Opportunities……...31

2.5. The Airspace Planning and Collaborative Decision-Making Model……35

Chapter 3: Modeling Weather-related Phenomena……..……..42

3.1. Selection of Weather Data Source……42

3.2. Availability of Probabilistic Data……..45

3.3. Modeling Approach……49

3.4. Model Application……52

3.5. Flight Plan Generation Tool……..56

3.6. Probability-Net Refinement……58

Chapter 4: Flight Generation, Probabilistic Delay Estimation, and Economic Impact Using the Proposed Weather-Based Models…….59

4.1. Extracting Exit Probabilities for Test Sets 1 and 2……..60

4.2. Superimposition of a Flight-trajectory-grid Network……...62

4.3. Incorporating Weather Delay Factors within APCDM……..……...……64

4.4. Evaluation of Economic Benefits Using *k*-means Cluster Analysis……..71

4.5. Expected Weather Delay and Disruption Factors Using a Decision-Theory Technique…75

Chapter 5: Modeling Slot Exchanges and Related Equity Concepts.……81

5.1. External Slot-Exchange Approach……81

5.1.1. Package-Deal Generation……81

5.1.2. Package-Deal Based Formulations ……85

5.2. Internal Slot-Exchange Approach……90

5.3. Equity Within Slot Exchanges……96

Chapter 6: Computational Results, Sensitivity Analyses, and Insights……107

6.1. Test Data Sets……...……..107

6.2. Computational Results Using Test Set #1……109

6.2.1. Results Using the Equity Concept in the Original APCDM Model…….110

6.2.2. Total Average Delay-based Equity Formulation Results: Method (a)……110

6.2.3. Net Delay Savings-based Equity Formulation Results: Method (b)……113

6.2.4. Downward-Move Ratio-based Equity Formulation Results: Method (c)……114

6.2.5. Upward-Move Value-based Equity Formulation Results: Method (d)…….114

6.2.6. Comparison of the Different Equity Concepts……117

6.2.7. Benchmark Runs……..119

6.2.8. Nonnegativity Restrictions on Net Passenger-minutes Delay Reductions…….120

6.3. Sensitivity Analysis of the Equity Weight Factors…….……121

6.3.1. Sensitivity Analysis with Respect to the Parameter μ_0 ……..121

6.3.2. Sensitivity Analysis under Increased Slot Competition (Test Set #2)……122

6.4. Computational Results Using Test Set #3……..126
6.5. Computational Effort Analysis……...…128

Chapter 7: Summary, Conclusions, and Recommendations for Future Research……..……..132
7.1. Summary and Conclusions……..132
7.2. Recommendations for Future Research……...134

References…….136

Vita…….....141

List of Figures

2-1 Flight Trajectory Transiting Through a Severe Weather System……..9
2-2 Convective SIGMETs from ADDS……..12
2-3 Example of an Area Forecast with Translation…….13
2-4 Example of a Terminal Area Forecast with Translation……...13
2-5 Variations in Terrain Resolution……16
2-6 SREF Precipitation Probability Plot……..17
2-7 Grid Square Covering a Portion of Denver……18
2-8 Diagram of a Neural Network……21
2-9 Compression Example……...…31
2-10 Directed Network of Potential Slot Offers……..32
2-11 Operational Framework for the APCDM……..36

3-1 Static Six-hour Forecast from GFS ……...……43
3-2 Convective SIGMETS from AWC……....44
3-3 NCWF Java Tool……...45
3-4 Short-range GFS and Eta MOS Stations……...47
3-5 Eta MOS Graphics: Six-hour Probability of a Thunderstorm……48
3-6 Example of an Eta MOS Text File……....48
3-7 Eta MOS Six-hour Thunderstorm Probability for February 7, 2005……50
3-8 MOS Reporting Station Thunderstorm Probabilities……50
3-9 Graphical Representation of a Probability-Net……51
3-10 Example of Single Probability-Net Evaluation……53
3-11 Example of Multiple Probability-Nets……...54
3-12 Exit Probability of Multiple Plans……55
3-13 Example of the Admissible Portion of a Probability Strand……57
3-14 Air Chart with Corresponding MOS Reporting Sites……57
3-15 Example of Reporting Site Clusters (k=15)……..58

4-1 Probability-Nets with 100-km and 150-km Adjacency Thresholds……60
4-2 Ellipsoidal Region……..……..63
4-3 Flight Trajectories Relative to Strand Thresholds……..……..63
4-4 Albany to Las Vegas Example…….……65
4-5 Illustration of Delay as a Function of σ……66
4-6 Delay Distribution…….……66
4-7 Two-step Distribution Function…….……67
4-8 Three-step Distribution Function…….…….68
4-9 Weather Delay Factor Flow-chart……..70
4-10 Potential Increase in Sector Count……..……..71
4-11 Variations in Probability-Net Refinement……72
4-12 Probability-Footprints……..……72
4-13 Economic Benefit Illustration…….…..73
4-14 Flight Plans as a Function of σ……..……75
4-15 Decision Tree for Routes A and B……..……..76
4-16 Decision Tree for Flight Plan Selection……78
4-17 Expected Delays for Strategic Level Planning……...……79
4-18 Disruption Factors for Strategic Level Planning……..……79

5-1 Slot Allocations from the imposed GDP……82
5-2 Airline Slot Offers……..83
5-3 Slot Offer Network…….…83
5-4 Package-Deal Graph, G_{PD}……..88
5-5 Flow-chart for Procedure MCC……88
5-6 Expanded Trade Offer Example……93
5-7 Slot Offer Network for Expanded Example…….……..94
5-8 Flight and Plan Specification Labels…..……95
5-9 Example Results……96
5-10 Collaboration Efficiency……98
5-11 Efficiency Based on Average Delay per Passenger……99
5-12 Efficiency Based on Net Delay Savings Per Passenger……101

5-13 Efficiency Based on the Proportion of Downward Trades……...……101
5-14 Various Value Functions……..……103
5-15 Efficiency Based on the Value per Offered Downward-Move……103
5-16 Alternative Value Function……104
5-17 Example of Airline Specific Value Functions……105

6-1 Miami IFR Rate……108
6-2 Total Net Reduction in Passenger-Minutes of Delay per $D^1_{\max}$ *adjustment* Factor..……111
6-3 Net Reduction of Delay by Airline……..……112
6-4 Net Reduction Percentage by Airline……...……112
6-5 Computational Time Versus $D^1_{\max}$ *adjustment* Factor…….……..……..113
6-6 Total Improvement for the Parameter λ……..115
6-7 Net Reduction of Delay by Airline.……116
6-8 Net Reduction Percentage by Airline…….……116
6-9 Computation Time Versus Parameter λ……...……117
6-10 Equity Comparison in Net Reduction by Airline……118
6-11 Equity Comparison in Net Reduction Percentage by Airline….……118
6-12 Comparison of Collaboration Efficiencies Across Respective Airlines…….119
6-13 Equity Comparison in Net Reduction for Benchmark Run 2……..……120
6-14 Nonnegativity Comparison…….……121
6-15 Sensitivity Analysis for Method (c) with Respect to μ_0……122
6-16 Identical Slot Competition Test Set……123
6-17 Identical Slot Competition Equity Comparison…….……123
6-18 Sensitivity Analysis for Method (a) Under Identical Slot Competition……..124
6-19 Method (b) Equity Comparison for Variations of p^*……..125
6-20 Airline Efficiency Comparison for Method (b)…….……..125
6-21 Variations in the Sum of Collaboration Efficiency and Equity Terms…….126
6-22 Equity Comparison in Net Reduction by Airline……...….127
6-23 Nonnegativity Comparison for Test Set #3……130

List of Tables

2-1 Categorical Outlook Terms from Area Forecasts……...……..12

3-1 Ceiling Height Categories ……..……52

4-1 Test Data Sets for Evaluating Convective Probability-Nets……..……61
4-2 Adjacency Threshold and SIPV Approach Results for Test Set 1…….……61
4-3 Computational Results for Test Set 2…..……...62
4-4 Expected Weather Delay and Disruption Factors……78

5-1 Directed Cycles Resulting from Different Runs of Model PDG…….85
5-2 Package-Deals Corresponding to the Cycles in Table 5-1……85
5-3 Maximal Clique Cover and Individual Maximal Cliques……89
5-4 Maximal Clique Cover and Individual Maximal Cliques Involving P_8…….89

6-1 Test Data Sets for Slot-Exchange Evaluations…….……108
6-2 Passenger Numbers for Test Set 1 at GDP Airport……..……109
6-3 SE-APCDM Results using APCDM Equity Approach……110
6-4 SE-APCDM Results using Net Delay Savings Equity Approach…….……..114
6-5 SE-APCDM Results using Downward-Move Ratio Equity Approach…….……114
6-6 Trade Offers and Passenger Counts……..126
6-7 Equity Method Performance under Time Limits…….128
6-8 Computational Effort for Alternative Test Sets Using Different Equity Formulations…129

Chapter 1
Introduction

1.1. Motivation

The Associated Press (AP) published an article describing the delays in air travel during the summer of 2004 as potentially the worst since the summer of 2000, in which nearly one of every four planes was late. As the number of passengers returned to their pre-September 11, 2001 levels, the largest contributing factor to flight delay was the presence of severe weather disrupting normal operations within the most congested airspace sectors. Severe weather can have a significant impact on the origin and destination airports as well as the planned flight routes. When an airport's arrival capacity is reduced due to severe weather and is incapable of slotting the scheduled number of arriving aircraft, the Federal Aviation Administration (FAA) implements a Ground Delay Program (GDP). Upon the execution of a GDP, specific flights are delayed at their respective departure airports in an effort to thin out the arrival rate at the destination airport. While the consequences of a GDP are undesirable for the airlines, the FAA Command Center prefers this technique to the riskier alternative involving in-flight delays. In instances where the severe weather intersects only the submitted flight route, the flight is rerouted as long as the proposed route is admissible. Otherwise, the flight is subject to a ground delay. The AP article was released only a few months after the present work commenced on an FAA sponsored research project regarding Collaborative Decision-Making and Air Traffic Flow Management under uncertainties due to weather, demand, and capacities. Providing methodologies to improve flight plan generation at both the strategic and tactical level under severe weather uncertainties and the subsequent reduction in associated delay costs is the primary motivation for this research effort.

The Federal Aviation Administration is sponsoring an overall 10-year, $11.5B, effort to increase the National Airspace (NAS) capacity by 30 percent by the year 2010 (Crawley, 2001). Given this expected increase in air and space transportation, it is of vital interest for the United States to remain involved with the development of techniques and methodologies to reduce the impending burden on the NAS. Richard P. Hallion (2004), a senior advisor to the U.S. Air Force for air and space issues, recently presented an argument referencing the lack of American academic contributions in the air and space fields. In addition, he emphasized that this issue is

not new when retracing American contributions throughout the history of the air and space industry. The present research effort pertains to addressing both of these issues.

According to Hallion (2004), America began its first major decline with respect to the growth of aviation shortly after the Wright Brothers' introduction of the airplane in 1903, as it fell behind other European countries in both aviation development and production and would not emerge from this position until 1938. Even during WWI, American pilots flew aircraft designed and built in France, Great Britain, and Italy. The resurgence of American ingenuity and predominance resulted from visits and migration of Europe's leading aviation technologists coupled with American designers' new willingness to adopt and exploit Europe's "structural and aerodynamic practices". The prominent European figures who contributed significantly to America's rebirth were Max Munk, Theodore von Karman, Anthony Fokker, and Igor Sikorsky.

America's development of commercial air transport was jump-started after certain key federal legislations (Kelly Act 1925 and Air Commerce Act 1926) were enacted. In the late 1930s, American commercial air transports were comparable to Europe's top transports and Europe began purchasing American Commercial Airliners. America's dominance in aircraft production during WWII is evident when comparing the number of platforms produced in America to those produced by the combined Axis Powers. America emerged from WWII producing the best bombers, fighters, and other aircraft types. The development and production capabilities of the United States at the time was a reflection on "American genius for building a system of systems approach….The knack for refinement, industrial organization, and output could be considered the great strength of American aviation" (Hallion, 2004, p. 7). Hallion expresses a concern that this is a pattern that America continues to repeat and gives examples referencing the radar, ballistic missiles, satellites, and other various improvements such as liquid fuel rockets. Because America has the raw materials necessary for development, it is relatively easy for us to catch up and eventually surpass other countries that are constrained by resources. This, however, is not the best way to do business. Hallion is even more concerned with the decline since the late 1980s in the industrial employment percentage and the number of American students studying air and space subjects at the universities. America has also lost its dominance in the airline industry and U.S. commercial space exports.

The greatest challenge, according to Hallion, is not motivated strictly towards economic or military dominance. Rather, the greatest challenge is to inspire the American youth to become

re-engaged with the air and space field. "We must excite our young people with new concepts that take us beyond the tired solutions of the past. We must be willing to shatter existing paradigms and patterns" (Hallion, 2004, p. 9). Many individuals from the past started with a concept and developed a product, which some said there was no need for, and now, they cannot live without. For America to be referred to as an Aerospace Nation, it must be involved in future advances and developments within the air and space field. Otherwise, it will be left behind again and will have to rely on playing catch-up.

The recent inaugural flight of the Airbus A380 in April 2005 is just another reminder of how Europe has taken the lead in aeronautical advances related to the expected increase in the NAS capacity. Boeing is scrambling to regain the lead over Airbus by introducing the Boeing 777-200LR with a planned extended range of 11,000 miles. While aircraft design is one approach taken to address the expected capacity increase, the efficient use of airspace in the presence of severe weather can significantly reduce costs that are typically associated with weather delays. Therefore, given existing weather forecasting tools and products, we choose not to play catch-up and recommend innovative methodologies within this dissertation for inclusion in the FAA's decision-making support system.

1.2. Scope of Research

In this dissertation, we propose and evaluate significant modeling concepts within the context of the Airspace Planning and Collaborative Decision-Making Model (APCDM) developed by Sherali et al. (2003 and 2006). The APCDM is a large-scale mixed-integer programming model designed to enhance the management of the National Airspace (NAS). Given a set of potential trajectories (referred to as surrogates) for each flight, the objective of the APCDM is to select an optimal set of flights subject to workload, safety, and equity considerations. This research is in support of the FAA's Collaborative Decision-Making (CDM) initiative.

The scope of research at the strategic level focuses on flight plan generation while incorporating probabilistic weather conditions that may have an impact along the existing flight network. The weather-modeling concept integrates severe weather information from a readily accessible forecast data source known as Model Output Statistics (MOS). The severe weather

probability data is used to compute an additional weather delay cost for a given flight for inclusion in the APCDM model's objective function.

At the tactical level, we include a slot-exchange mechanism within the APCDM model (designated SE-APCDM) and, thereby, focus on providing viable methodologies to incorporate various practical issues pertaining to the Ground Delay Program (GDP). Following the execution of the current Ration-by-Schedule (RBS) and Compression procedures of the GDP, airlines are allocated slots based on flight arrival times listed in the Official Airline Guide (OAG). As a byproduct related to the notion of airline "slot-ownership" (Vossen and Ball, 2004), an airline may relinquish an earlier slot in return for acquiring an improved slot for a later flight through a mediated bartering process. We explore both internal and external slot-exchange formulations and include various proposed equity formulations related specifically to slot exchanges. The resulting SE-APCDM solutions will instinctively decrease the overall passenger delay when compared to the passenger delay generated by the imposed GDP without slot exchanges.

The proposed modeling concepts are tested using the FAA's traffic demand scenario flight data, the Enhanced Traffic Management System (ETMS) database. The test sets consist of flight plans characterized by a set of four-dimensional coordinates (latitude, longitude, altitude, and time). An additional input for evaluating the SE-APCDM model is the trade offer data that is submitted by participating airlines. Different model variations are evaluated and various sensitivity analyses are performed to provide insights into model implementation issues.

1.3. Summary of Contributions

This dissertation makes the following specific contributions in support of the FAA's Collaborative Decision-Making initiative.

We integrate within the APCDM model a significant severe weather-modeling paradigm that can be used to assess existing tactical en route flight plan strategies such as the Flight Management System (FMS) as well as to provide rerouting strategies. A discretized representation of various weather phenomena that affect aviation operations is developed using the data provided by the National Centers for Environmental Prediction (NCEP). The discretized representations are structured in the form of *probability-nets* that are dynamic with respect to time and space. We incorporate point-by-point forecast data from the CONUS Model Output

Statistics (MOS) reporting stations to serve as the primary data sources for probabilistic weather. As a flight plan traverses through a probability-net, we extract probability data corresponding to the points where the flight plan and probability-net strand(s) intersect. The ability to quickly extract this trajectory-related probability data is essential to our severe weather rerouting concepts and delay cost calculations. We also consider the superimposition of a flight-trajectory-grid network upon the probability-nets and develop a time-dependent, shortest path approach for generating flight plans in order to circumvent severe weather phenomena with specified probability levels. By constructing alternative flight plans pertaining to specified threshold strand probabilities, we prescribe a methodology for computing expected weather delay values and, subsequently, appropriate weather delay or disruption factors for inclusion within the APCDM model. Additionally, we include an economic benefit analysis using a *k*-means clustering mechanism in concert with our delay assessment methodology in order to evaluate delay costs and system disruptions associated with different levels of probability-net refinement-based information.

Next, we develop a modeling construct that concerns the mediated bartering of slot exchanges involving airline trade offers for arrival/departure slots at an arrival airport that is affected by the Ground Delay Program (GDP), while simultaneously considering issues related to sector workloads, airspace conflicts, as well as overall equity concerns among the airlines. The proposed slot-exchange mechanism provides a unique perspective for addressing slot ownership in the prescription of surrogates for each flight in support of tactical level flight planning. The slot trading concepts introduced by Vossen and Ball (2004) focus only on the delay costs associated with potential slot trades. However, it is important to also examine such slot trades on the entire mix of the resulting flight paths from the respective origins to destinations. Therefore, we incorporate certain "at-least, at-most" type trade offers and augment the APCDM model to accommodate specific types of slot exchanges. We first develop an external Package-Deal Generation model in order to identify a number of acceptable trades that conform with stated trade restrictions, and propose a Package-Deal Based Selection model for including these sets of trades within the current framework of the APCDM model. Accordingly, the model then prescribes a set of flight plans corresponding to selected trade package-deals. We further tighten the model representation using maximal clique cover-based cuts that relate to the joint compatibility among the individual package-deals. We then develop a more efficient

approach that generates feasible package-deals as necessary within the framework of the APCDM model, in contrast to the first approach that utilizes a restricted, prescribed set of proposed acceptable trades. In addition to the APCDM model's current equity representation, we propose new concepts for equity, which focus primarily on achieving perceived "fairness" with respect to the selected slot exchanges. These alternative equity formulations are embedded within the APCDM model by specifying suitable performance ratios and related efficiency functions. The proposed alternative equity methods, as well as the original APCDM equity formulation, are evaluated using real data to provide insights into the nature of their corresponding slot-exchange solutions produced with respect to the resulting equity achieved while attaining a net reduction in passenger-minutes of delay for each airline. Furthermore, we evaluate and compare the computational-effort performance, under both time limits and optimality thresholds, for each equity method in order to glean insights regarding the efficiency of the model under realistic implementation scenarios.

A detailed experimentation of the proposed weather-modeling paradigm and slot-exchange mechanisms is conducted and evaluated using test sets constructed from real flight data obtained from the FAA, which pertains to the Miami-Jacksonville Air Route Traffic Control Centers (ARTCC), as derived from the FAA's Enhanced Traffic Management System (ETMS). The flight data information used relates. Computationally, our proposed modeling constructs provide effective decision-making support to the FAA that can be implemented in a timely fashion at both the strategic and tactical levels.

1.4. Organization of the Dissertation

The remainder of this dissertation is organized as follows. In Chapter 2, we review the relevant literature, beginning with weather forecasting tools and products related to flight operations. We provide an overview of the regional forecasting models and highlight the methodologies used to provide high-resolution local forecasts. We discuss several approaches that attempt to incorporate weather uncertainty in generating flight trajectories along with the optimization models that address hub closures and aircraft rerouting problems. Additionally, we review the fundamental components of the enhancements to the Ground Delay Program followed by a discussion on the slot-trading concepts proposed by Vossen and Ball (2004). Chapter 2 concludes with a brief overview on the composition and formulation of the Airspace Planning

and Collaborative Decision-Making model used to provide quantifiable results in support of this research.

Chapter 3 presents the severe weather-modeling paradigm. We begin by addressing the suitability of current weather data sources available to the aviation community. Next, we describe the probabilistic weather data available through the National Weather Service's Meteorological Development Lab (MDL) and extract the relevant information from the Model Output Statistics (MOS) to construct the probability-nets that we superimpose on a flight network. These probability-nets are then utilized to design various approaches that govern the generation and evaluation of flight plans. Finally, we develop an additional cost term associated with weather uncertainty for inclusion in the objective function and discuss measures to evaluate the accuracy of the probability-nets.

Chapter 4 provides the computational results related to the severe weather rerouting procedures and evaluates the accuracy of our weather-based approach using cluster analysis. We further develop and demonstrate our time-dependent flight-plan-generation tool using an ellipsoidal region technique proposed by Sherali, Hobeika, and Kangwalklai (2003).

The slot-exchange mechanism is developed in Chapter 5. We begin with an illustrative trade offer example from which we develop the framework of a slot offer network. An external slot-exchange approach is described in order to generate a set of feasible exchanges that serve as inputs to the APCDM model. We then propose an internal slot-exchange formulation within the constructs of the APCDM model itself. In addition to the equity terms and constraints developed by Sherali et al. (2006), we propose four additional equity concepts specific to the characteristics of trade offers.

Computational results are reported for the recommended internal slot-exchange approach in Chapter 6. We describe several ETMS scenarios that include slot trade offers from participating airlines. Each scenario is evaluated using the five aforementioned equity methods. In addition, we conduct sensitivity analyses on the equity related cost terms.

In Chapter 7, we discuss the effectiveness of the proposed modeling concepts within the context of the APCDM model and summarize their respective contributions to the FAA's CDM initiative. We conclude by recommending future research opportunities that will continue to improve NAS operations and strive to motivate future American graduate students to become re-engaged with the sciences related to air and space operations.

Chapter 2
Literature Review

One of the major expenses in the airline industry is the cost associated with flight delays. Most of the delays are weather induced and the cost of these delays amounts to billions of US dollars per year. In an attempt to minimize the cost associated with weather related delays, the Federal Aviation Administration currently adjusts flight routes in accordance with the guidelines specified in the National Playbook, which is a collection of Severe Weather Avoidance Plans (SWAPs) (FAA, 2005). As an alternative to the FAA's current approach, we address a complex idea that involves the incorporation of severe weather on flight plan generation in this dissertation. Our approach focuses on two separate modeling concepts within the context of the Airspace Planning and Collaborative Decision-Making Model (APCDM). The first is a strategic level concept designed to select flight plans relative to local severe weather probabilities. The second is a tactical level concept designed to generate slot exchanges at an airport that is affected by a Ground-Delay Program (GDP), following the submission of slot trade offers from the participating airlines. Both of these modeling constructs require evaluating several aircraft flight plans, each of which are proposed along with several alternatives, under existing and forecasted severe weather conditions.

Accordingly, in Section 2.1, we provide a review of weather forecasting tools and methodologies used to generate severe weather forecast products for the aviation community. This review includes a discussion on the levels of resolution required for forecast accuracy and the attempts made to improve the accuracy of local forecasts. We extract key probability data from existing weather forecasting products to develop our proposed application of weather uncertainty on flight path generation in Chapter 3. Section 2.2 reviews previous methodologies used to incorporate weather related uncertainties and affects in Air Traffic Management (ATM). In Section 2.3, the enhancements to the Ground-Delay Program are described and in Section 2.4, we review the concepts from Vossen and Ball regarding slot-trading opportunities utilizing a mediated bartering process. We conclude in Section 2.5 by providing a review of the original Airspace Planning and Collaborative Decision-Making Model developed by Sherali, Staats, and Trani (2003 and 2006) that serves as the mechanism used to generate slot exchanges and to quantify the impact of weather on flight paths.

2.1. Weather Forecasting Tools and Methodologies

Given the costly downstream effects that severe weather has on Air Traffic Management, a great deal of time and effort has been expended on the development and continuous improvement of various atmospheric circulation and numerical weather forecasting models. With a focus on tactical level weather decisions, Evans (2001) proposed a system in which routes are frequently revised in light of automatically generated weather predictions. He pointed out, in particular, that new routes must be tied to air traffic conflict decision support systems, a feature we adopt in our approach presented herein. Aviation weather forecasts used in conjunction with aviation weather advisories play a critical role in the optimization of aircraft trajectories and airspace operations. The ability to maximize the utilization of existing airspace is strongly dependent on the accuracy of hourly forecasts. An accurate forecast that provides credible details on the movement of convective weather can theoretically permit the prescription of an optimized trajectory that circumvents the severe weather system as shown in Figure 2-1, while ensuring that such a flight plan can be closely realized in practice. On the other hand, poor forecasting models could result in the elimination of a beneficial flight path from consideration based on an erroneous prediction that its trajectory would intersect the convective weather system.

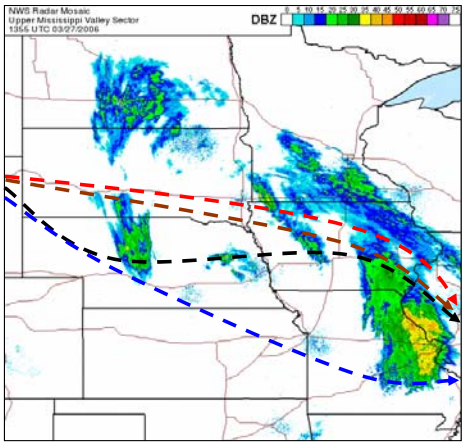

Figure 2- 1: Flight Trajectory Transiting Through a Severe Weather System.

2.1.1. Evolution of Weather Forecasting

The European Centre for Medium-Range Weather Forecasts (ECMWF) (ECMWF, 2002) traces the beginning of Numerical Weather Prediction (NWP) to 1904, when Norwegian hydrodynamist, V. Bjerknes, suggested the use of hydrodynamic and thermodynamic equations

to quantitatively predict atmospheric states; just one year after the Wright brothers sustained the first flight at Kitty Hawk. However, he lacked the means to successfully develop and implement such equations and thus, settled on a simplified qualitative approach known as the "Bergen School". Advances in numerical prediction methods remained relatively dormant until the introduction of the first electronic computer and the development of hemispheric network of upper air stations after World War II. The availability of atmospheric conditions at various altitudes above specified surface locations is critical to weather forecasting (Britannica, 2004). Additionally, the introduction of the radar (and satellite imagery in later years) for tracking storm movements allowed meteorologists to better understand the characteristics and behavior of certain weather phenomena. Jule Charney was the first to successfully derive a mathematical weather model in 1948. However, the limitations on computing power prevented any large-scale applications of his models. In 1950, a simplified version of Charney's models was used to successfully create a 24-hour forecast of atmospheric flow over North America.

Improvements in NWP models continued as countries strove to incorporate the effects from the vertical motion of weather and the influence from frontal boundaries (Baroclinic). In 1962, the United States introduced the first operational NWP model to account for vertical motion, followed by Great Britain in 1965. These improvements were, however, perceived as unrealistic and the search for more realistic weather models began with the development of the Primitive Equations (PEs) that govern fluid motion in thermodynamics. The Primitive Equations allowed for the interaction between winds and geopotential (height) fields that were constrained under the baroclinic models. The first global PE model, with a 300-kilometer grid and a six-layer vertical resolution, began operation in 1966 (ECMWF, 2002). Improvements in the field of PE models continued in the 1970s as countries developed models to handle a wide range of forecasting requirements from the global level down to high-resolution models for local forecasts.

The next significant advancement in NWP models came with the introduction and application of mesoscale models in the 1980s. Previous forecasting models lacked the ability to forecast weather phenomena at the level between a cyclone storm and individual clouds. The development of the mesoscale model addressed this shortfall and is capable of predicting critical atmospheric conditions such as thunderstorms, hurricane bands, and the location of jet streams (Britannica, 2004). Eta and the Rapid Update Cycle (RUC) models are two mesoscale models in use today. The most recent development in numerical weather forecasting is the Ensemble

Prediction System (EPS), and is currently used by many forecasting agencies to include the National Centers for Environmental Prediction (NCEP) in the United States and the ECMWF in Europe. A description of the EPS is presented later in this chapter following an overview of regional weather advisories and forecasting approaches that are in current use today.

2.1.2. Weather Advisories

In addition to numerical weather forecasts, numerous reports and advisories are generated in order to provide pilots and air traffic managers with a clear weather picture prior to aircraft departure as well as updates while the aircraft is en route. These advisories and reports are provided by both voice, through aircraft telecommunication systems, and via internet on the Aviation Digital Data Service (ADDS) web site. The ADDS is funded and directed by the FAA under the Aviation Weather Research Program (AWRP). The five weather advisories used by pilots as supplements to the weather forecasts are the: Airman's Meteorological Information (AIRMETs); Significant Meteorological Information (SIGMETs); Convective SIGMETs; Center Weather Advisories (CWAs); and Severe Weather Forecast Alerts, more commonly referred to as Alert Weather Watches (AWW).

These advisories are used to provide information on hazardous weather situations and are typically widespread, requiring coverage of at least 3,000 square miles before inclusion as an advisory. Therefore, even though an advisory may not exist for a particular airspace sector, one cannot exclude the potential for localized severe weather within the airspace (FAA, 2004). A reporting format, PIREP, also exists where the pilot can report observed hazardous weather conditions. Figure 2-2 is an example of Convective SIGMETs from the ADDS. The Convective SIGMETs are shown in red and the yellow region represents potential thunderstorm activity. The information is provided in both a graphical format as well as raw report data. The Convective SIGMETs and Alert Weather Watches are used to inform pilots of existing thunderstorms or thunderstorm related phenomena. Dependent upon the characteristic of a particular flight, the information from the SIGMETs can be used as initial conditions when determining the probabilistic path of a storm in relation to the planned flight route. In Chapter 3, we address the apparent shortfalls associated with the Convective SIGMETS in relation to flight plan generation and, in turn, introduce forecast data sources that provide a greater degree of resolution.

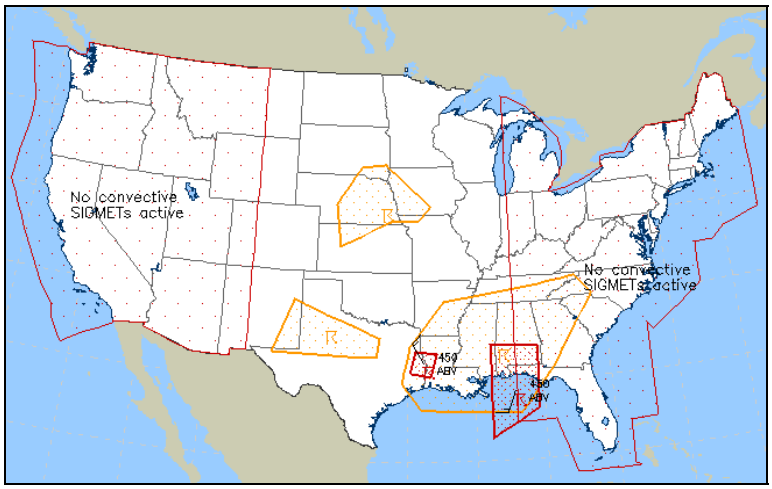

Figure 2-2: Convective SIGMETs from ADDS (AWC, 2005).

2.1.3. Weather Forecasts

Currently, two categories of weather forecasts are used by the Aviation Weather Center (AWC). They are the Area Forecast and the Aerodrome (or Terminal) Forecast (TAF). The Area Forecast is a twelve-hour forecast plus a six-hour estimate of Visual Flight Rules (VFR) for clouds and weather over a large area that may cover one or more airspace sectors. Table 2-1 lists the various Area Forecast categorical terms in reference to ceiling and visibility (FAA, 2004). The Area Forecasts are insufficient by themselves and must be supplemented with the information found in the AIRMETs. More specifically, the Area Forecasts must be supplemented by the AIRMETs SIERRA, TANGO, and ZULU, which contain advisories for IFR and mountain obscuration, turbulence, and icing and freezing, respectively (FAA, 2004 and AWC, 2003). Area Forecasts are issued three times a day from the National Weather Center in Kansas City, Missouri, for the six regions that cover the 48 states located on the mainland of the United States. Forecast amendments and/or corrections are submitted when necessary. Figure 2-3 illustrates a segment of an Area Forecast in both raw data form and its translated version for an area within Virginia.

Categorical Outlook	Ceiling	and/or Visibility
Low Instrument Flight Rules (LIFR)	< 500 feet	< 1 statute mile
Instrument Flight Rules (IFR)	< 1000 feet	between 1 and 3 statute miles
Marginal Visual Flight Rules (MVFR)	< 3000 feet	between 3 and 5 statute miles
Visual Flight Rules (VFR)	>3000 feet	> 5 statute miles

Table 2-1: Categorical Outlook Terms from Area Forecasts.

Example of an Area Forecast:

VA MD DC DE
SWRN VA...BKN040-050. TOPS 120-140. WDLY SCT TSRA DVLPG.
...CB TOPS FL370. TSRA ENDG OR BECMG ISOL 00Z-03Z...BECMG
SCT050 SCT-BKN120-140. TOPS 160. OTLK...MVFR BR.

Translation: Area Forecast for Virginia, Maryland, District of Columbia, and Delaware Southwest Region of Virginia…Ceiling 4000 to 5000 feet broken AGL, tops 12000 to 14000 feet AGL. Widely scattered Thunderstorms and Rain Developing.
… Cumulonimbus Cloud tops Flight Level of 37000 feet. Thunderstorms ending or becoming isolated between Midnight and 0300 Coordinated Universal Time (UTC)… Becoming scattered at 5000 feet AGL and scattered and broken at 12000 to 14000 feet AGL, tops 16000 feet AGL. Outlook… Marginal VFR due to Mist.

Figure 2-3: Example of an Area Forecast with Translation.

Aerodrome or Terminal Area Forecasts (TAF) are forecasts for specific airports and cover a region spanning five statute miles from the center of the runway complex. The TAF is valid for a 24-hour period and is amended or corrected when required. The information contained with the TAF relates specifically to weather, visibility, surface winds, and cloud coverage for the specified terminal (FAA, 2004). For terminals that do not have existing TAFs, Area Forecasts and AIRMETs are used to interpolate the conditions at the terminal. Figure 2-4 provides an example of a TAF for Boston in both forecast format and the translated version. The accuracy of the TAFs is extremely important given that poor conditions at a terminal dictate FAA's implementation of a GDP rather than flight re-routes. Improving the accuracy of TAFs can lead to substantial cost savings according to a study conducted by the National Weather Service in 2000 (Riordan and Hansen, 2002). TAFs are revisited in this chapter during the discussion on local forecasting models.

Example of an Aerodrome Forecast:

TAF
KBOS 0411452 1212 34015G25KT 5SM SHSN- SCTO10
BKN018 TEMPO 1215 1/2SM SHSN VV008 BECMG 15-17
33012G22KT P6SM BKNO5O

Translation: Boston Aerodrome Forecast for the 4th day of the month, valid time 122-122. Surface wind from 340" at 15 knots with peak gusts to 25 knots; visibility 5 statute miles; light snow showers; scattered clouds at 1,000 feet AGL; ceiling 1,800 feet broken AGL; occasionally, visibility one-half mile in moderate snow showers; indefinite ceiling 800 feet (an indefinite ceiling represents a surface- based phenomena obscuring the whole sky). Becoming between 15Z and 172 surface wind from 330" at 12 knots with gusts to 22 knots; visibility greater than 6 miles; ceiling 5,000 feet broken AGL.

Figure 2-4: Example of a Terminal Area Forecast with Translation.

2.1.4. Weather Forecasting Errors

When it comes to forecasting models, unless the system is in a constant state, the model will always have an associated degree of uncertainty within the results. This uncertainty becomes even more prevalent when creating numerical models for forecasting weather phenomena and can potentially lead to significant forecasting errors. Peter Manousos, at the National Oceanic and Atmospheric Administration (NOAA), provides four primary reasons why deterministic weather forecasting models are plagued with errors (NCEP, 2004). Manousos refers to weather forecasting models that take initial conditions, run a simulation, and provide a single output as deterministic. The first reason identified relates to the number of processes captured within the model's equations. A majority of the models focus on wind, temperature, and moisture as the primary processes. Other atmospheric conditions exist that contribute to weather phenomena as it transitions from one state to the next. However, Manousos argues that inclusion of these additional conditions would only complicate the already highly nonlinear equations and drive the required computational effort beyond that suitable for operational use. Therefore, most models address these additional conditions through parametric means, which introduces errors into the model results.

The second reason is based on the model's inability to resolve atmospheric processes within a given threshold. Take for example the 10-kilometer Eta forecasting model. In this model, the region of interest is divided into grid squares 10 kilometers in width. While this is considered as high resolution in the forecasting world, any influential conditions that exist within a region smaller than 10 kilometers wide are omitted from the model and propagate through the model as a forecasting error. The third and fourth reasons respectively focus on the availability and the accuracy of the initial conditions. Without a meteorological observation available at every point within the region of interest, initial conditions for some points must be interpolated. Additionally, the initial conditions from one or more locations that are obtained using an observation device are occasionally rejected. As far as the accuracy of the initial conditions is concerned, Manousos argues that the current technology does not permit measurements at the level of precision required to make the forecast perfect. While there exist other reasons for supporting deterministic weather forecasting models, the aforementioned reasons motivate the choice of the current models selected by the National Centers for Environmental Prediction

(NCEP), which provides numerical weather information for the National Weather Service and the Aviation Weather Center.

2.1.5. Regional Forecasting Models and Systems

The National Centers for Environmental Prediction uses mesoscale models for providing regional forecasts. The five regional atmospheric models used by NCEP (EMC, 2004) are the Eta coordinate models, Global Forecast System (GFS), Watch Wave III, Rapid Update Cycle (RUC) model, and the Nested Grid Model (NGM). One significant point of differentiation between each of these models is their respective levels of resolution. Variations of resolution also occur within each model separately. For example, the Eta model, named after the ETA coordinate system, has versions with horizontal resolutions of 29, 32, and 48 kilometers. The level of resolution refers to the subdivision of the region into grid squares of a specified length and width (in kilometers). The smaller the grid square, the higher the resolution of the forecasting model. Figure 2-5, modified from UCAR (1998), represents the difference in resolution between two Eta models. The scale to the right of each terrain box represents elevation classifications. An immediately apparent concern associated with increasing the level of resolution (number of grid squares used to define the terrain) is the increased computational complexity of the mathematical model. In addition to variations in horizontal resolution, these models also differ in vertical resolution and are differentiated by the number of layers. Model developers use the horizontal and vertical resolutions together to classify a specific model. For example, the Meso-Eta model is a 50-layer model with a 29-kilometer resolution.

The NWP models are used to provide both short-range and medium-range forecasts. The short-range forecasts cover a period up to 48 hours (72 hours in some models), while the medium-range forecasts extend from 48 hours out to 240 hours using the Medium-Range Forecasting (MRF) model. Given that our concern is air traffic management, the medium-range forecasts beyond 72 hours have no added value and will not be discussed further. The remainder of the review on regional forecasting methods will focus on how the NCEP and ECMWF apply their prediction models.

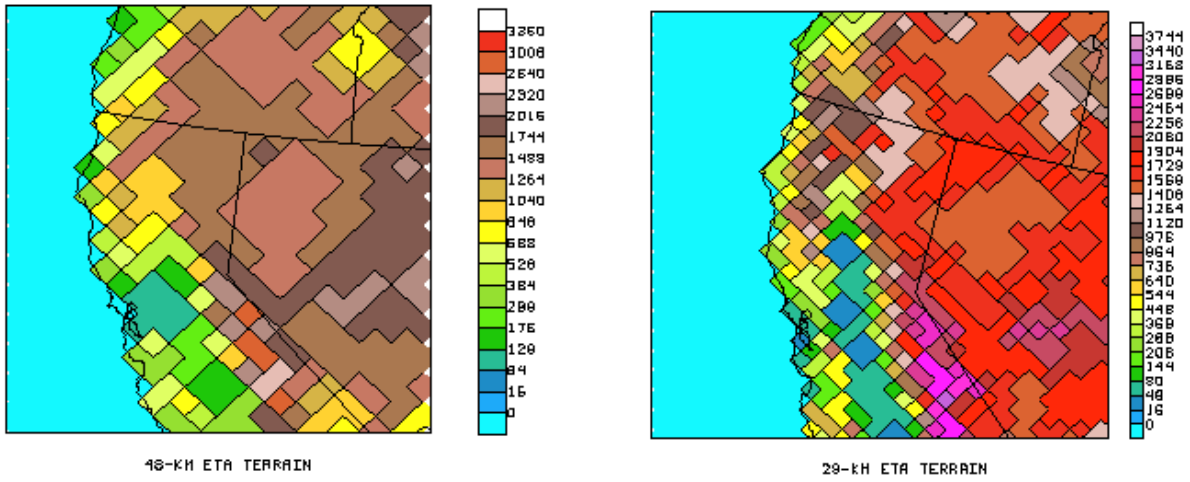

Figure 2-5: Variations in Terrain Resolution.

As stated earlier, there is a degree of uncertainty associated with each forecast, given the chaotic nature of weather. Therefore, using the mesoscale NWP models, how is this uncertainty accounted for? This is accomplished by the introduction and implementation of the Ensemble Prediction System (EPS). A single run of an Eta model has no uncertainty associated with the output. Using initial atmospheric conditions, the model accounts for the effects of terrain and variations between the vertical levels and produces a forecast for a given period. The Short-Range Ensemble Forecasting (SREF) system currently in use by NCEP is one example of a successful implementation of the EPS. The ECMWF uses the ensemble system for medium-range forecasting.

SREF was designed to provide probabilistic multi-regional forecasts out to 72 hours (McQueen et al, 2004). Manousos (NCEP, 2004) provides an online training manual for Ensemble Prediction Systems (EPS). An ensemble is a collection of two or more forecasts for a specific region and period of time. The premise behind EPS is to generate a probabilistic forecast from a collection of member forecasts, where a member is defined as a single forecast. The current SREF used by NCEP contains 15 members. The ECMWF EPS contains 50 members as of February 2002. A member can be either a forecast from the same mesoscale model, using a perturbation concept, or a forecast from a different mesoscale model. The role perturbations play in ensemble forecasting is that of attempting to capture atmospheric uncertainties within the model input for each member. The initial conditions are perturbed from

a control member to generate another member and are controlled to ensure that the initial conditions for a member remain within reason. An example of a perturbation is to increase the surface temperature at a given location by 0.1^{o} C (NCEP, 2004). Once the members are generated, variations within the forecast from the different members allow for the generation of a probability distribution function.

The three primary outputs from the SREF are: the Mean and Spread plots, the Spaghetti plots, and the Precipitation Probability plots. As of June 2004, NCEP provides SREF plots online at: http://wwwt.emc.ncep.noaa.gov/mmb/SREF/SREF.html. Figure 2-6 depicts an example of a Precipitation Probability plot from a 15 member SREF for 12 hours, starting from the commencement of the plot generation. The online site allows looping of SREF plots from 12 to 63 hours. Similar online sources exist for the retrieval of RUC, RSM, and NGM forecasts. In addition to plots, the raw data for the SREF is available. While satisfied with their current prediction capabilities, NCEP strives to improve SREF results in research projects by varying the number and classification of members.

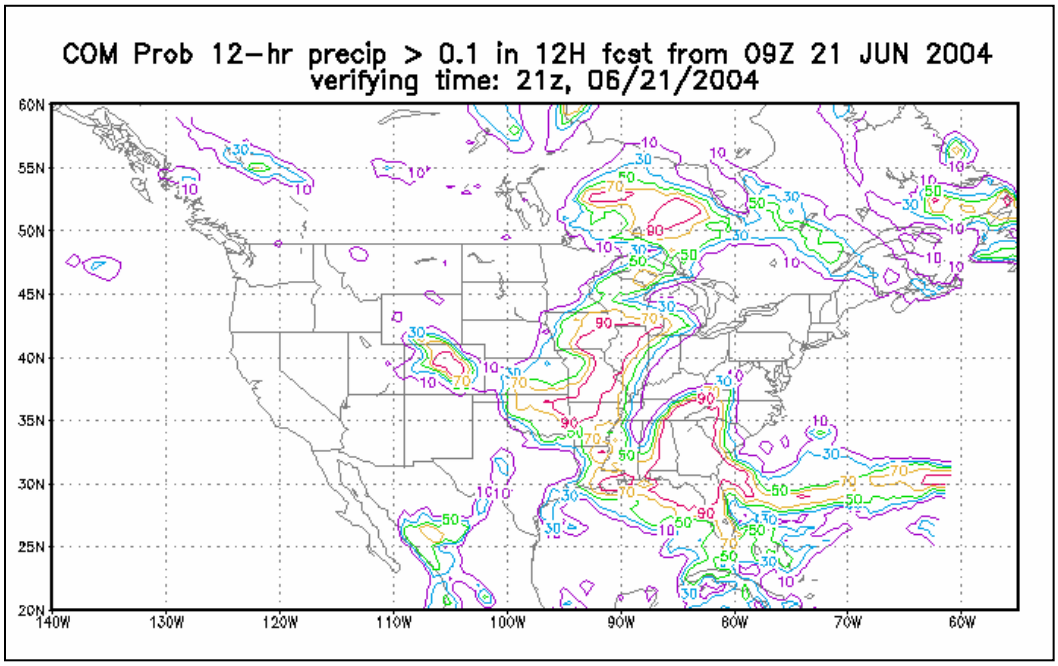

Figure 2-6: SREF Precipitation Probability Plot (SREF, 2004).

Our review so far has focused on the regional forecasting models. Given that the desire for accurate weather forecasting has grown significantly over the past two decades, organizations such as the NCEP will continue to strive for improvements to existing forecasting

models and techniques. The extent of forecast information, prediction sources, and products available today is so abundant that one can become overwhelmed. Even so, unfortunately, the available data appears to be at a resolution that remains below what is desired for local forecasts. Is there a local model out there that can forecast the path of a storm as it moves from City A to City B located 20 kilometers apart? And if so, is the model accurate enough to predict the storm's departure prior to the aircraft's arrival in the specific area? Given the desired level of accuracy as prompted by these questions, we shift our focus to the branch of local forecasting models.

2.1.6. Local Forecasting Models

The NWP models focus their primary attention on global and regional forecasts that typically lack the resolution to accurately provide local forecasts. Figure 2-7 demonstrates one example of incomplete resolution for the Denver area. The NWP models divide the region of interest into grid squares of predetermined length and width. A condition may exist, as shown in Figure 2-7, in which dramatic changes in terrain can occur within a given grid square. The NWP models uniformly classify the terrain within the box and do not account for extreme changes within the box that can significantly influence local weather. Therefore, additional forecasting methods are necessary to address conditions within the grid square.

Figure 2-7: Grid Square Covering a Portion of Denver.

During the literature search on local weather forecasting models, numerous modeling techniques surfaced that either had potential but were later discarded, or are still in existence today. This overview will focus on: the Bayesian or Bayesian Network models, Neural Network

models, and Fuzzy Logic in Case-Based Reasoning (CBR) models. While other modeling techniques not listed here may exist, the intent of this overview is to address alternative methods to local forecasting that may be relevant to our future work on the impact of weather uncertainties with respect to Air Traffic Management.

Abramson et al. (1996) developed a Bayesian system, known as Hailfinder, to forecast severe weather in Northern Colorado. The development of the model was in response to a series of competitions established by the NOAA in 1989 and 1991, known as Shootouts. Hailfinder is considered to be the first such system that uses Bayesian techniques in the area of meteorology in which meteorological data is combined with a Bayesian model structure along with subjective inputs from experts. Pole et al. (1994) suggested that Bayesian forecasting methods work extremely well in dealing with "non-routine" events. Given that weather phenomena is anything but routine, it is the additional subjective inputs from the modeler that may reduce the model error. For example, experts on Northern Colorado weather trends devised ten scenarios within Hailfinder that accounted for over eighty percent of the potential weather conditions during the months of interest. An eleventh scenario accounted for all others. The premise behind the Hailfinder model is the development of the initial state probabilities (priors) with respect to each scenario. Then, using one-step-ahead forecasting techniques, the most recent observation is used to update the prior probabilities for the next step. These are known as the posterior probabilities, which are proportional to the priors and are calculated using a likelihood function (Pole et al. 1994). A Belief-Network (BN) was the selected framework for Hailfinder in which the states of each of the variables were represented by the nodes in a directed graph. An arc between a pair of nodes was constructed in this network if there was a direct influence from one corresponding variable to the other.

The complete Hailfinder network consisted of 56 nodes and 68 arcs. The development of Hailfinder demonstrated a necessity for the infusion of models and trained meteorologists in the construction of such models. Unfortunately, the last Shootout occurred prior to the completion of Abramson et al.'s Bayesian Forecasting Model. Therefore, Hailfinder did not have an opportunity to be compared against other existing forecasting methods at that time, using a baseline meteorological data set from the Shootout sponsors. Even when Abramson et al. finally published their article on their Bayesian model, the amount of meteorological data for Northern Colorado required to test the effectiveness of Hailfinder remained insufficient. Therefore, the

article only addresses the structure of Hailfinder. The ensuing literature is devoid of any further testing of the Hailfinder model. This, however, did not mark the end of Bayesian attempts at weather forecasting.

At the European Conference on Artificial Intelligence (ECAI-2002) in 2002, Cofino et al. presented a paper on weather predictions using Bayesian Networks. Their intent was to provide a forecasting model for local areas that are not covered by the numerical Atmospheric Circulation Models (ACMs) as described earlier in the section on regional models. Their current ACMs provide a resolution of between 50 and 100 kilometers, which becomes a significant limitation when attempting to provide a local forecast inside of 50 kilometers. The particular point of interest in this work was to provide rainfall forecasts for the northern section of the Iberian Peninsula. Cofino et al. developed a Bayesian Network based on dependencies between various weather reporting stations. The dependency between weather stations was captured through a directed acyclic graph where a directed arc between stations *A* and *B* is used to represent a causal effect on Station *A* from Station *B*.

The difficulty with the Bayesian Network structure is the calculation of the conditional probability of each node, given that of its parent nodes. This occurs due to either the lack of information of the local topography or lack of supporting historical data. Cofino et al. referenced two techniques for establishing the conditional probabilities through either quality measures or search algorithms. Once the conditional probabilities of the Bayesian Network are developed, the remaining steps of this forecasting method follow standard Bayesian techniques. A Brier Skill Score (BSS) method was used to validate their numerical forecasting technique using the winter months in 1999. The actual model described above was developed using only historical data. Cofino et al. also introduced a technique to combine the historical data with forecasts provided by the ACMs. A major benefit of this hybrid technique is the linkage between the operational model and the daily weather forecast products (Cofino et al., 2002). This forecasting technique remains relevant today as the authors continue to make model improvements.

The method of Neural Networks has also surfaced as a useful modeling technique for local weather forecasting. “The utility of Neural Networks is most present in disciplines where intrinsic nonlinearities in the dynamics preclude the development of exactly-solvable models (Marzban and Stumpf, 1996),” as is the case with weather. Neural Networks are an artificial intelligence tool used for pattern recognition (McCann, 1992). The primary use of Neural

Networks for weather forecasting within the literature appears to focus on rainfall level predictions (Hall et al., 1997) with relatively fewer models focusing on tornados (Marzban and Stumpf, 1996) and severe weather. The Severe Weather Forecast Center (SWFC) uses Neural Network models to forecast the frequency and intensity of storms and provides current severe weather watches (SWFC, 2000). In 1992, McCann from the National Severe Storms Forecast Center developed a Neural Network tool to forecast thunderstorm activity with a prediction period between three and seven hours.

The premise behind the use of Neural Networks is one in which the forecasting model learns and establishes weather patterns through the use of historical data and training sets. Once these patterns are defined, the model takes initial weather conditions as the input layer, and transforms the initial conditions into model outputs by means of a "hidden layer" (Figure 2-8, derived from Hsieh and Tang (1998)). While Neural Networks have been successfully applied to a wide variety of other forecasting problems (stock market and other financial entities), initial attempts to apply this technique to large-scale weather prediction revealed little promise of success. Hsieh and Tang (1998) addressed the difficulties inherent to Neural Networks with respect to weather forecasting and provide solutions based on recent computational advances. Of primary concern was the difficulty associated with the inherent nonlinearity of the forecasting problem. Advances in ensemble forecasting approaches have allowed the modelers to address this nonlinearity. Neural Networks continue to play an important role in local weather forecasting today.

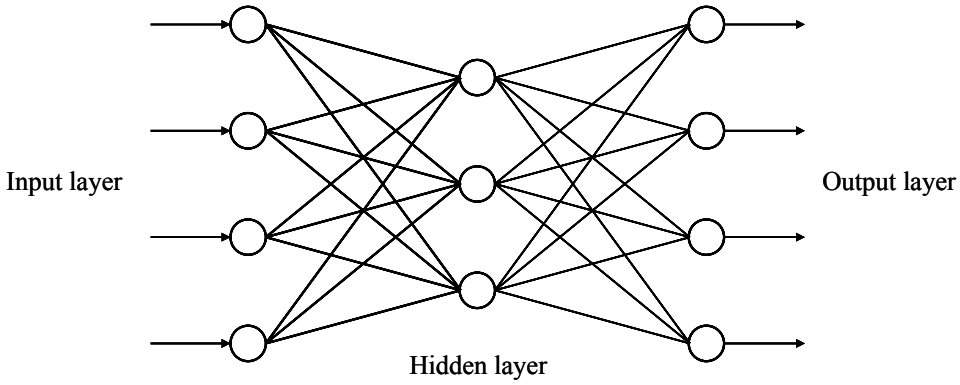

Figure 2-8: Diagram of a Neural Network.

The application of Fuzzy Logic within a Case-Based Reasoning (CBR) methodology to weather forecasting is another artificial intelligence approach to addressing weather uncertainties.

Riordan and Hansen (2002) argue that the small-scale utilization of Numerical Weather Prediction models for local weather may be difficult to apply in real-time given the characteristic lack of complete data sets for a specified region. They have successfully developed two Fuzzy Logic weather prediction models, with one focusing on ceiling and visibility and the other on marine forecasts.

The premise behind Fuzzy Logic is that the inputs into the system are oftentimes defined in imprecise terms. It is the grouping of these inputs into common sets that provide structure and manageability of available data (Sowell, 1998). Manner and Joyce (1997) provided three reasons why Fuzzy Logic is suitable for weather forecasting. The first and primary reason is that the terminology and characterization of weather forecasting (partly cloudy, occasional rain, etc.) fits well into the definition of fuzzy sets. Second, existing work such as that of Riordan and Hansen (2002) supports the use of fuzzy logic in weather prediction models. Third, the domain of weather meets the general conditions for fuzzy solutions.

Riordan and Hansen's project, WIND (Weather Is Not Discrete), focused on predicting horizontal visibility and cloud ceilings over airport terminals as a replacement for the current TAFs. They targeted the TAFs for improvement given that in 2001, the National Weather Service estimated a savings between $500 million and $875 million from reduced weather related delays associated with accurate visibility and ceiling forecasts with less than 30 minutes lead-time. As presented earlier, TAFs cover a 24-hour period and are updated as necessary. Given that routine aviation weather observations (METARs) are generated every hour for all major airports, sufficient historical data existed for the development of the WIND project. Riordan and Hansen used 315,576 hourly observations from 1961 to 1996 for the Halifax International Airport. Results from project WIND indicated a significant improvement in terminal forecasts over existing forecasting methods used to produce the TAFs. "The main contribution of Fuzzy Logic to CBR is that it enables us to use common words to directly acquire domain knowledge" (Riordan and Hansen, 2002, p. 139). The Harris Corporation has also achieved success using Fuzzy Logic weather systems to provide information on short-term ceilings and visibility to the FAA using a verification period of two years (Hicks et al., 2004).

Success of these three methodologies: Bayesian, Neural Networks, and Fuzzy Logic, for local forecasting rests on the existence of complete and accurate historical data in order for the individual learning mechanisms to be effective. Incomplete or incorrect data sets can lead to

faulty pattern recognition, resulting in poor forecasts from the overall model. In addition to complete historical data sets, the inclusion of information from local weather experts can only serve to enhance the accuracy of the local weather forecast. As the desired level of resolution required for local forecasts increases, so will the requirement for increased computational power. Timeliness of the model output will continue to dictate the model's feasibility for future application.

It is interesting to note that just one year after the Wright Brothers succeeded at Kitty Hawk, the ideas for numerical weather forecasting were conceived. Today, these two modern concepts remain inextricably linked. Norwegian hydrodynamist, V. Bjerknes, suggested the idea of using mathematical models to predict the weather one-hundred years ago. Even though he was unable to develop functional models, his revolutionary ideas serve as the foundation of today's successful weather forecasting models. Advances in mesoscale models, along with the application of an Ensemble Prediction System, allow NCEP and ECMWF to provide accurate regional and global forecasts for both short-range and medium-range periods. Where the mesoscale model fails is forecasting at the local level due to limitations inherent within the model's resolution based on its grid-square terrain classification. Given this shortfall, attempts have been made to provide accurate local forecasts using Bayesian, Neural Network, and Fuzzy Logic techniques.

2.2. Incorporating Weather Effects in Air Traffic Management

2.2.1. Europe's Air Traffic Flow Management Problem (TFMP)

Alonso et al. (2000) presented a stochastic approach for Europe's Air Traffic Flow Management Problem (TFMP) under uncertainty due to weather conditions. By 2000, it was predicted that 16 of Europe's airports and 100 airspace sectors would exceed capacity. Given the nature of the problem, the capacities on the ground and in the air are not constant and must be addressed probabilistically. Therefore, the three aspects of uncertainty that the authors addressed were related to the capacities of the arrival and departure airports and the relevant segment of the airspace. The majority of the air traffic management models up to this point focused on the short-term solution that included ground-holding policies. This modeling objective was clearly driven by the fact that ground-holding costs were significantly lesser than air-holding costs. Two

models found in the literature that address ground-holding costs are the Single-Airport Ground Holding Problem (SAGHP) and the Multi-Airport Ground-Holding problem (MAGHP).

The Air Traffic Flow Management Problem (TFMP), introduced by Bertsimas and Stock (1994), not only considers the MAGHP but also addresses the airspace capacity issue. The work of Bertsimas and Stock (1994), Matos et al. (1996), and Alonso (1997), along with others in the literature, adopt a deterministic modeling approach. This simplifying assumption reduces the computational effort required to find a solution, but fails to address the variability associated with air traffic.

Alonso et al. (2000) proposed a stochastic approach to the Air Traffic Management problem using two different policies. The first policy was one of simple recourse to "anticipate any decisions at the beginning of the time horizon." The second policy was one of full recourse to "anticipate decisions for only the first stage by taking into account all scenarios but without subordinating to any of them." The authors modified the 0-1 deterministic model of Bertsimas and Stock to account for weather related uncertainties. The objective function of the Bertsimas and Stock 0-1 deterministic model is to minimize the total cost of ground and air delays constrained by departure and arrival airport capacities and airspace capacity for each air sector. The problem is also bounded above by a maximum allowable ground and air delay for each flight. The 0-1 deterministic nature of the model stems from the usage of binary variables representing whether or not an aircraft arrives at a required sector by a specified time.

Rather than pursue a stochastic approach utilizing probability distributions, Alonso et al. selected the scenario analysis technique, which they felt was more appropriate for addressing uncertainty in situations involving limited historical data, as is the case with most weather related behavior. Each scenario, which they represented graphically using tree diagrams, represents one realization of uncertainty. The first scenario method proposed was to average the capacities over all the scenarios and to use these averages as additional constraints in the Bertsimas and Stock TFMP deterministic model. Their computations revealed that the optimal solution thus found was infeasible to almost every scenario. As a result, they concluded that the average scenario method is an inappropriate approach to modeling the minimization of flight delays. The authors also considered determining an optimal solution for each scenario. Fortunately, they soon realized that this approach could generate a "good" flight selection for one scenario that could have "disastrous consequences" if an alternate scenario is realized. Alonso et al. settled,

therefore, on the scenario analysis scheme of Dembo (1991), which selects flights that best track the different scenarios by minimizing the weighted difference between a recommended solution and the optimal solution obtained for each scenario.

The first stochastic model Alonso et al. (2000) presented determines a best track using a simple recourse policy. This policy, however, introduces non-linearity into the objective function that motivates the authors to recommend two alternative model formulations, each one removing the non-linearity of the base model. The linearity requirement becomes very important, in relation to the model run-time, as the dimensions of the problem size increase with the introduction of stochastic input. The second stochastic model presented determines a best track using a full recourse policy, which focuses only on future uncertainty when looking for a better solution at a particular stage. While using the full recourse policy, the authors implemented the non-anticipatory principle, Rockafellar and Wets (1991), which implies that if two stages are identical up to a certain time *t*, then the decisions variables up to that time *t* are the same for both scenarios. This principle removes the solution dependency on information that has yet to be obtained.

In both the simple and full recourse policy models for a realistic problem size, the number of required computations could potentially result in an optimal solution too late for implementation. Therefore, the authors proposed a Fix-and-Relax heuristic to reduce the run time, thus improving the usefulness of the model solution. This heuristic considers the integrality of the 0-1 variables successively rather than all at once. A computational comparison between this heuristic and the relaxation of the 0-1 variables resulted in very little to no integrality gap for a majority of the scenarios. The remainder of the paper presented by Alonso et al. (2000) provides computational comparisons between the deterministic model and the two recourse policy models discussed above using seven test cases. The largest test case consisted of 160 flights using four airports and five airspace sectors.

While Alonso et al. (2000) addressed the stochastic nature of the Air Traffic Flow Management problem; their approach using scenarios for each realization of weather uncertainty requires detailed scenario structures for each area of interest. Their implementation of a heuristic that is guaranteed to find a near-optimal solution in reasonable time is necessary for air traffic management.

2.2.2. Trajectory-based Air Traffic Management under Weather Uncertainty

Given the potential disruption of a planned flight trajectory for an aircraft due to severe weather conditions, the current strategic air traffic management strategy adopted by the FAA is predicated on weather avoidance through the implementation of either Ground Delay Programs (GDPs) or re-routes under the Severe Weather Avoidance Plan (SWAP) as part of the National Playbook (FAA, 2005). Nilim et al. (2001) pointed out that this current approach for handling inclement weather in the Airspace-Based Air Traffic Management System is too conservative. As an alternative, they developed a Trajectory-Based Air Traffic Management (TB-ATM) system, in which "only one controller is responsible for each aircraft from gate-to-gate". Accordingly, they addressed the problem of routing a single aircraft using Markov chains and a dynamic programming algorithm. The single aircraft problem is the first of three major phases introduced by the authors to support the transition to a Trajectory-Based ATM. The authors also emphasized the requirement for an automated system that "explicitly deals with the dynamics and the stochasticity of the storms and provides solutions that reduce the expected delay in the air traffic control system" (Nilim et al., 2001).

The current Air Traffic Management system is based on the division of airspace into a number of sectors. The size of a sector is dependent upon the expected number of aircraft within the sector. The capacity of a sector is around 40 aircraft at any given time with each sector managed by two controllers: Planning Controller and Executing Controller, who are responsible for each aircraft as it moves through the sector. The Planning Controller is responsible for minimizing the number of conflicts at the strategic level, while the Executive Controller ensures that no conflicts exist at the tactical level. As the number of aircraft increase in a small region, the size of the sector becomes relatively smaller.

While constructing an optimal two-dimensional flight plan for a single aircraft, there exist obstacles that must be avoided as the aircraft moves from point A to point B. These obstacles are either deterministic or stochastic in nature. The deterministic obstacles are invariant with known dimension and duration such as military operations areas or other Special Use Airspaces (SUAs). Storms and related weather conditions fall into the stochastic obstacle classification in which variations exist in time, location, and size. Weather teams are available that provide associated storm locations and time probabilities that are updated approximately every 15 minutes. The current method used to account for these stochastic obstacles is to

consider them unstable and treat them as deterministic constraints within the optimization problem. Thus, this approach to flight plan generation is conservative and under-utilizes the existing airspace since the storm departs the area after a predictable period of time.

Using a simple example, the authors discuss a potential flight plan for one segment in which the aircraft proceeds on a path until it is at some predetermined distance from the storm. At this point, a decision is made, based upon the storm characteristics, as to whether the aircraft can proceed directly to its destination or if re-routing is required to move around the storm. A probability p is associated with the storm characteristics and the authors minimize the flight length of that particular segment. Unfortunately, this simplistic viewpoint must be expanded to account for multiple flight segments and the probabilities associated with the storm durations and their changing intensities.

Nilim et al. (2001) presented an extension to account for weather probabilities. They discretized the time into 15-minute intervals within their Markov chain, assuming known probabilities associated with the existence of a storm or no storm in the region within each subsequent 15-minute interval. A transition matrix for the Markov chain was then developed using a transition model for each storm $1,\ldots,m$ moving from its current state to the next state. The total number of stages is calculated based upon the worst-case flight time T and the total number of states is $2m$. For a demonstration of their methodology, Nilim et al. develop the transition matrix for two storms. A significant assumption made is that there is no storm movement and that sectors without storms will remain storm free throughout the flight time.

Similar to the method used to discretize time, the authors used a rectangular airspace region with grids to construct flight paths using fixed waypoints. Grid points are considered attainable if they can be reached within 15 minutes. After describing their method for reducing the search space by looking at only a limited number of shortest paths from the aircraft's current position, Nilim et al. developed the recursive equations for formulating a stochastic dynamic programming routine for routing aircraft under weather uncertainties.

The Markov Decision Process algorithm is an eight-step process in which the authors are mainly concerned with the portion of the flight in which the velocity remains relatively constant. By focusing on this portion only, minimizing the expected delay is the same as minimizing the distance traveled. In their algorithm, the distance for which the pilot knows precisely the information on the storm is $15*V$ where V is the aircraft velocity (miles per minute), and where

the multiplier 15 represents the 15 minutes for which perfect information is achieved. The algorithm assigns a high cost for those flight paths that encounter storms. Flight paths that do not encounter storms are assigned a cost equal to the Euclidean distance for that flight segment.

Nilim et al. (2001) implemented their algorithm in MATLAB for two test scenarios. The dynamic routing of each scenario was then compared to two Traditional Strategies (TS1 and TS2) using a "performance metric referred to as the Improvement Measure (IM)". TS1 was a flight path that completely avoided the storm region. TS2 was a flight path that initially traveled along the nominal path until it reached a potential storm zone. If the storm was present, it circumvented the storm. If there was no storm, the aircraft continued on the nominal path until reaching its destination. In summary, the dynamic routing algorithm using updated information on the weather provided a higher IM value in comparison with the traditional strategies.

2.2.3. Hub Closures and Schedule Recovery

The presence of severe weather at an airport can either reduce the airport's capacity (defined by the number of arriving and departing aircraft per hour) or in the worst-case, force an airport to close for a period of time until flight operations can safely resume. When the arrival rate is reduced, the FAA imposes a GDP in order to thin out the arrival process. For the case of an airport closure, aircraft may need to be rerouted depending upon the duration of the closure. Thengvall et al. (2003) presented an approach for a more specific situation in which the airport is a hub for a particular airline. For example, the Hartsfield-Jackson Atlanta International Airport is a hub for Delta Airlines. As a central point for multiple flights, the closure of a hub can cause major disruptions that ripple through published flight schedules. Following such a closure, the problem becomes one in which the affected airline(s) must reroute aircraft in order to minimize the impact on the passengers. This problem within the literature is referred to as the *aircraft schedule recovery problem*. Thengvall et al. (2003) proposed the application of a bundle algorithm to solve the aircraft schedule recovery problem, after transforming it into a multi-commodity network flow model.

Rosenberger et al. (2003) also addressed the aircraft schedule recovery problem for situations when a planned flight route is no longer feasible due to weather conditions or due to unscheduled maintenance problems. They formulated a set-packing model for this problem and

developed an optimization routine for aircraft recovery following either a flight route disruption or an airport disruption.

While we do not address hub closures or the aircraft schedule recovery problem in this dissertation, we emphasize that the rerouting of flights remain subject to sector workload, conflict risk, and equity considerations and, therefore, should be evaluated in concert with these related, impacted features. We address this aspect in our approach via the APCDM model.

2.3. Enhancements to the Ground Delay Program

The enhancements to the Ground Delay Program (GDP) were the first major steps in the Federal Aviation Administration's (FAA) adoption of the Collaborative Decision-Making (CDM) paradigm. In addition to the improvements in situational awareness, the two key concepts developed under the enhancements were the Ration-by-Schedule (RBS) and Compression procedures. The Ration-By-Schedule and compression procedures, developed by Metron Inc. and Volpe National Transportation Systems Center, were designed to provide incentives for the airlines to report flight delays and cancellations under the CDM initiatives (Chang et al. (2001), and Vossen and Ball, (2001)). This was accomplished by means of a significant paradigm shift in the way that FAA allocated arrival slots. Under the original GDP process, the FAA allocated slots based solely upon the latest reported arrival estimates from the airlines. "Flights were then assigned to slots by a first-come-first-served algorithm, affectionately known as Grover Jack" (Vossen and Ball, 2001, p. 4). The defining characteristic of RBS is the philosophical change with respect to slot allocations. Rather than using the latest reported arrival estimates, RBS prioritizes flights based on their original scheduled arrival times found in the Official Airline Guide (OAG). Thus, airlines that report delays or cancellations no longer forfeit their originally scheduled arrival slots, but rather, they retain ownership of those slots, giving them the freedom to either use these slots for their own flights or to exchange them according to their best interests. Airlines manage their arrival slot allocations (i.e., canceling and substituting flights) through the use of the Enhanced Substitution Module (ESM), developed by Metron Aviation Inc. The ESM, an optional add-on to the Flight Schedule Monitor (FSM), is an automated flight substitution decision support tool used to evaluate scenarios relating to potential flight swaps (Metron, 2004).

When the delay or cancellation of a flight results in a slot vacancy, efficient methods are required for slot reassignment to ensure that a slot does not go unused (Chang et al., 2001). The compression algorithm was designed specifically to address the reassignment issue while providing the incentive for airlines to report flight cancellations. Compression begins internally with the specific carrier that owns the vacant slot. The algorithm searches for other flights pertaining to this same carrier that can be assigned to that slot. For example, if the cancellation of some Flight 1 from carrier A creates a vacancy in a slot having an arrival time of 0900, the algorithm will find the first available flight, say, Flight 2, from carrier A that has been delayed to arrive at a later slot time, and will reassign this flight to the time of the vacated slot, creating another vacant slot originally belonging to Flight 2. One key stipulation is that a flight cannot be assigned to the vacant slot if its published (OAG) scheduled arrival time is later than the time associated with the vacant slot. The algorithm repeats this process until carrier A can no longer fill the remnant vacant slot, and then considers the assignment of this slot to some other airline B, say, whose vacant slot is accordingly thereby reassigned to airline A. This is where the incentive for airlines to report delays and cancellations becomes truly evident. Vossen and Ball (2004) imply that, in this situation, airline A is being "paid back" for its released slot. The compression algorithm will then determine if carrier A can utilize its newly allotted slot and, if not, repeat the process looking for flights from other airlines. While equity is a primary consideration within the compression algorithm, priority is given to airlines that participate in CDM (Chang et al., 2001). An example of the compression algorithm is shown in Figure 2-9 (derived from Vossen and Ball, 2004) involving airlines AAL, DAL, and COA in which flight AAL2 is cancelled. The compression algorithm potentially allows an airline to cancel a flight, and as a result of the creation of the vacant slot, to reduce the GDP-imposed delays of other flights. Ball et al. (2002) present a layout of the RBS and compression algorithms. Following the implementation of RBS and compression procedures in January 1998, the compression algorithm alone resulted in savings of approximately $39 million from January 20, 1998 to July 15, 1999 (Ball et al., 2000).

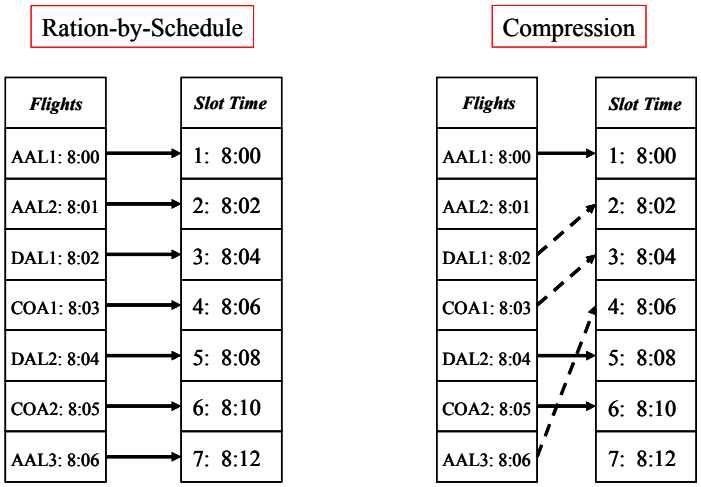

Figure 2-9: Compression Example.

2.4. Slot Trading Opportunities

When Vossen and Ball (2001) first introduced the concept of inter-airline slot exchanges, it was based on the principle that given a fixed set of allocated slots under a GDP, each airline would be willing to trade its assigned slot(s) if and only if the trade would be beneficial with respect to the cumulative delay induced from the GDP. Offers presented by airlines in this context fall into two types. The first type, referred to as *default offers*, occurs when an airline proposes to relinquish its allocated slot in exchange for an earlier slot that pertains to a time no earlier than the earliest time of its arrivals listed in the OAG. The second type occurs when an airline considers either canceling or delaying a flight (*downward-move*) in return for a reduction in the delay (*upward-move*) of a subsequent flight. In essence, the default offers are of the form: Airline $a \in A$ is willing to give up a slot $s \in S_a$ in return for a slot earlier than s, where A is the set of airlines and S_a is the set of slots allocated to airline $a \in A$. The second offer type is of the form: Airline $a \in A$ is willing to cancel or delay the flight in slot $s_1 \in S_a$, in return for a slot earlier than $s_2 \in S_a$, $s_2 > s_1$, where s_2 is the slot allocated to a subsequent flight of airline a. A directed network can be used to represent potential slot-exchange offers. Each node of the network represents an available slot that is currently assigned to a specific flight and its associated airline, while the arcs represent the offers. Figure 2-10 illustrates a directed network involving seven slots under a GDP. The number at the top of each box is the flight number. The bottom number is the time of the allocated slot for the respective flight. An example of a default

offer from flight US1620 is depicted in the directed network by any one of the three arcs to slot times 0806, 0808, and 0810. Arcs from US1620 to slots earlier than 0806 do not exist given that the earliest flight arrival time for US1620 listed in the OAG is 0806. The arc from UA635 to slot time 0812 depicts an offer of the second type in which United Airlines is willing to delay flight 635 in return for moving flight UA647 to an earlier slot. The problem then becomes one in which the FAA, acting as the mediator, selects a feasible set of slot exchanges from all offers provided by the airlines, where any feasible set of slot exchanges corresponds to a set of directed cycles in this graph and can be generated by an optimization problem formulated as an assignment problem (Vossen and Ball, 2001). One critical stipulation in this approach is the insurance that if an offer from an airline is not accepted, it retains its current slot. The offer of a flight cancellation or delay initiates the requirement for slot exchanges in order to ensure efficiencies in slot utilization. If United Airlines removed the offer associated with flight 635 (see Figure 2-10), no slot exchanges would occur (i.e., no directed cycles would exist in the resulting network). Furthermore, the model ensures that no flight specific to any airline is delayed without reducing the delay of some other flight for that airline.

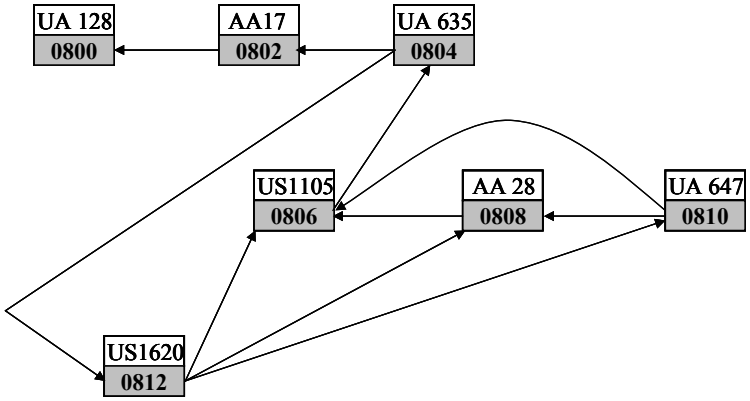

Figure 2-10: Directed Network of Potential Slot Offers.

As stated previously, the mediated slot exchange problem can be modeled as an assignment problem. Vossen and Ball (2001) started from a mediated bartering model for goods between various agents. The set of agents, A, own one or more goods, and each agent, $a \in A$, submits potential offers for the exchange of goods between agents. The objective of the assignment problem is to minimize the cost of the allowable trades. The constraints within the bartering model formulation contain provisions for trades that are not accepted. Vossen and Ball then modified this model to account for the above two types of offers, and adopted a bi-level

programming approach, giving priority within the objective function to the second type of offers. A general form of their bartering model is shown below (Vossen and Ball 2001).

$$\text{Minimize} \quad \sum_{s \in N} \sum_{t \in T_s} c_{st} x_{st} \tag{2.1}$$

$$\text{subject to} \quad \sum_{t \in T_s} x_{st} + y_s = 1, \quad \forall\, s \in N \tag{2.2}$$

$$\sum_{t:s \in T_t} x_{ts} + y_s = 1, \quad \forall\, s \in N \tag{2.3}$$

$$x_{st}, y_s \in \{0,1\}, \qquad \forall\, (s,t) \in E \text{ and } s \in N\,. \tag{2.4}$$

Offers are of the form $(s,t), t \in T_s$, where s is the slot offered by airline a, and T_s is the set of slots that the airline is willing to accept in return for the exchange. The set E is the set of arcs in the directed network representing all possible exchanges. The binary variable $x_{s,t}$ is equal to 1 if the trade between slot s in exchange for slot $t \in T_s$ is accepted, and is 0 otherwise. The set N is the collection of all slots assigned under the GDP. The variable y_s is equal to 1 when an offer is rejected and is 0 otherwise. In essence, y_s activates a self-loop at node s. The first constraint ensures that slot s is traded only once, which includes a trade to itself (i.e. the airline maintains slot s). Likewise, the second constraint ensures that if an airline accepts a trade for slot s, it receives another slot in return. Optimal solutions to the model above are represented in the network by directed cycles. We omit the development of the cost parameters in the objective function and refer the reader to Vossen and Ball (2001). Note that these authors later abandoned this model formulation in favor of a more restricted approach with regard to offer types.

From this initial work, Vossen and Ball (2004) suggested several possible extensions. One of these deals with conditional exchanges in which the airlines can "test-the-water" by offering a conditional cancellation in return for a reduction in the delay of a subsequent flight. This extension has been implemented and is more commonly referred to as Slot Credit Substitution (SCS). Another important extension, which is central to our works involves more complex slot-exchange offers. In this instance, airlines are able to offer multiple slots in exchange for multiple slots in return. This extension is the foundation for their slot trading opportunities proposed in 2004, where Vossen and Ball introduced the idea of airlines submitting "at-least, at-most" type offers. The premise behind such offers is that it may be beneficial for an airline to exchange an earlier slot for a later slot for some flight, in return for moving up a subsequent flight. For example, an airline may submit an offer to extend the delay of a flight

serving only a few passengers in return for reducing the delay of a flight that serves several more passengers. Vossen and Ball provide an example using delay costs as the metric to show how such offers can mutually benefit a pair of airlines involved in such a trade. The authors formulated a set partitioning model to select among such offers as well as default offers so as to maximize the number of trades.

Vossen and Ball (2004) also proposed an alternative formulation that assigns flights to classes based on the submitted offers, where a class represents the direction of change in the amount of delay (i.e. an increase or decrease). Given the range of the offer, flights can be assigned to more than one class. The model also assigns the classes to slots, guaranteeing that each slot is assigned exactly once, and that the slot exchanges are valid with respect to the submitted offers. For example, slot exchanges that reduce the delay time of two flights from the same airline violate the restriction that requires one flight to move down in time when another is selected to move up in time. The objective function is selected to maximize the number of downward trades, thus reducing the delay for as many flights as possible that are designated for upward trades. Vossen and Ball also presented empirical results to support their conjecture that extended slot-trading mechanisms can improve airline efficiencies.

On November 15, 2000, the FAA, at the request of the Port Authority of New York and New Jersey (PANYNJ), announced a temporary capacity restriction on the number of hourly arrival and departure operations at LaGuardia Airport (LGA) in order to reduce the increasing number of air traffic-related delays. The operational cap, which was imposed on January 31, 2001, reduced the number of High-traffic Density Rules (HDR) slots and exemption slots (as prescribed by the Wendell H. Ford Aviation Investment and Reform Act for the 21st Century) from 104 to 81 per hour. To facilitate the distribution of the limited number of available exemption slots among the existing and new entrant carriers, the FAA conducted a lottery on December 4, 2000. Following the implementation of the operational cap, the delays at LGA decreased by 71% as determined using the FAA's Air Traffic Operations Network Database. The initial FAA-imposed capacity restriction, however, was scheduled to expire on September 15, 2001. As such, the FAA proposed a two-phased approach to implement further demand management solutions at LGA. The first phase extended the December 4, 2000 lottery results and included a second lottery to allocate the unused slots from the initial lottery, which provided an opening for new entrant carriers. The focus of the second phase was on finding a long-term

solution in order to establish an equilibrium between demand and capacity at LGA. Since LGA is unable to expand its airfield capacity due to land restrictions, the FAA considered two market-based options. The first option proposed the implementation of a congestion price for arrivals and departures set by PANYNJ. The second option considered the auctioning of a percentage of the HDR/exemption slots each year, where the FAA determined the number of slots available. Possible extensions proposed by the FAA included the assessing of auction fees, which could be adjusted to accommodate new entrant carriers (Federal Register, 2001).

2.5. The Airspace Planning and Collaborative Decision-Making Model

In response to the Federal Aviation Administration's sponsored effort to enhance the management of the U.S. National Airspace System (NAS), Sherali et al. (2003) developed the Airspace Planning and Collaborative Decision-Making Model (APCDM). The overall intent in this model is to select a set of flight plans from among alternatives, called surrogates, subject to flight safety, air traffic control workload, and airline equity. Each flight plan is required to meet the feasibility requirements specified by the system constraints and as a result of this research will be generated to avoid dynamically moving weather.

The model consists of five separate subroutines that range from the Air Occupancy Model (AOM), developed by Sherali et al. (2000), to the Flight Plan Selection subroutine, developed by Sherali et al. (2003). Figure 2-11 illustrates the essential framework for the APCDM. Inputs into the APCDM consist of sector geometries, flight plans, special use airspaces (SUAs), and weather closures. The sector geometries represent the division of the available airspace into polygonal cross-sections defined by boundaries, and floor and ceiling altitudes. The size and geometry of the airspace sectors is often determined by the potential number of aircraft that can exist within a region at any given time (Nilim et al., 2001). These airspace sectors remain static and presently maintained by the FAA for regulating air traffic. The flight plans, grouped into surrogates, are provided for each aircraft. Currently, flight plan inputs for the APCDM are generated devoid of information from existing weather systems.

The AOM subroutine determines the airspace sectors traversed by each surrogate flight plan. The information extracted from this subroutine includes the time intervals each flight spends in a corresponding airspace sector. In addition, the AOM subroutine contains a workload

function used to generate a cost associated with monitoring the number of flights that can potentially coexist within each given airspace sector.

The second subroutine is the Probabilistic Aircraft Encounter Model (PAEM), which conducts conflict analyses based on probabilistic trajectory realizations that are induced by wind effects or by random errors around a planned flight trajectory. This subroutine identifies durations for which conflicts at various severity levels can occur within each sector with specified conflict threshold probabilities. The outputs from these first two subroutines are utilized in a third subroutine to generate the workload constraints per sector, based on the sector's capacity to monitor air traffic and to resolve co-existing conflicts.

The fourth subroutine addresses the issue of achieving equity amongst the various airlines with respect to absorbing the costs associated with delays and cancellations. The equity in this context is measured with respect to the relative collaboration efficiencies attained by the different airlines based on the fuel and delay costs incurred for the solution generated by the APCDM model in comparison with the individually optimized costs. The final subroutine integrates the workload constraints and the equity constraints into a mixed-integer programming formulation for determining an optimal mix of flight plans.

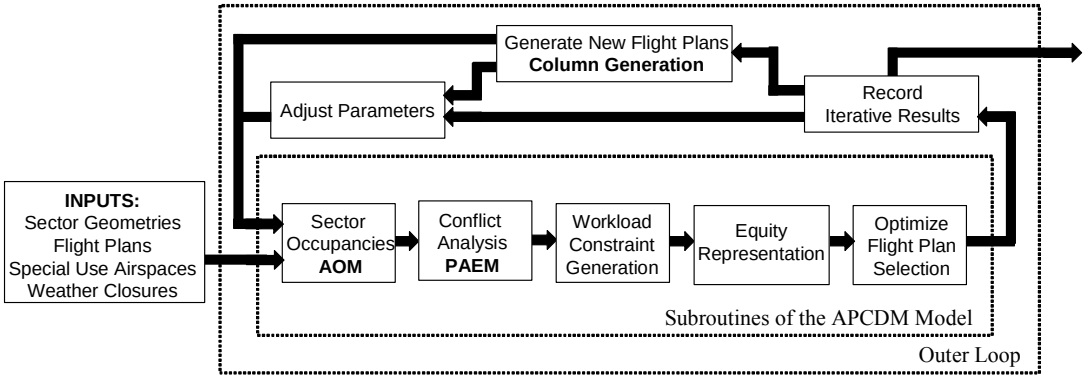

Figure 2-11: Operational Framework for the APCDM (Sherali et al., 2003 and 2006).

We present a review of the mathematical formulation of the APCDM model that is developed in Sherali et al. (2003, 2006). We will be integrating our modeling concepts into this model in Chapters 3, 4, and 5 to include the impacts of weather uncertainty and to consider slot-exchange mechanisms, respectively. Therefore, we provide a summary of this model here for the sake of completeness. Below we first list the sets of indices, variables, parameters, and coefficients, and then state the model formulation.

(a) **Index Sets**:

$s = 1,...,S$: Sectors involved in the model analysis.

$\alpha = 1,...,\overline{\alpha}$: Airlines involved in the model analysis.

$f = 1,...,F$: Flights to be scheduled.

$p \in P_f$: Alternative flight plans or surrogates for flight *f*.

$P_{f0} = P_f \cup \{0\}$, with *p*=0 representing the flight cancellation surrogate, if offered by the particular airline as a possible option, and being ascribed an inordinately high penalty otherwise (including the case of airborne flights).

(b) **Decision Variables**:

(i) **Principal Decision Variables**:

x_{fp} : Binary variable, which equals one if flight plan $p \in P_{f0}$ is selected for flight *f*, and zero otherwise, for $f=1,\ldots,F$. (These are sometimes denoted by x_P or x_Q (etc.) where each of *P* and *Q* (etc.) represent some actual flight plan combination (*f*, *p*) for $p \in P_f, f \in \{1,\ldots,F\}$.)

(ii) **Auxiliary Decision Variables**:

n_s : Peak occupancy level (number of flights) for sector *s*.

w_s : Average occupancy level (number of flights) for sector *s*.

$y_{sn} \in [0,1]$, $n=0,\ldots,\overline{n}_s$: Convex combination weights attached to the breakpoints of a piecewise linear increasing convex penalty function, which represents the penalty ascribed to the difference between the peak and the average workload in sector *s*.

z_{PQ} : Binary variable, which equals one whenever conflicting flight plans *P* and *Q* are selected. (It is assumed in the model description that $z_{PQ} \equiv z_{QP}$.)

$E_\alpha(x)$: Collaboration efficiency for airline α.

$E^e_\alpha(x)$: Collaboration equity for airline α.

$x^e \equiv \sum_{\alpha=1}^{\overline{\alpha}} \omega_\alpha \left| E^e_\alpha(x) \right|$: (ω-) Mean collaboration inequity.

ν_α : Variable used to represent the term $\left| E^e_\alpha(x) \right|$ for airline α.

(c) **Model Parameters and Coefficients:**

ω_α : The weight factor ascribed to each airline α (prescribed in proportion to the number of flights or passengers handled).

c_{fp} : The cost to execute flight plan $p \in P_{f0}$ for flight f (prescribed as $c_{fp} = F_{fp} + D_{fp}$, $\forall p \in P_f$, $f=1,\ldots,F$, where F_{fp} and D_{fp} are respectively the associated fuel and delay costs as derived in Sherali et al. (2006)).

c_f^* = Minimum $\{c_{fp}: p \in P_f\}$, for each flight f.

H : The length of the time horizon under consideration (in minutes).

γ_s : The airspace monitoring cost factor for sector s, per unit average occupancy level workload (prescribed as \$0.361H).

μ_{sn} : The (penalty) cost assessed when the peak monitoring workload in sector s exceeds the average workload by n (prescribed as $\left(\frac{\gamma_s}{5}\right)n^2$, which yields a convex increasing rate penalty function).

φ_{PQ} : The (penalty) cost ascribed to resolve an en-route conflict between flight plans P and Q (ordinarily prescribed as \$0.301, but could depend on the conflict geometry).

μ^D : The (penalty) cost factor associated with the total weighted collaboration inefficiency attained (designated as $0.1\sum_{f=1}^{F} c_f^*$).

μ^e : The (penalty) cost factor associated with the level of total weighted collaboration inequity attained (designated as $0.1\sum_{f=1}^{F} c_f^*$).

$E_{\max}^e$: Bounding constant (designated as $0.07/\overline{\alpha}$) imposed on each weighted inequity.

t_{fp}^s : The length of time (in minutes) that flight plan $p \in P_f$ of flight f occupies sector s.

Ω_s : The set of flight plans that occupy sector s during some subset of the time horizon.

$\overline{n}_s$: The maximum allowable peak monitoring workload (simultaneous flight occupancies) in sector s.

r_s : The maximum number of simultaneous conflict resolutions permitted to exist in sector s.

$D_{\max}$: The maximum allowable ratio for any airline of the cost for the selected surrogates to that for the individually optimized surrogates (prescribed as 1.2).

A_α : The set of flights belonging to airline α.

W_f : Relative priority weight attached to flight $f \in A_\alpha$ by airline α, where $\sum_{f \in A_\alpha} W_f = 1$, $W_f \geq 0$, $\forall f \in A_\alpha$.

ν^e : The maximal limit imposed on x^e, the ω-mean collaboration inequity.

C_{si}, $\forall i=1,\ldots,I_s$: The maximal overlapping sets of occupying flight plans for sector s.

M_{sk}, $\forall k=1,\ldots,K_s$: The maximal overlapping sets of conflicting pairs of flight plans for sector s.

$G_{sk}(N_{sk},M_{sk})$: The conflict subgraph of conflicting flight plans represented by M_{sk}, where the node set N_{sk} represents the respective flight plans (labeled as P, Q, R, etc.) that are involved within the edge set M_{sk}.

$J_{sk}(P)$: The set of flight plans Q that are adjacent to P within the graph G_{sk}.

FC : The set of fatally conflicting pairs of flight plans (P,Q).

A : The entire set of resolvable conflicting pairs of flight plans (P,Q).

APCDM:

Minimize

$$\sum_{f=1}^{F} \sum_{p \in P_{f0}} c_{fp} x_{fp} + \mu^D \sum_{\alpha=1}^{\bar{\alpha}} \omega_\alpha \left[1 - E_\alpha(x)\right] + \mu^e x^e + \sum_{s=1}^{S} \gamma_s w_s + \sum_{s=1}^{S} \sum_{n=0}^{\bar{n}} \mu_{sn} y_{sn} + \sum_{(P,Q) \in A} \varphi_{PQ} z_{PQ} \quad (2.5a)$$

subject to:

$$\sum_{p \in P_{f0}} x_{fp} = 1, \quad \forall f = 1,\ldots,F \quad (2.5b)$$

$$\sum_{(f,p) \in C_{si}} x_{fp} \leq n_s, \quad \forall i = 1,\ldots,I_s, s = 1,\ldots S \quad (2.5c)$$

$$w_s = \frac{1}{H} \sum_{(f,p) \in \Omega_s} t_{fp}^s x_{fp}, \quad \forall s = 1,\ldots,S \quad (2.5d)$$

$$n_s - w_s = \sum_{n=0}^{\bar{n}_s} n y_{sn}, \quad \forall s = 1,\ldots,S \quad (2.5e)$$

$$\sum_{n=0}^{\bar{n}_s} y_{sn} = 1, \quad \forall s = 1,\ldots,S \quad (2.5f)$$

$$x_P + x_Q \leq 1, \quad \forall (P,Q) \in FC \quad (2.5g)$$

$$\sum_{(P,Q) \in M_{sk}} z_{PQ} \leq r_s, \quad \forall k = 1,\ldots,K_s, s = 1,\ldots,S \quad (2.5h)$$

$$x_P + x_Q - z_{PQ} \leq 1, \quad \forall (P,Q) \in A \quad (2.5i)$$

$$\sum_{Q \in J_{sk}(P)} z_{(PQ)} \le r_s x_P, \quad \forall P \in N_{sk} : \left|J_{sk}(P)\right| \ge r_s + 1, \ \forall k = 1,...,K_s, s = 1,...,S \tag{2.5j}$$

$$E_\alpha(x) = \frac{D_{\max} \sum_{f \in A_\alpha} W_f c_f^* - \sum_{f \in A_\alpha} \sum_{p \in P_{f0}} W_f c_{fp} x_{fp}}{\left(D_{\max} - 1\right) \sum_{f \in A_\alpha} W_f c_f^*}, \quad \forall \alpha = 1,...,\bar{\alpha} \tag{2.5k}$$

$$E_\alpha^e(x) = E_\alpha(x) - \left(\sum_{\alpha=1}^{\bar{\alpha}} \omega_\alpha E_\alpha(x) \right), \quad \forall \alpha = 1,...,\bar{\alpha} \tag{2.5l}$$

$$\nu_\alpha \ge -E_\alpha^e(x), \quad \nu_\alpha \ge E_\alpha^e(x), \quad \forall \alpha = 1,...,\bar{\alpha} \tag{2.5m}$$

$$x^e = \sum_{\alpha=1}^{\bar{\alpha}} \omega_\alpha \nu_\alpha \tag{2.5n}$$

$$z_{PQ} \ge 0, \ \forall (P,Q) \in A, \ x_{fp} \text{ binary}, \ \forall p \in P_{f0}, \ \forall f = 1,...,F, \ y_{sn} \ge 0, \forall n = 1,...,\bar{n}_s, s = 1,...,S,$$

$$E_\alpha(x) \ge 0, \ \forall \alpha = 1,...,\bar{\alpha}, \ n_s \le \bar{n}_s, \forall s = 1,...,S, \ x^e \le \nu^e, \ \omega_\alpha \nu_\alpha \le E_{\max}^e, \forall \alpha = 1,...,\bar{\alpha}. \tag{2.5o}$$

The first objective term is the summation of the fuel, delay, and cancellation costs for the selected flight plans. The next two terms impose penalties on the attained levels of the ω-mean collaboration inefficiency and the ω-mean collaboration inequity, respectively. Note that although the cost factors $c_{fp}x_{fp}$ appear in both the first two terms in (2.5a), the first term represents the total system cost, whereas the second term is dimensionless and includes weighting priority factors among airlines, as well as weighting priorities for flights pertaining to each individual airline. Moreover, the second term is weighted with a factor μ^D, which provides the flexibility of running the model with different degrees of relative importance attached to this term. Sherali et al. (2006) prescribe values for μ^D and μ^e that, in extreme cases of the ω-mean collaboration inefficiency and inequity, would yield a penalty of some μ_0% of $\sum_{f=1}^{F} c_f^*$ via the second and third terms. Sherali et al. (2006) also provide a sensitivity analysis with respect to μ_0. Additionally, note that the priority weights $W_f, f \in A_\alpha$, attached to the flights for an individual airline essentially affect its defined efficiency, which then governs the selection of flight plans via the three equity-based terms. Since the entire objective function (2.5a) represents a systems perspective, the influence of these equity terms is naturally offset by the remaining cost terms, depending on the value of μ_0 or that of the parameter vector (μ^D, μ^e). The fourth

term in the objective function (2.5a) ascribes a penalty to the average sector workloads, the fifth term penalizes the differential between the peak and the average sector workloads according to a piecewise linear increasing convex function, and the final term penalizes the resolvable conflicts that will need to be addressed by the air traffic controllers (ATC).

Constraint (2.5b) requires exactly one flight plan to be selected from among the set of available surrogates. The next four constraints are associated with sector occupancies, where (2.5c) limits the maximum simultaneous occupancy for each sector *s*, (2.5d) evaluates the average sector workloads, (2.5e) computes the peak-average workload differential, and (2.5f) requires the convex combination weights ascribed to the breakpoints of the peak-average workload differential penalty function to sum to one. All fatal conflicts are prohibited via (2.5g). The conflict constraint formulation, described in detail in Sherali et al. (2003), is expressed via (2.5h) through (2.5j), where (2.5h) and (2.5i) jointly ensure that no more than r_s resolvable conflicts coexist within sector *s* at any point in time, and (2.5j) further tightens this representation via a set of star-subgraph convex hull based valid inequalities. The airline collaboration efficiencies and collaboration equities are determined by (2.5k) and (2.5l), respectively. Constraints (2.5m) and (2.5n) provide a linear function for computing the ω-mean collaboration inequity. Finally, (2.5o) imposes the necessary logical and bounding conditions. As expounded in Sherali et al. (2003), in case a model run indicates infeasibility, additional sensitivity analysis runs can be made by relaxing $E_\alpha(x) \geq 0$ and $x^e \leq \nu^e$ from these latter bounding constraints.

Chapter 3
Modeling Weather-related Phenomena

In order to incorporate weather uncertainty within the APCDM model, certain tradeoffs between model fidelity and model tractability need to be considered when selecting a suitable weather forecasting approach from Chapter 2. Given that the primary goal of the APCDM model is to generate an optimal set of flight plans in support of FAA's Collaborative Decision Making (CDM) initiative, we cannot afford to expand the constructs of the APCDM model to the extent that the weather-related component would inhibit the execution of the APCDM model beyond the bounds of the decision-making cycle. In essence, we need to input weather forecast data from a "trusted" source, then preprocess this data appropriately for incorporating the relevant weather effects into the APCDM model, and finally ascertain its impact on the selection of an optimal set of flight plans, all while meeting the timelines for either a strategic or a tactical level decision-making process.

3.1. Selection of Weather Data Source

Given that a great deal of emphasis is given towards accounting for weather effects in most aspects of our daily lives, there is an abundance of daily forecasting data produced in multiple formats from a variety of weather prediction models. Our search for reliable weather forecasting probability data began with the National Weather Service (NWS), a sub-division of the National Oceanic and Atmospheric Administration (NOAA). A critical component of the NWS is the National Center for Environmental Prediction (NCEP), which is the primary U.S. source for nearly all weather forecast products (NWS, 2003). NCEP consists of nine centers that are responsible for the generation of both national and international weather products for the NWS, government offices, and other meteorological agencies. The Aviation Weather Center (AWC) is just one of the nine centers, and "provides aviation warnings and forecasts of hazardous flight conditions at all levels within domestic and international airspace" (NWS, 2003).

NCEP provides two categories of forecasting models: numerical models and statistical models. As described in Chapter 2, the suite of numerical models consists of five separate models (Eta, Global Forecast System (GFS), Wave Watch III, Nested Grid Model (NGM), and Rapid Update Cycle). The information from these numerical models is converted to static and

looping graphical representations, which are provided to the various users on the NCEP website. Figure 3-1 illustrates a static six-hour precipitation forecast from the Global Forecast System (GFS) model. While this type of forecast is available across the United States for precipitation, temperature, and wind data, it is very difficult to extract the associated probabilities for convective weather.

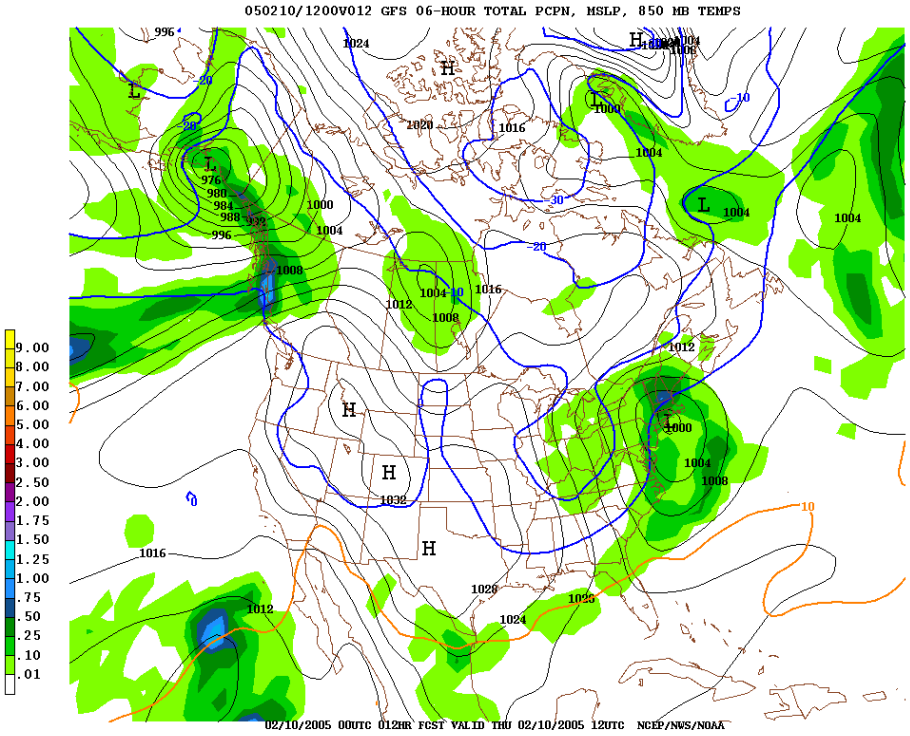

Figure 3-1: Static Six-hour Forecast from GFS (NWS, 2003).

The data from the numerical models is used by the Aviation Weather Center (AWC), to provide weather warnings to the aviation community in the form of both graphical representations and raw data format. The most common tool for accomplishing this is the Collaborative Convective Forecast Product (CCFP), which identifies possible convective regions for a specified time interval. Figure 3-2 depicts a CCFP product issued for February 7, 2005 until 2155Z. According to the AWC's CCFP Product Description Document (2005), convection is defined as a polygon of at least 3,000 square miles that attains:

- A coverage of at least 25% of the region with echoes of at least 40 dBZ composite reflectivity;
- a coverage of at least 25% of the region with echo tops of FL250, or greater, and
- a confidence level of at least 25%.

Unfortunately, because of its coarse features, the CCFP does not provide the level of detail required for our weather analysis.

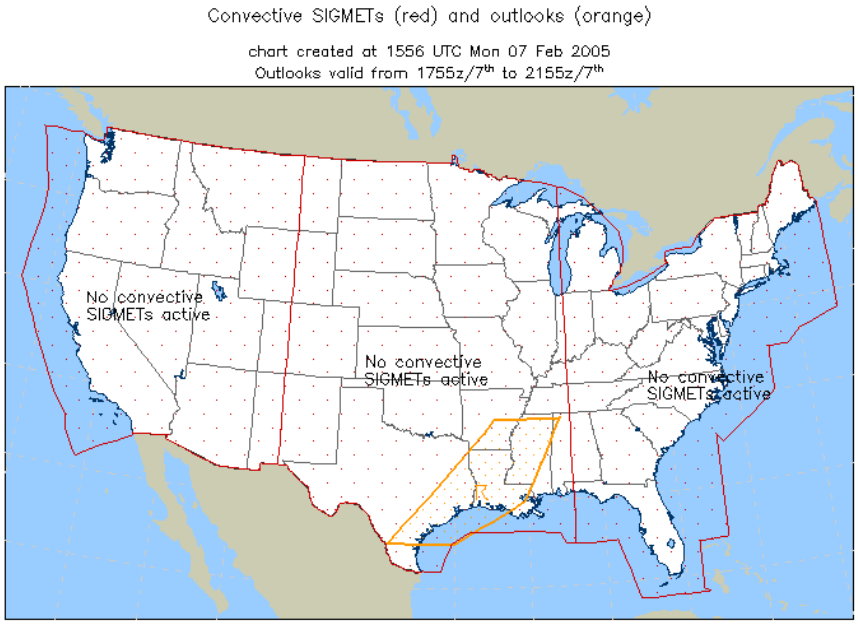

Figure 3-2: Convective SIGMETS from AWC (AWC, 2005).

A more detailed forecast information suite, which is available to the aviation community through the AWC, is the Aviation Digital Data Service (ADDS) website. Recall from Chapter two that there are five weather advisories used by pilots as supplements to the weather forecasts are the: Airman's Meteorological Information (AIRMETs); Significant Meteorological Information (SIGMETs); Convective SIGMETs; Center Weather Advisories (CWAs); and Severe Weather Forecast Alerts, more commonly referred to as Alert Weather Watches (AWW). These advisories are used to provide information on hazardous weather situations and are typically widespread, again, requiring coverage of at least 3,000 square miles before inclusion as an advisory, similar to the case of the CCFP. Therefore, even though an advisory may not exist for a particular airspace sector, we cannot exclude the potential for localized severe weather within the airspace (FAA, 2004).

The AWC also provides a suite of Java Tools that allows the aviation community to plot flight routes using real-time information pertaining to temperature, wind, convection, icing, and turbulence. Figure 3-3 depicts the real-time convection information for February 7, 2005, generated by the National Convective Weather Forecast (NCWF) Java Tool. This tool produces

an overlay containing the current convective hazard regions as well as a one-hour forecast hazard region when available. By remaining consistent with our temporal framework of February 7, 2005, we compared the real-time information from the NCWF Java Tool and the Convective SIGMET from CCFP, as depicted in Figure 3-2. By superimposing the large CCFP polygon region on top of the real-time information, we concluded that the information from the numerical model lacks adequate detail, and that one-hour convective forecasts are insufficient. Therefore, we shifted our attention to the available statistical models, which will be covered in the next section.

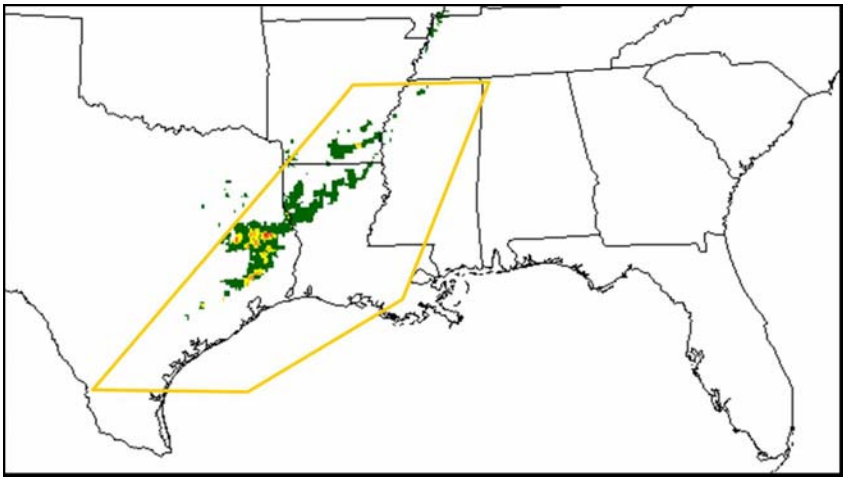

Figure 3-3: NCWF Java Tool.

3.2. Availability of Probabilistic Data

Given that weather uncertainties can wreak havoc on Air Traffic Management, we can no longer ignore problematic weather when selecting an optimal set of flight plans. The difficulty associated with capturing weather uncertainties in any model lies in the generation and application of forecast probabilities. Additionally, one must consider the continuous nature of weather when developing a probability map to describe the weather forecasts. The amount of data required to provide a continuous weather representation within the APCDM model would, however, quickly overburden the model and drastically reduce the model's efficiency. In order to maintain the model's tractability, we propose the development of a discretized representation of various weather phenomena that affect aviation operations using the data provided by the NCEP's statistical forecast models. These representations will be structured in the form of *probability-nets* as defined in the sequel, which are essentially lattices that are specific to the

spatial intensity of the weather. For example, using the probabilities associated with convective weather over a specified region, we will create a convective probability-net to monitor the probabilities of encountering severe weather throughout a given flight's trajectory. We will then appropriately penalize these trajectories within the objective function of the APCDM model. What follows is a detailed description of the data from the statistical forecast models, the development of the probability-nets for a given weather observation, and our proposed methodology for capturing weather uncertainty within the APCDM model.

The fundamental requirement for the development of the probability-nets is the existence of reliable site-specific forecast data over the area of interest. Of primary concern is the availability of probability data relating weather of aviation interest such as convection, snow, and visibility. The National Weather Service's Meteorological Development Lab (MDL), whose mission is "to develop and implement scientific techniques into National Weather Service Operations" (NWS, 2005), produces the necessary information in three-hour time intervals using a statistical modeling method known as Model Output Statistics (MOS). The pertinent aviation MOS text forecasts are available in short-range GFS (6-84 hours), Eta (6-72 hours), and extended-range GFS (12-192 hours) formats. MOS forecasts are also available in graphical form, which will be discussed later.

MOS is a technique that introduces objectivity into weather forecasting by interpreting the data produced from the aforementioned numerical models, and provides specific probability results for numerous sites throughout the United States. The primary predictors that serve as inputs into MOS include the forecasts from the Numerical Weather Prediction (NWP) model, prior surface weather observations, and other geo-climatic information. A multiple linear regression technique is then used to generate the required probabilities. Two significant advantages of the MOS technique are the removal of systemic biases inherent within the numerical models and the availability of weather specific probabilities (i.e., convection, ceiling, temperature, etc.) at every location in the MOS site structure (Antolik, 2003). Currently, there are over 1,500 reporting sites throughout the United States and Puerto Rico. Figure 3-4 depicts the locations of these reporting sites by region for the short-range GFS and Eta MOS forecast products. The exact latitude and longitude of each reporting site is available through the MOS website in text format.

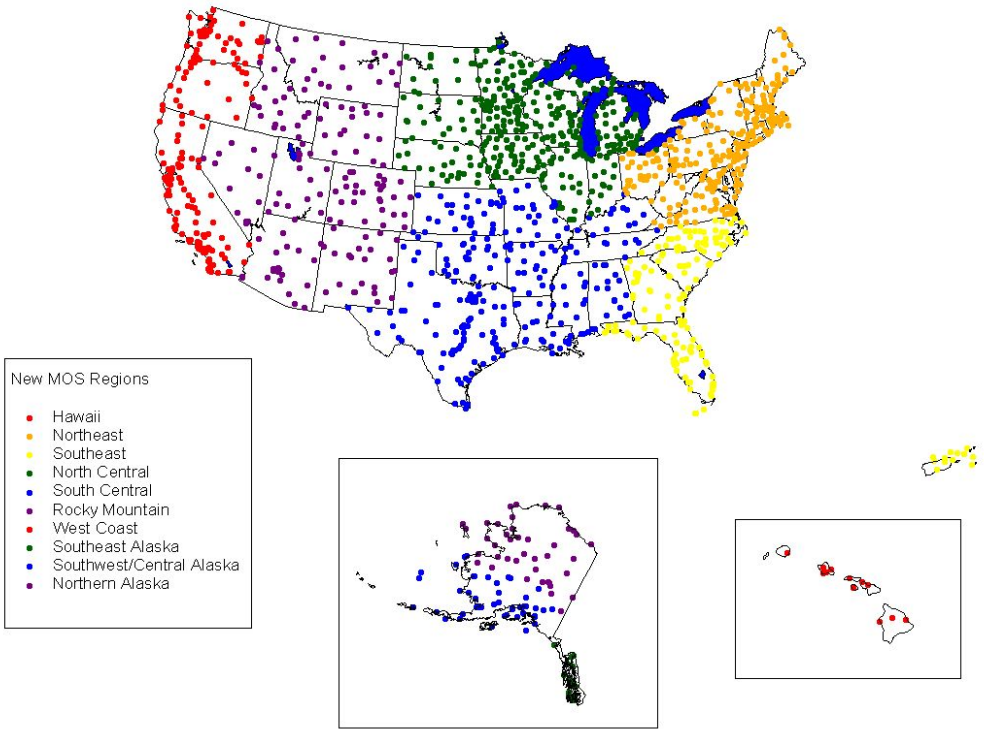

Figure 3-4: Short-range GFS and Eta MOS Stations (MDL, 2004).

The MOS graphics website allows the user to select the pertinent forecast products and displays the requested information superimposed on a map of the United States, using different colors to indicate the probability levels of a thunderstorm occurring over a 40-kilometer grid box (depending on the resolution of the numerical forecasting model used to produce the forecast) during a specified six-hour interval (see Figure 3-5). While the graphical displays provide a sufficient overview of the weather probabilities, they lack the necessary details our modeling purposes. In addition to the graphical representation, there is a supporting text message for each site. Figure 3-6 displays the text message for Casa Grande, Arizona, during the same time interval as depicted in the graphical forecast in Figure 3-5. The row highlighted in red represents the six-hour thunderstorm probability with an ending time corresponding to the hour listed in line four of the text message. For example, there is a 32% chance of thunderstorm activity in Casa Grande from 1800Z, February 11, 2005, until 0000Z, February 12, 2005 (all times are measured from Coordinated Universal Time). Each text message from each MOS site contains a significant amount of probabilistic weather data for various types of weather phenomena. For instance, we can extract information with regard to snow, ceiling, temperature, precipitation, etc.

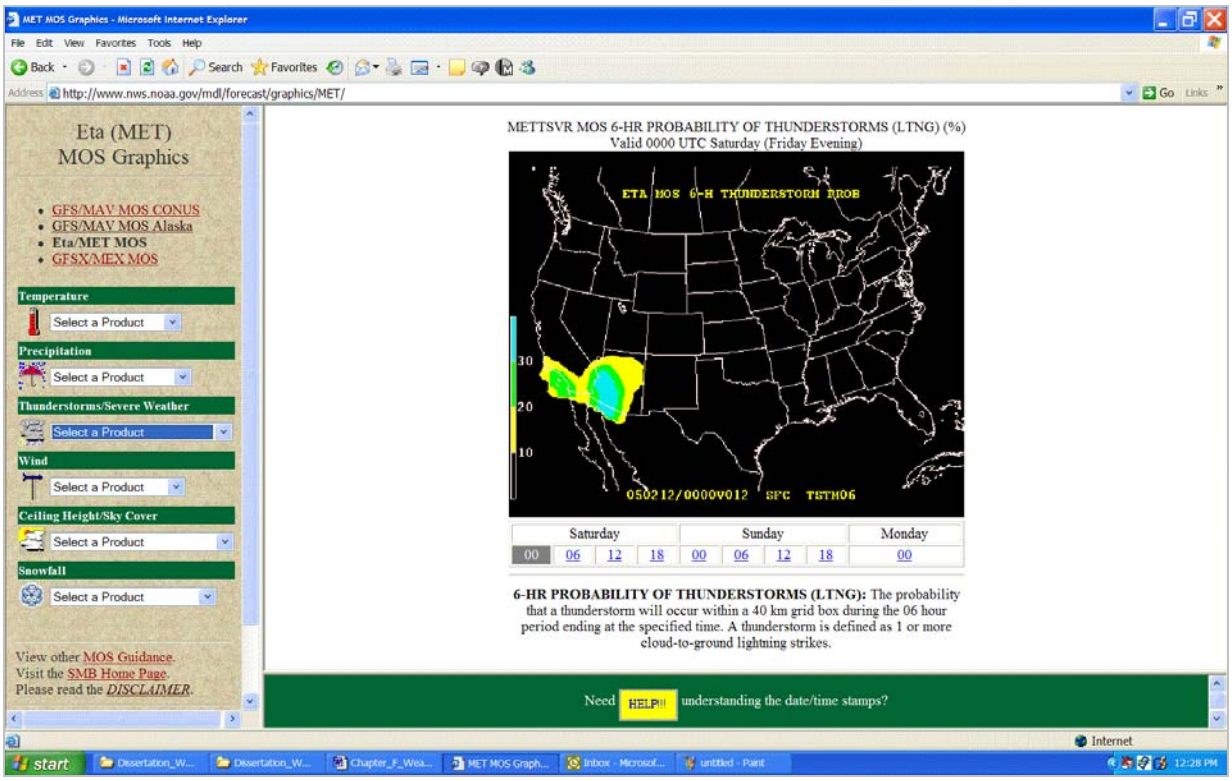

Figure 3-5: Eta MOS Graphics: Six-hour Probability of a Thunderstorm (NWS, 2005).

CASA GRANDE																					
KCGZ ETA MOS GUIDANCE																					
DT	/FEB	11/ FEB			12							/ FEB	13						/ FEB	14	
HR	18	21	00	03	06	09	12	15	18	21	00	03	06	09	12	15	18	21	00	06	12
N/X							52				64				45				67		46
TMP	58	62	61	59	57	55	54	52	58	63	62	56	52	49	47	48	60	65	65	53	48
DPT	54	55	56	56	55	54	51	49	49	47	45	46	42	41	40	43	47	45	43	48	46
CLD	OV	OV	OV	OV	OV	OV	OV	OV	OV	OV	OV	OV	OV	OV	OV	OV	OV	BK	BK	BK	BK
WDR	9	12	6	4	2	10	17	23	21	23	29	28	1	4	2	0	8	30	32	2	2
WSP	10	7	5	4	2	3	2	4	7	6	6	1	1	1	1	0	3	3	4	1	1
P06			83		83		73		38		41		21		4		5		1	1	1
P12							84				65				22				5		1
Q06			3		4		3		1		1		0		0		0		0	0	0
Q12							4				2				0				0		0
T06			32/0		38/0		24/0		16/0		15/0		10/0		2/0		0/0		2/1	999/99	
T12					46/0				39/0				18/0				2/0		999/99		
SNW							0								0						0
CIG	6	5	6	6	6	6	7	6	6	6	6	6	6	6	5	6	7	7	8	8	8

Figure 3-6: Example of an Eta MOS Text File.

We will revisit the information contained in the site-specific MOS text messages throughout the development of our modeling approach. Note that the data provided is based on discrete time intervals of three or six hours, depending upon the forecast product. This fact lends itself to the development of our discrete time probability-nets, which will maintain the tractability of the weather-based formulations within the APCDM model. We will then examine

the flight trajectories in 4-D (specified by latitude, longitude, altitude, and time), in light of the dynamically varying probability-nets.

3.3. Modeling Approach

Consider the analogy of a salmon swimming upstream, assuming that it instinctively selects a route that minimizes the travel distance in the stream, while being also aware of the scattered number of fishing nets present in the stream. Therefore, as the salmon proceeds, the probability of being caught in a fishing net increases with the number of nets that are in close proximity to the salmon. In addition, the catch-probability increases proportionately to the net size and its relative location with respect to the net. We now translate this analogy to that of flight trajectories. When generating flight surrogates under perfect weather conditions, the airlines are free to focus on optimized trajectories between the origin and destination airports and the related arrival times. Under conditions of weather uncertainty, there exists a range of probabilities with which the flight plans might be "caught" in a specific weather phenomenon, thereby resulting in a delay. The number of weather systems is analogous to the number of nets in the stream, whereas the intensity and coverage of the weather system are analogous to the size of the nets.

We will illustrate the construction of a convective probability-net with an example using data taken from February 7, 2005. Figure 3-7 is the graphical representation of an Eta MOS six-hour thunderstorm probability, which depicts the location probabilities associated with two convective weather systems covering the interval from 1800Z until 0000Z. This representation clearly provides more detail when compared with the results from the CCFP in Figure 3-2. Note that the probabilities range from zero to thirty percent with probability contour intervals of ten percent (i.e., a reading of 37% would be represented within the blue color interval). Relating this situation back to the salmon analogy, the stream has two nets varying in both size and intensity.

To capture the probability data associated with the convective weather vicinity over Louisiana, Mississippi, Arkansas, and Eastern Texas, we imported the relative text data from 82 MOS reporting stations. The 82 stations included all of the available reporting sites in Louisiana, Mississippi, and Arkansas. A key characteristic of the MOS text data is the availability of specific severe weather probabilities, in contrast to the ten percent contour intervals found in the

graphical representation. An important step was to compare the text data with the visual information displayed in the map (see Figure 3-7). This step is critical in order to construct the suitable convective probability-nets using the reporting sites. Figure 3-8 depicts the location and the thunderstorm probability forecast for each station. Notice that when visually compared with the graphical representation of Figure 3-7, the probabilities specified at the reporting sites are equivalent and provide point-by-point probability readings, which we will use as the building blocks of the probability-net for this region.

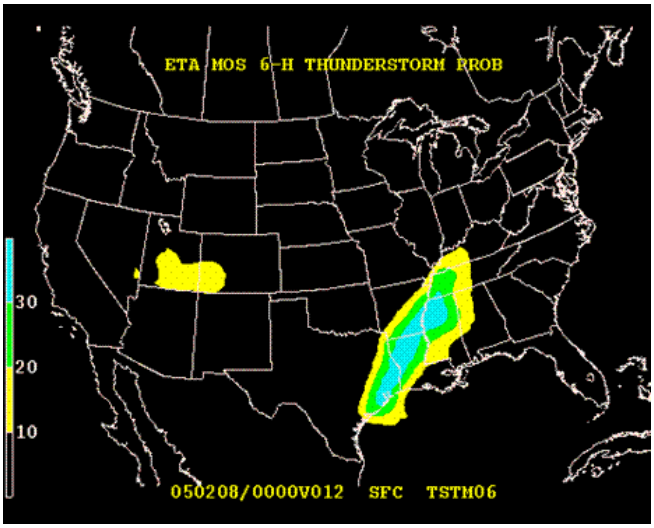

Figure 3-7: Eta MOS Six-hour Thunderstorm Probability for February 7, 2005.

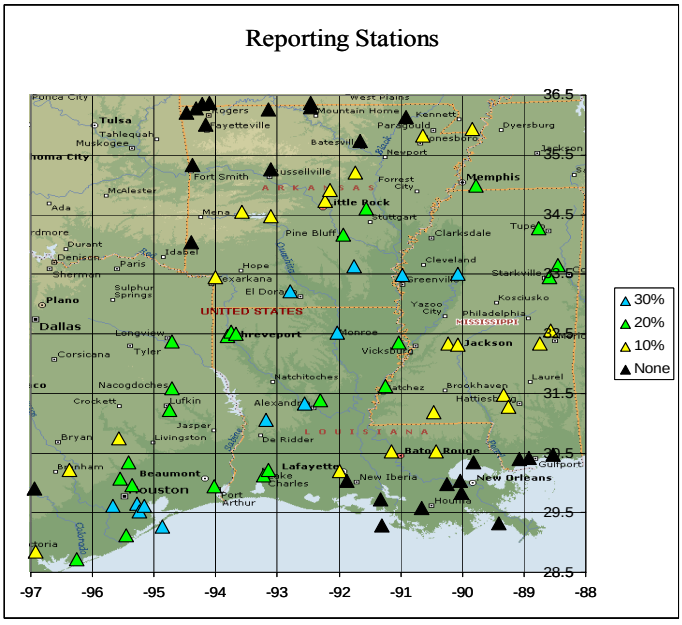

Figure 3-8: MOS Reporting Station Thunderstorm Probabilities.

The probability-nets are constructed by specifying an *adjacency threshold* that creates the strands that link the reporting site locations. Figure 3-9 illustrates an example of a probability-net constructed from the region shown in Figure 3-8. Every pair of reporting sites is linked by an edge, or a *strand*, as long as the great circle distance between the pair does not exceed the specified adjacency threshold. Naturally, we must be careful that the adjacency threshold is not too small so as to inadvertently create a "hole in the net" for an area in which there exists a significant weather probability, or too large making the probability-net unnecessarily dense. Additionally, reporting sites with a probability forecast of less than 5% are not linked to any other site, assuming that there would exist other reporting stations having a more significant convective weather probability in the relative vicinity of the most severe weather area(s). This will greatly reduce the number of computations required during the analysis of each flight plan.

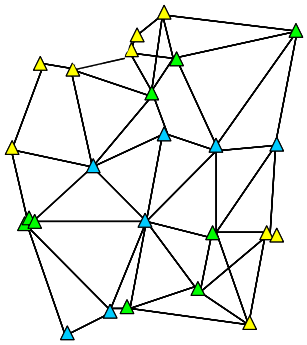

Figure 3-9: Graphical Representation of a Probability-Net.

While the reporting sites remain fixed, the data from the MOS text messages contain changing probabilities over time in six-hour increments for convective weather. Therefore, we must update the links within a probability-net every six hours to ensure that we account for the appropriate probabilities for the flight plans in question. Using the additional data from the text message, we are able to construct other weather-related probability-nets that influence airspace operations to include snow and visibility if required.

Before we continue with the application of our probability-net concept, we need to address two limitations regarding our modeling approach. The first limitation stems from the existing inaccuracies associated with the NWS current ceiling forecasts. NOAA (2005) recently reported that the ability to provide an accurate ceiling forecast remains a critical issue given that the current accuracy of aviation ceiling forecasts remains at 46% (unchanged from 2002). NOAA asserts that improvements to ceiling forecasts can result in an estimated $250 million

reduction in fuel costs for the airline industry. Given these known inaccuracies, the ceiling data ("CIG" in Figure 3-6) provided by the MOS reporting stations is categorized into altitude intervals as shown in Table 3-1. Therefore, while aircraft continuously traverse three-dimensional space, the categorical ceiling data will inherently reduce the efficiency of the flight trajectories, which are generated assuming that the weather ceiling extends to the upper limit of the interval. The second limitation stems from the location and spread of the MOS reporting stations. Apparent in Figure 3-8 is the clustering of MOS sites in some locations such as major cities, while other areas have relatively fewer reporting stations covering a larger area. The minimum distance from any station to the other stations varies from 2.2 km (two separate reporting sites in Olathe, KS) to 168.9 km (Havre to Great Falls, MT). Therefore, we will be required to interpolate probabilities between adjacent reporting stations that vary dramatically in their respective reporting values.

Table 3-1: Ceiling Height Categories.

Category	Ceiling
1	< 200 feet
2	200 - 400 feet
3	500 - 900 feet
4	1,000 - 1,900 feet
5	2,000 - 3,000 feet
6	3,100 - 6,500 feet
7	6,600 - 12,000 feet
8	> 12,000 feet or unlimited

3.4. Model Application

Once the respective probability-nets have been constructed, the weather uncertainty analysis is conducted by evaluating each surrogate flight plan as it potentially passes through the probability-net structures. Flight plans that avoid the existing probability-nets are not subject to a weather delay penalty and can be removed from this portion of the analysis using preprocessing methods. A flight plan that enters only one probability-net will be assigned an *exit probability* (EP) based upon the highest probability strand it encounters while being "caught" in the net. Flight plans that encounter more than one probability-net will be assigned a probability based upon an accumulated probability rating across all nets.

We begin with the evaluation of multiple flight plans through a single probability-net as depicted in Figure 3-10. The figure is a simple illustration that represents two alternative flight

plans (#1 and #2) for a single flight as they traverse through a single probability-net. The triangles are the MOS reporting sites and the line segments A through D are the strands that link the reporting sites as a function of the adjacency threshold. For this example, the displayed values at each reporting station are the six-hour thunderstorm probabilities. As previously stated, the overall probability used to determine the delay penalty is based on the highest probability strand that the flight plan intersects, which we call the exit probability, *EP*. In this example, flight plan #1 intersects only strand A while flight plan #2 intersects both strands B and C.

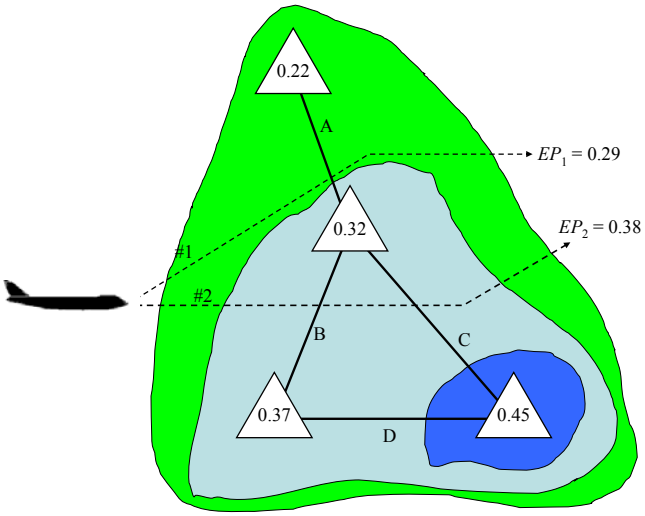

Figure 3-10: Example of Single Probability-Net Evaluation.

The discrete representation of the probability data lends itself to a subjective assignment of probability values at the point of intersection between the flight plan and the strand of interest, referred to as the *strand intersection probability value* (SIPV) approach throughout the remainder of the dissertation. We consider three SIPV approaches. The first approach calculates the probability through a linear interpolation between the two reporting stations' probabilities, as done in Figure 3-10. For example, suppose that flight plan #1 is 1 kilometer from the reporting station having a probability value of 0.32 and 3 kilometers from the station having a probability value of 0.22. The overall probability assigned to the strand at the point of intersection, using a standard linear interpolation equation, is $EP_1 = 0.295$. The second approach provides an upper bound on the probability assignment by using the larger probability of the two reporting stations at which the intersected strand is incident. Likewise, the third approach provides a lower bound on the probability assignment by using the smaller probability of the two reporting stations. The second and third SIPV approaches provide worst-case and best-case scenarios, respectively, in

our weather uncertainty analysis. In Chapter 4, we will discuss how the exit probability is used to calculate the weather delay factor for integration within the APCDM model objective function.

A condition may also exist in which a flight plan encounters multiple probability-nets. Figure 3-11 is a simple illustration of this event in which two probability-nets, separated by at least 300 kilometers (figure not to scale), are encountered by the submitted flight plan. Again, our goal is to calculate the exit probability as the flight exits the second (final) system. We start by calculating the exit probabilities for each net as described above. Using the individual exit probabilities, we then calculate the total probability of traversing both systems without experiencing a weather delay assuming independence between the two systems. The final exit probability is the compliment of the total probability of not experiencing a delay. For example, suppose that the exit probabilities for the probability-nets are 0.45 and 0.26, respectively, using the upper bound SIPV approach. The exit probability, *EP*, for the combined system is then computed as $EP = 1 - (1 - 0.45) * (1 - 0.26) = 0.593$. In general, the exit probability for a single flight plan encountering $n \geq 1$ probability net(s) is computed as follows:

$$EP = 1 - \prod_{i=1}^{n} \left(1 - EP_i^{SIPV}\right), \tag{3.1}$$

where EP_i^{SIPV} is the exit probability for probability-net *i* using the specified SIPV approach.

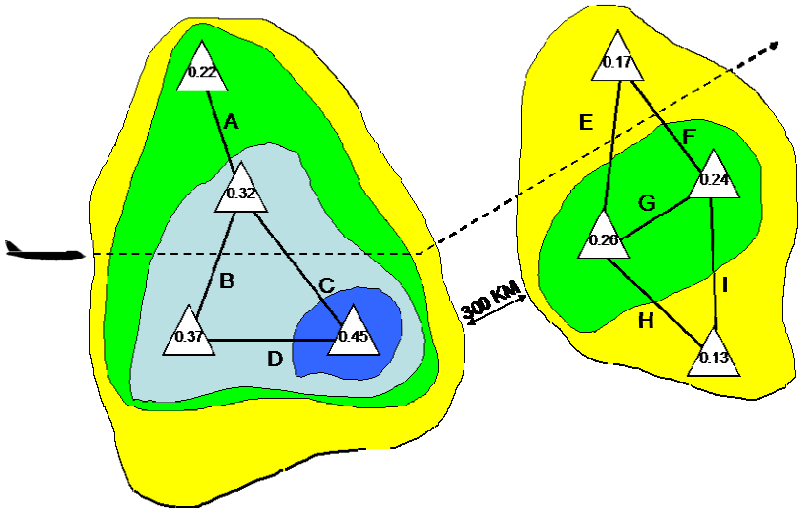

Figure 3-11: Example of Multiple Probability-Nets.

During the construction of the probability-nets, the specification of the adjacency threshold may generate a strand that, on the surface, appears to skew the probabilistic

representation based on the positional relationship between reporting sites. For example, Figure 3-12 depicts the situation where strands A, B, and C are generated between three reporting sites within the adjacency threshold from one site to the other. Using an upper bound SIPV approach, the flight trajectory for Plan #1 would incur a probability penalty associated with the reporting site value of 0.48. If the angle θ between strands B and C is relatively small, a more appropriate probability penalty might be that associated with the reporting site value of 0.32. In this instance, one might consider omitting strand C during the construction of the probability-net. However, given our intent to include a linear interpolation SIPV approach, we demonstrate, as illustrated by Plan #2 in Figure 3-12, how the omission of strand C can produce an inaccurate exit probability with respect to two separate flight paths for a given flight. Assuming strands A, B, and, C have lengths of 50, 31, and 80 kilometers, respectively, and determining the intercept point on strands A and C as the distance from the point of intercept on the respective strands to the reporting station having the probability value of 0.22, the exit probabilities for each plan can be determined as shown in Figure 3-12. Notice that the omission of strand C would result in the same exit probability for both plans, which might be misleading. This example also underscores the efficacy of relying on the linear interpolation SIPV approach.

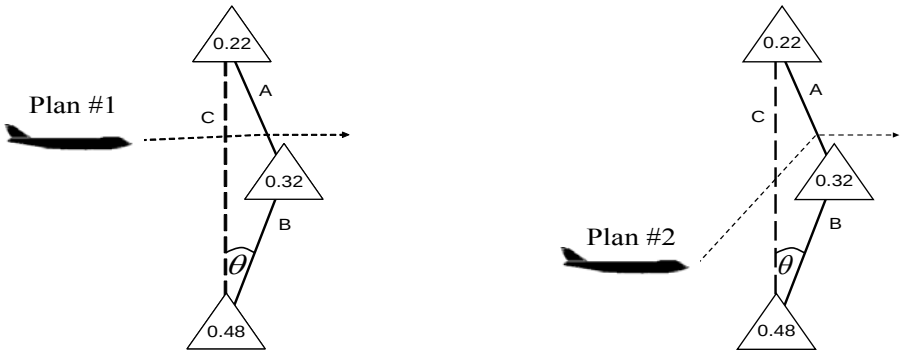

Flight Plan	Intercept Point on Strand C	Intercept Point on Strand A	Exit Probability
Plan #1	15 km	35 km	0.29 (Strand A)
Plan #2	40 km	35 km	0.35 (Strand C)

Figure 3-12: Exit Probability of Multiple Plans.

Once we have established the exit probability for each flight plan p belonging to some set P_f of alternative plans for each flight $f = 1,...,F$, the final step of our modeling approach is to generate an appropriate weather delay factor for inclusion within the APCDM model that will

influence the cost of the specific flight plan c_{fp}. The original APCDM cost function is as follows (Sherali et al., 2006):

$$c_{fp} = F_{fp} + D_{fp}\ ,\ \forall p \in P_f, f=1,\ldots,F, \tag{3.2}$$

where F_{fp} and D_{fp} are, respectively, the associated fuel and delay costs. We will focus primarily on a proposed modification to the delay cost. The original APCDM delay cost is as follows (Sherali et al., 2006):

$$D_{fp} = \left(t_{fp}^{d} d_{f}^{c}\right)\left(l_{f}\right)\left(\delta\right), \tag{3.3}$$

where t_{fp}^{d} is the arrival delay time, d_{f}^{c} is a connection delay cost factor associated with the arrival airport, l_f is the load factor for the particular aircraft type, and δ is the average delay cost per passenger-minute. We will penalize the arrival delay time t_{fp}^{d} by an additive (or multiplicative) weather delay factor t_{fp}^{w} to be determined in the following chapter. The weather delay factor must adequately reflect the effect of the probability of encountering severe weather or delay.

3.5. Flight Plan Generation Tool

In this section, we discuss the superimposition of a flight-trajectory-grid network onto the probability-nets in order to facilitate generating flight plans that are within a specified threshold of circumventing severe weather. The ADDS website (2005) contains a flight path generation java tool that allows the user to plot a flight path using point-and-click waypoint and altitude selections from origin to destination. The flight path is superimposed upon user-selected backgrounds that provide three-dimensional weather data in terms of icing likelihood, temperature, wind speed, relative humidity, and the potential for turbulence. While suitable for tactical level flight planning, its three-hour time horizon renders this tool irrelevant when addressing the impact of weather uncertainty beyond three hours, which is the typical time horizon for a strategic level analysis.

Using our probability-nets, we ascribe a *threshold strand probability* σ and impose the constraint that the trajectory generated should not intersect any strand at a probability level exceeding σ. Using the linear interpolation SIPV approach and a specified threshold strand probability, we can identify which portion of a strand will exclude links in the network for flight

plan generation. For example, given $\sigma = 0.2$ and the strand with its associated probabilities as depicted in Figure 3-13, links that intersect within the dotted area are admissible for consideration in the network, whereas those links that intersect the strand within the brick area are excluded from the network. Flight plans that are generated using this tool satisfy a specified minimal threshold safety level and, as prescribed earlier, are then assigned a weather delay factor based upon their expected delay times, which are in turn applied within the APCDM.

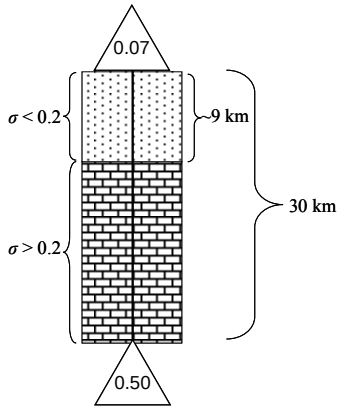

Figure 3-13: Example of the Admissible Portion of a Probability Strand.

For illustrative purposes, Figure 3-14 shows an en route air chart for the Salt Lake City area. Superimposed on the air chart are the six MOS reporting sites (linked by an adjacency threshold) that are near Salt Lake City. Given an instance when the probability on strand A exceeds σ (using the linear interpolation SIPV approach), the two flight routes that intersect strand A would be restricted from inclusion in a flight plan. With respect to APCDM, if all the flight plans submitted for flight *f* contain a trajectory link that intersects a strand exceeding σ, the only remaining flight plan within the surrogate that would be selected is the cancellation plan if offered by the airline.

Figure 3-14: Air Chart with Corresponding MOS Reporting Sites.

3.6. Probability-Net Refinement

Two critical components within the construction of the probability-nets are the selection of the adjacency threshold and relative strand probabilities. Each will have an impact on the resulting weather delay factor, which is a function of the flight plan exit probability. The accuracy of the probability-nets is also dependent upon the number of reporting sites used as the linkage points. Inclusion of all MOS reporting stations will generate the most refined probability-nets possible. A reduction in the number of reporting stations used will undoubtedly decrease the computational effort required, but at a price in terms of accuracy. We inherit another problem when reducing the number of reporting stations in that we cannot afford to indiscriminately select the reporting sites to remove. The haphazard removal of reporting sites could denigrate the model's effectiveness, potentially allowing the selection of poor flight plans that have a higher likelihood of experiencing severe weather. Therefore, given the latitude and longitude of each MOS reporting site, we propose the application of a *k*-means cluster algorithm to reduce the number of sites, as depicted in Figure 3-15 for Florida where we reduced the number of links from 59 to 15. The centroid of each cluster becomes a reporting *faux-site*. The probability associated with the faux-site is determined by either averaging the probabilities of each reporting site located within the cluster or by assigning the highest probability within the cluster to the faux-site. By specifying the number of clusters, we can create various levels of refinement. We will illustrate the economic benefits associated with various probability-net refinement levels, from a very coarse representation to the maximum refined level (inclusion of all MOS reporting sites), using cluster analysis. The next chapter provides details for flight generation, delay estimation, and economic impact analysis, along with computational results using the different weather-related modeling constructs proposed herein.

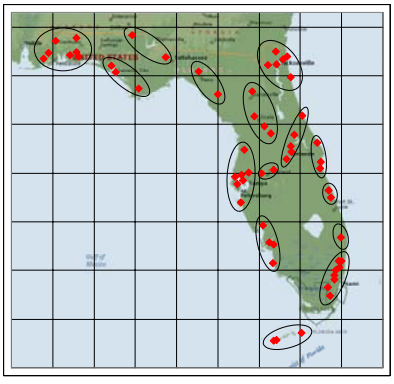

Figure 3-15: Example of Reporting Site Clusters (k = 15).

Chapter 4

Flight Generation, Probabilistic Delay Estimation, and Economic Impact Using the Proposed Weather-Based Models

In this chapter, we perform experiments to evaluate our probability-net concept and its application in support of the weather-induced decision-making process. We start by evaluating the retrieval of the essential probability data along with the characteristics of various probability-nets by altering adjacency thresholds and applying our three SIPV approaches. Second, we examine the utilization of our probability-nets as a flight-plan-generation tool. Third, we provide a probabilistic analysis to derive weather delay factors for inclusion within the APCDM model and its sub-modules. We conclude with an assessment of the economic impact of various probability-net refinements using a *k*-means cluster analysis approach. Additionally, we provide an alternative economic impact assessment using decision theory techniques. The test cases for our computational experiments were constructed using real data based on the Enhanced Traffic Management System (ETMS) flight data information. Our weather scenarios were derived from the Model Output Statistics (MOS) forecast data provided by the National Weather Service. All reported computations have been performed on a Dell Inspiron 8500 laptop computer equipped with a 2.0 GHz Pentium 4 processor and 256 Mb Random Access Memory, and running the Microsoft Windows XP operating system.

With our focus on the Continental United States (CONUS), we used probabilistic weather data from 1,395 MOS reporting sites and excluded those sites located in Hawaii, Alaska, the Western Pacific Islands (Guam, Saipan, etc.) , and the Mid Atlantic (Cuba, Puerto Rico, and the Virgin Islands). Using an initial adjacency threshold of 50 kilometers, the computational time required to extract the essential weather data (inclusive of time intervals and ceiling data) from all reporting sites, along with the time required to determine adjacency relationships between all reporting site pairs, was a mere 8.271 cpu seconds. Of the 1,395 reporting sites, 73% have at least one adjacent site within 50 km, whereas 97% have a least one adjacent site within 100 km. An increase in the adjacency threshold would obviously generate a denser probability-net, which in turn would increase the number of computations required as a flight traverses the airspace. Figure 4-1 depicts two separate probability-nets with adjacency thresholds of (a) 100-km and (b) 150-km, respectively. By increasing the threshold by only 50 kilometers, we greatly increase the

number of strands along with the required number of computations. For illustrative purposes, we constructed the probability-nets in Figure 4-1 using all the CONUS reporting stations. During our analysis of the flight plans, the probability-nets will contain only those reporting stations having an associated probability value exceeding 0.05.

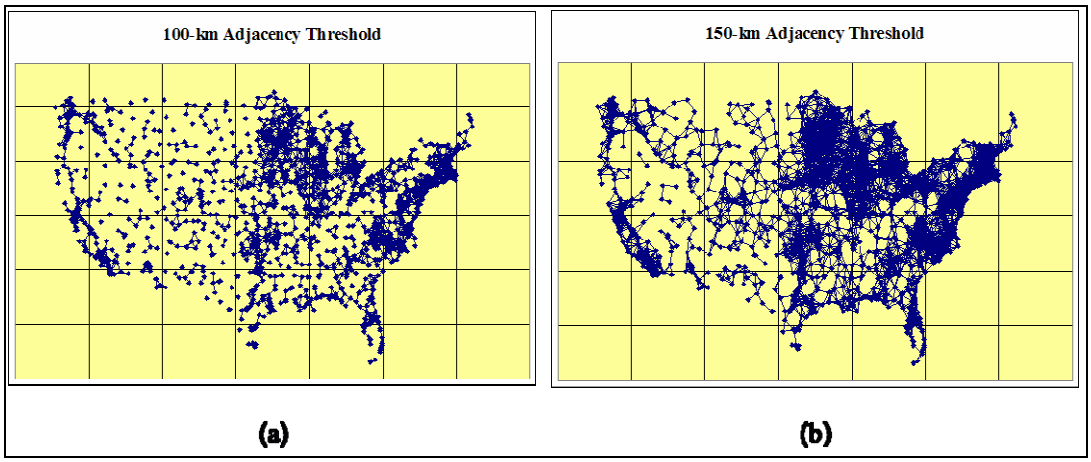

Figure 4-1: Probability-Nets with 100-km and 150-km Adjacency Thresholds.

4.1. Extracting Exit Probabilities for Test Sets 1 and 2

To gain a perspective on the probabilistic weather impact, we used the first two test sets in Table 4-1 from Sherali et al. (2006). Using the first test set, comprised of 180 flight plans (six flight plans each for 30 flights), we evaluated the efficiency of our algorithm by varying both the adjacency threshold and the three SIPV approaches defined in Chapter 3. We selected a particular MOS data set guaranteeing that a portion of the flight plans in Test Sets 1 and 2 would intersect the constructed probability-nets. Table 4-2 presents the detailed computational results for Test Set 1. In addition to the computational effort required to extract the exit probabilities, Table 4-2 provides the results for the maximum exit probability computed over all the flight plans for each SIPV approach and the number of flights that have an exit probability greater than 0.50.

Notice that the maximum probabilities associated with the 50 km adjacency threshold are significantly higher than the maximum probabilities for the other adjacency thresholds. This is a result of the density of the probability-net. As mentioned earlier, only 73% of all MOS reporting stations have at least one adjacent site within 50 km. Consequently, a particular region of the 50-km probability-net became strand-free, and a flight traversing this region perceived the weather situation as one represented by multiple probability-nets instead of a single one. Hence, the algorithm generated a correspondingly higher exit probability for all three SIPV approaches.

This particular probability-net phenomenon was not encountered using adjacency thresholds of 100 km or more. Therefore, all future probability-nets will have an adjacency threshold of at least 100 km.

Table 4-1: Test Data Sets for Evaluating Convective Probability-Nets.

	Test Set 1	Test Set 2
Number of Flights	30	80
Surrogates per Flight	6	6
Centers	ZMA/ZJX	ZMA/ZJX
Number of Airlines	5	5
Airlines: Flights per Airline	AAL: 10	AAL: 18
	ABX/ACA/AMT: 5	ABX/ACA/AMT: 5
	CAA: 7	CAA: 7
	COA: 3	COA: 25
	DAL: 5	DAL: 25

Table 4-2: Adjacency Threshold and SIPV Approach Results for Test Set 1.

		SIPV Approach			
Adjacency Threshold	Measures	Lower Bound	Upper Bound	Linear Interpolation	Time (cpu seconds)
50 km	Max Prob: # Plans > 0.5:	0.657 20	0.668 20	0.657 20	173.14
100 km	Max Prob: # Plans > 0.5:	0.495 0	0.584 18	0.517 14	174.76
150 km	Max Prob: # Plans > 0.5:	0.428 0	0.577 17	0.509 6	177.42
200 km	Max Prob: # Plans > 0.5:	0.428 0	0.606 30	0.509 6	181.71
250 km	Max Prob: # Plans > 0.5:	0.428 0	0.606 42	0.509 6	186.18
300 km	Max Prob: # Plans > 0.5:	0.428 0	0.635 102	0.509 6	192.22

As we increased the adjacency threshold beyond 150 km for Test Set 1, the maximum probability values for the lower bound and linear interpolation SIPV approaches level off, whereas those for the upper bound method increased as indicated in Table 4-2. This increase is a function of the strand length. By increasing the adjacency threshold, we may include a probability-net strand that has a large probability associated with one of the endpoints (MOS reporting site) and, consequently, incur exit probabilities that exceed previously realized probabilities for smaller threshold distances. However, if the reporting site having the large probability value is relatively far from the flight trajectory, it should in reality have a minimal impact on the exit probability (see Figure 3-12). Therefore, we conclude that, while the upper and lower bound results provide added information, the linear interpolation method provides the most appropriate results for determining exit probabilities. The computational effort required for Test Set 2 (see Table 4-3) indicates that our proposed algorithm can generate probability-nets

and flight related exit probabilities in a sufficiently timely fashion to support strategic level flight planning.

Table 4-3: Computational Effort for Test Set 2.

Adjacency Threshold	Time (cpu seconds)
100 km	435.79
150 km	441.42
200 km	452.7
250 km	461.27
300 km	469.2

4.2. Superimposition of a Flight-trajectory-grid Network

As detailed in Section 3.5, we can generate flight plans that are within a specified threshold of circumventing severe weather by superimposing a flight-trajectory-grid network onto the probability-nets. We constructed our initial flight-trajectory-grid network using the U.S. Navigational Aids (Navaids) consisting of 2710 points as the network nodes. To reduce the computational effort required to generate the time-dependent shortest path between a pair of origin (*O*) and destination (*D*) airports, we then curtailed the size of the network under construction based on the Ellipsoidal Region Technique developed by Sherali, Hobeika, and Kangwalklai (2003). Unlike their technique, which involves multiple ellipsoidal regions for assessing various elements of ground transportation, we need to consider only one ellipsoidal region that represents a natural widening of the airspace as the aircraft departs from *O* followed by a natural decrease of the airspace as the aircraft approaches *D* (see Figure 4-2). The length of the major axis of our ellipsoidal region is taken as $\gamma\|OD\|$, where $\gamma > 1$ and $\|OD\|$ is the great circle distance from *O* to *D*. The curtailed network nodes would then consist of all Navaids (*NA*) within the closed ellipsoidal region. The arcs between the nodes represent feasible flight segments and are labeled with the distances between the Navaids using the great circle distance [*]formula since each Navaid point is identified by its longitude and latitude. Temporary flight

[*] Let (ϕ_1, λ_1) and (ϕ_2, λ_2) be the (latitude, longitude) vectors for two locations, respectively. If *r* is the great-circle radius of the sphere, then the great circle distance is $r\theta$, where θ is calculated by (see Wikipedia, 2006, for example):

$$\theta = \arctan\left\{\frac{\sqrt{[\cos\phi_2 \sin(\lambda_2 - \lambda_1)]^2 + [\cos\phi_1 \sin\phi_2 - \sin\phi_1 \cos\phi_2 \cos(\lambda_2 - \lambda_1)]^2}}{\sin\phi_1 \sin\phi_2 + \cos\phi_1 \cos\phi_2 \cos(\lambda_2 - \lambda_1)}\right\}.$$

restrictions such as Special Use Airspaces (SUA) and over-water flights can be accommodated by removing the arcs in our curtailed network that intersect the boundaries of the restricted areas.

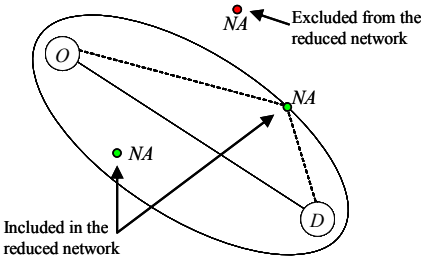

Figure 4-2: Ellipsoidal Region.

To illustrate the generation of a flight plan in the presence of multiple probability-nets, we selected a flight from Seattle to Miami departing at 0800 hours on April 17, 2005. We constructed a flight-trajectory-grid network using an ellipsoidal region specified by $\gamma = 1.25$ (as prescribed by Sherali et al. (2003) based on their extensive experiments). Using the MOS data corresponding to the flight departure date and time, we then constructed two severe weather probability-nets that are intersected by the weather-independent shortest path from Seattle to Miami (4,378 km). As indicated in Figure 4-3, when specifying a threshold strand probability of $\sigma = 0.15$, the shortest path from Seattle to Miami increases (to 4,427 km) as the flight route circumvents the strands having intersection probabilities exceeding σ. As expected, the shortest path continues to increase in distance as we further reduce σ. Note that the time-dependent shortest path algorithm considers the fact that both the location and structure of the probability-nets are time-varying. For example, if the Seattle to Miami flight departed twelve hours later, the time-dependent shortest path would coincide with the weather-independent shortest path as the predicted severe weather veers to the northeast.

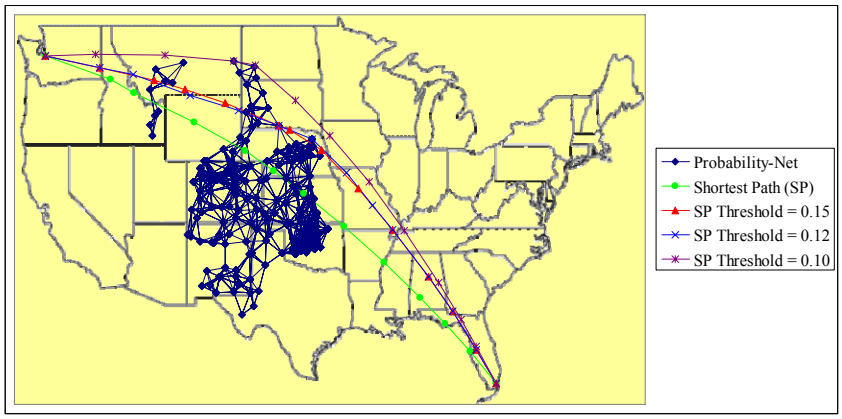

Figure 4-3: Flight Trajectories Relative to Strand Thresholds.

4.3. Incorporating Weather Delay Factors within APCDM

In order to demonstrate the potential benefits of our probability-net concept, we need to generate suitable delays as a function of (a) the exit probability, EP_{fp}, for plan p of flight f and/or (b) the threshold strand probability σ. The most significant challenge in generating appropriate weather delay factors for inclusion within the APCDM model is in determining a relationship between forecasted probabilities and the actual airport delays resulting from realized severe weather. While no historical data exists that relates probabilistic severe-weather encounters to actual airport delays, the FAA does maintain historical weather delay data records within the Aviation Service Quality Performance (ASQP) and the Aviation System Performance Metrics-Complete (ASPM-Complete) databases for 75 major airports, extending as far back as January 1, 2000 (FAA, 2006). From this data, we can extract daily, monthly, and yearly average delays (minutes) for arriving aircraft as a function of the *impact* from en-route thunderstorm activity, where ASQP and ASPM-Complete define impact as a categorical variable specified by $impact \in$ (None, Minor, Moderate, Severe). This categorical value is related to the number and intensity of the storm(s) encountered throughout the flight trajectory as reported by up to five Air Transportation Oversight System (ATOS) stations (FAA, 2006).

Initially, we considered a rather simple approach in which we could partition the range of exit probabilities to match the four categorical impact values. Using six years of historical data for the destination airport, this would enable us to compute the average delay in minutes for each impact value. Given any flight plan, we could then determine the exit probability and, subsequently, output the average delay in minutes as a function of the impact value associated with the exit probability. This approach, however, has two significant drawbacks. First, note that the delay data acquired from the ASQP and the ASPM-Complete databases is not likely to be purely weather-based, in that it involves other airline-related factors such as equipment, crew, and departure slot availabilities. Second, this approach maintains the status quo in terms of historical average delay in minutes based on a wide impact category specification and, thus, would mask the relevant detailed information available via our probability-net concept. Accordingly, we propose a more in-depth procedure that accommodates the concepts developed above regarding exit probabilities and flight plan generation using the ellipsoidal region technique, based on a specified threshold strand probability σ.

To motivate this procedure, we generated four flight plans as a function of different threshold strand probabilities σ for a single flight from Albany (ALB) to Las Vegas (LAS) scheduled to depart at 1930Z (1530 EDT) on April 18, 2005. The aircraft type for this example is a B737-700 with an economical cruising speed of 850 km/h (Boeing, 2006). Figures 4-4(a) and 4-4(b) respectively depict the probability-nets for convective weather at various probability intervals, and the four resulting flight routes using different threshold probabilities. In the absence of severe weather, the arrival time associated with the shortest path (3591.5 km) is estimated at 0001Z on April 19 (1701 PDT, April 18) using the ASPM-Complete historical data, which also corresponds to the departure and arrival times listed in the OAG. When we superimposed the flight-trajectory-grid network onto our probability-nets and generated a flight plan based upon a small value for the threshold strand probability ($\sigma = \varepsilon$), where $\varepsilon = 0.01$ for this example, the resulting time-dependent shortest path increased the total distance to 4106.3 km (an increase of 514.8 km). Historical records for the past month indicate that the average ground speed for this route (east-west route) is approximately 650 km/h due to atmospheric effects (FlightAware, 2006). Therefore, using this average ground speed as opposed to the economical cruising speed, the ε-threshold delay is computed as 47.52 minutes. We will address the other time-dependent shortest paths that are displayed in Figure 4-4(b) for $\sigma = 0.20$ and $\sigma = 0.30$ later in this section.

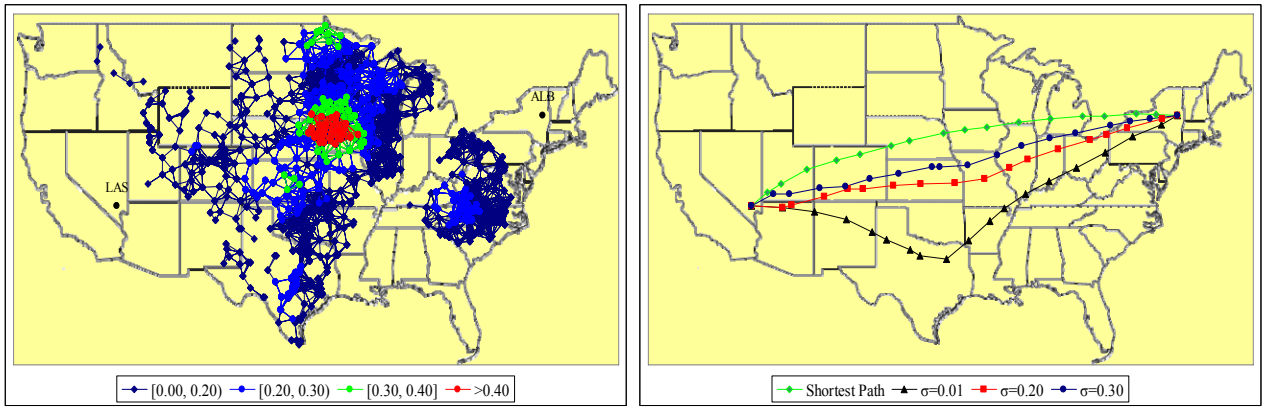

(a) (b)

Figure 4-4: Albany to Las Vegas Example.

As illustrated in the previous example, when generating flight plans using a threshold strand probability σ, we are capturing delays and trajectory times in a probabilistic sense. For

instances in which a GDP is executed, there is an arrival slot for a particular flight plan and the associated departure time is determined by tracing the trajectories back to the corresponding origin. So, while the delay is based on that slot time, its value holds with a probability of $(1-\sigma)$, which is the probability with which severe weather is circumvented. For non-GDP (non-slot-based) flights, our approach in APCDM considers different alternative departure and arrival times, and for each case, it generates a path through the probability-nets as above to obtain a delay having an estimated probability of $(1-\sigma)$.

Suppose that for some flight *f*, we have delays d_1 and d_2 (resulting from increased flight plan distances) using threshold probabilities of σ and ε, respectively, as depicted in Figure 4-5.

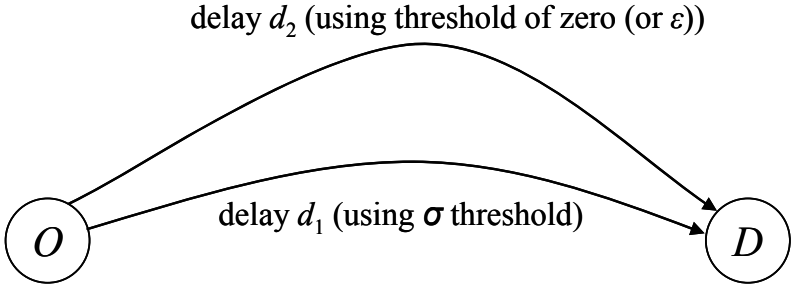

Figure 4-5: Illustration of Delay as a Function of σ.

Hence, we can estimate that the delay for the planned flight trajectory *p* will be d_1 with probability $(1-\sigma)$, and the delay will be greater than d_1 with probability σ. Assuming in the latter case that the delay is uniformly distributed between d_1 and d_2, given that d_2 is generated with a near-zero threshold probability, we obtain a delay distribution function as depicted in Figure 4-6.

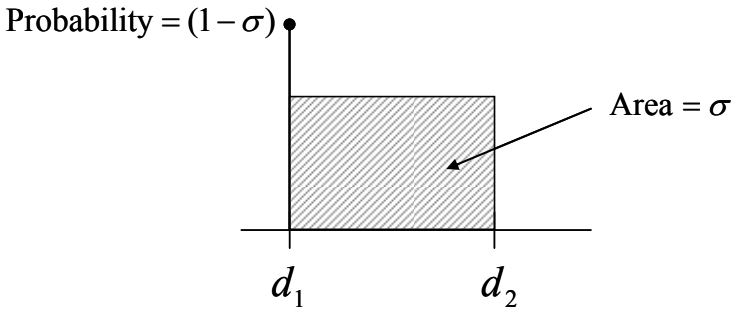

Figure 4-6: Delay Distribution.

We can then determine the *expected weather delay*, t_{fp}^{EWD}, for plan *p* of flight *f* as a function of d_1 and d_2 as defined by:

$$t_{fp}^{EWD} = (1-\sigma)d_1 + \sigma\left(\frac{d_1+d_2}{2}\right) = \left(1-\frac{\sigma}{2}\right)d_1 + \frac{\sigma}{2}d_2, \tag{4.1}$$

and include this expected weather delay within the delay cost D_{fp} in the original APCDM model, as explained in the sequel.

We could refine this computation somewhat further by considering an intermediate threshold value σ', where $\varepsilon < \sigma' < \sigma$, and determining the corresponding delay d' with respect to σ'. In this case, we can then approximate the delay distribution by a two-step function as depicted in Figure 4-7. Note that $P(\text{delay} \le d') = (1-\sigma')$, and as before, we have that $P(\text{delay} \le d_2) = 1$ and that the probability value $P(\text{delay} \le d_1) = (1-\sigma)$ is assumed concentrated on d_1.

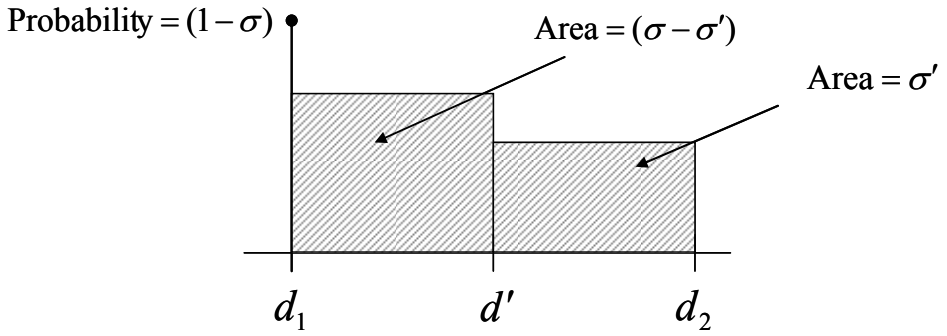

Figure 4-7: Two-step Distribution Function.

Accordingly, the *expected weather delay* can be computed as:

$$t_{fp}^{EWD} = (1-\sigma)d_1 + (\sigma-\sigma')\frac{(d_1+d')}{2} + \sigma'\frac{(d'+d_2)}{2}, \tag{4.2}$$

which can then be incorporated within the delay cost D_{fp} of APCDM as discussed below. Note that when either $\sigma' = \sigma$ (whence $d' = d_1$) or $\sigma' = 0$ (whence $d' = d_2$), Equation (4.2) coincides with Equation (4.1), as it should.

Returning to the ALB-LAS example, flight plans generated using threshold strand probabilities of $\sigma = 0.30$ and $\sigma' = 0.20$ increased the total flight distance by 51.2 km and 103.4 km, respectively, when compared to the weather-independent shortest path. Using the average ground speed of the aircraft, the associated trajectory delays are approximately 4.73 and 9.54 minutes, respectively. Letting $d_1 = 4.73$, $d' = 9.54$, and $d_2 = 47.52$ minutes, the one-step

approximation yields $t_{fp}^{EWD} = 11.14$ via (4.1), whereas the two-step approximation results in $t_{fp}^{EWD} = 9.73$ minutes via (4.2). Note that by selecting σ' appropriately, one can better account for the long-tailed effect of the distribution, in contrast with the one-step approximation.

With increased computational effort, we could further refine our approximation of the delay distribution by utilizing a three-step function based on selecting another intermediate threshold value σ'', where $\varepsilon < \sigma'' < \sigma' < \sigma$, and determining the corresponding delay d'' with respect to σ'' (see Figure 4-8). Similar to the two-step approximation, note that for the present case we have $P(\text{delay} \le d') = (1-\sigma')$, $P(\text{delay} \le d'') = (1-\sigma'')$, $P(\text{delay} \le d_2) = 1$, and $P(\text{delay} = d_1) \equiv P(\text{delay} \le d_1) = (1-\sigma)$.

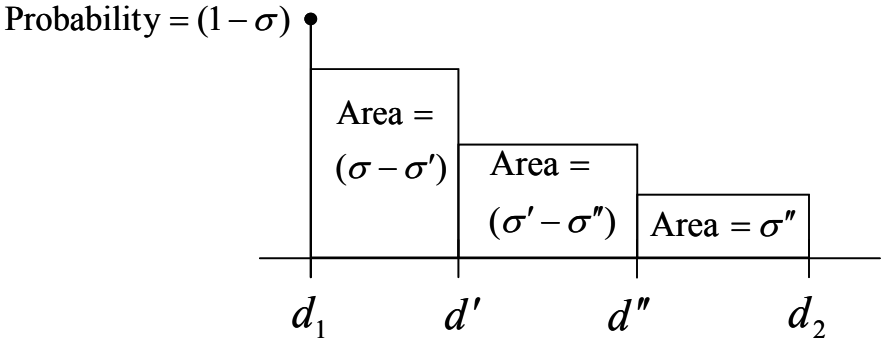

Figure 4-8: Three-step Distribution Function.

Likewise, the *expected weather delay* to be included within the delay cost D_{fp} of APCDM can be computed as:

$$t_{fp}^{EWD} = (1-\sigma)d_1 + (\sigma - \sigma')\frac{(d_1 + d')}{2} + (\sigma' - \sigma'')\frac{(d' + d'')}{2} + \sigma''\frac{(d'' + d_2)}{2}. \quad (4.3)$$

Continuing with our example, the delay for the threshold value $\sigma'' = 0.15$ is $d'' = 27.39$, which results in $t_{fp}^{EWD} = 10.56$ minutes using the three-step approximation. (Note that for this instance, the three-step approximation is not monotone decreasing as depicted generically in Figure 4-8, and provides a more reliable delay estimation based on recognizing this feature of the underlying distribution.)

Once we have obtained the expected weather delay, we can determine a weather delay factor for the given flight plan. The original APCDM model delay cost D_{fp} in (3.3) contains an

arrival delay time expressed as $t_{fp}^{d} = \max\{0, \tau_{fp} - \tau_{f}^{*}\}$, where τ_{f}^{*} is the originally scheduled arrival time of a given flight *f*, and τ_{fp} is the arrival time for a particular flight plan *p* of the flight *f*. Now let d_{fp}^{σ} be the trajectory delay pertaining to a particular flight plan *p* of *f* based on the threshold strand probability σ. This trajectory delay, as previously stated, is determined by calculating the time required to travel the additional distance in order to circumvent the severe weather. From our ALB-LAS example, $d_{fp}^{\sigma} = d_1$ for $\sigma = 0.30$. Since d_{fp}^{σ} is the delay associated strictly from the flight trajectory, it is already included in the arrival delay time t_{fp}^{d} based on the structure of our flight data sets. Therefore, to prevent from double counting the delay generated solely by the flight trajectory, we define the *weather delay factor* or *disruption factor*, t_{fp}^{w}, as follows:

$$t_{fp}^{w} = t_{fp}^{EWD} - d_{fp}^{\sigma}. \tag{4.4}$$

Note that we cannot just replace t_{fp}^{d} with t_{fp}^{EWD}, because t_{fp}^{d} may contain other delays associated with equipment, crews, etc. This weather related delay factor is then added to the arrival delay time t_{fp}^{d} in the delay cost D_{fp} in the original APCDM model yielding:

$$D_{fp} = \left(t_{fp}^{d} + t_{fp}^{w}\right)\left(d_{f}^{c}\right)\left(l_{f}\right)\left(\delta\right). \tag{4.5}$$

By generating flight plans based upon a given threshold strand probability σ, the two-step approximation ensures that we are using purely weather-related information in the derivation of the weather delay factor. Figure 4-9 presents a flow-chart that summarizes the entire procedure for incorporating weather effects within the APCDM model. Once we obtain the flight surrogates from the participating airlines, we check if the flight plans within the surrogate were created using our proposed flight plan generation tool. If an alternative tool is used to generate the flight plans, the associated threshold probability σ_{p} can be determined for each such surrogate plan *p* using the corresponding exit probability defined earlier. This step is critical in order to compute the value for t_{fp}^{EWD} in (4.4). We can then use the two-step approach (or the three-step approach if the time and the relevant delay and threshold information are available) in order to generate the relevant weather delay factors for inclusion within the modified delay cost in (4.5). Furthermore, observe that given σ, we could additionally restrict the admissible arcs in the overlaid grid network to generate alternative surrogates that

circumvent the weather system with the specified probability $1-\sigma$ from different sides of this system (refer to Figure 4-10 for an illustration), in order to promote the ultimate generation of a desirable mix of flight plans via the APCDM model from the viewpoint of collision risk and sector workload contributions.

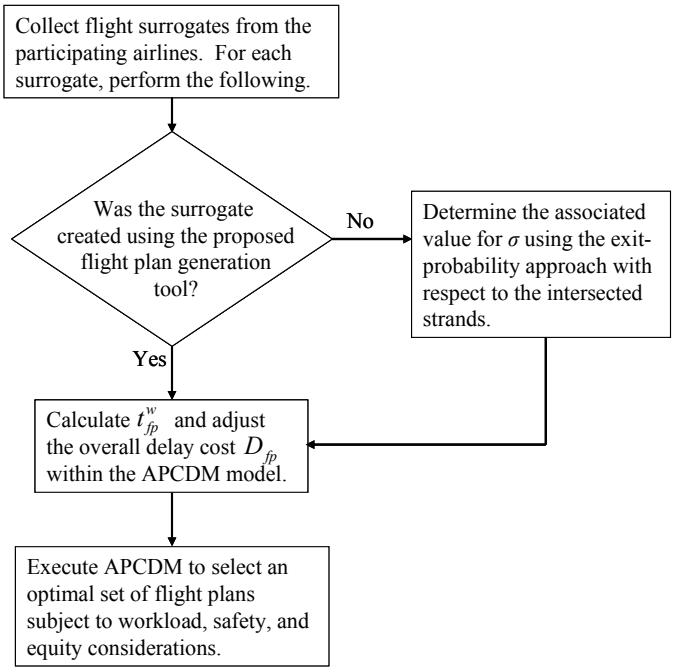

Figure 4-9: Weather Delay Factor Flow-chart.

By requiring airlines to generate flight plans that conform with the threshold strand probability σ, a situation could develop, as illustrated in Figure 4-10, where the flight plans increase the potential number of routes traversing a given sector. This weather-related development underscores the importance of using the APCDM model to select an optimal set of flight plans. For example, assume that flight plan #1 for each flight A and B is considerably longer in distance than the two alternative plans for each flight that intersect the sector depicted in Figure 4-10. While both flights would prefer a shorter route, if the sector capacity is violated as a result of including the shorter routes for each flight in addition to the other flight plans (not shown) traversing this sector, the APCDM model might exclude either one or both of the routes. Additionally, there is the potential for fatal airspace conflicts as a result of the planned routes, which is also prohibited by the APCDM model. Note that by applying our probability-net concept to strategic level flight planning, we could dynamically adjust sector capacities if the situation dictates such a requirement.

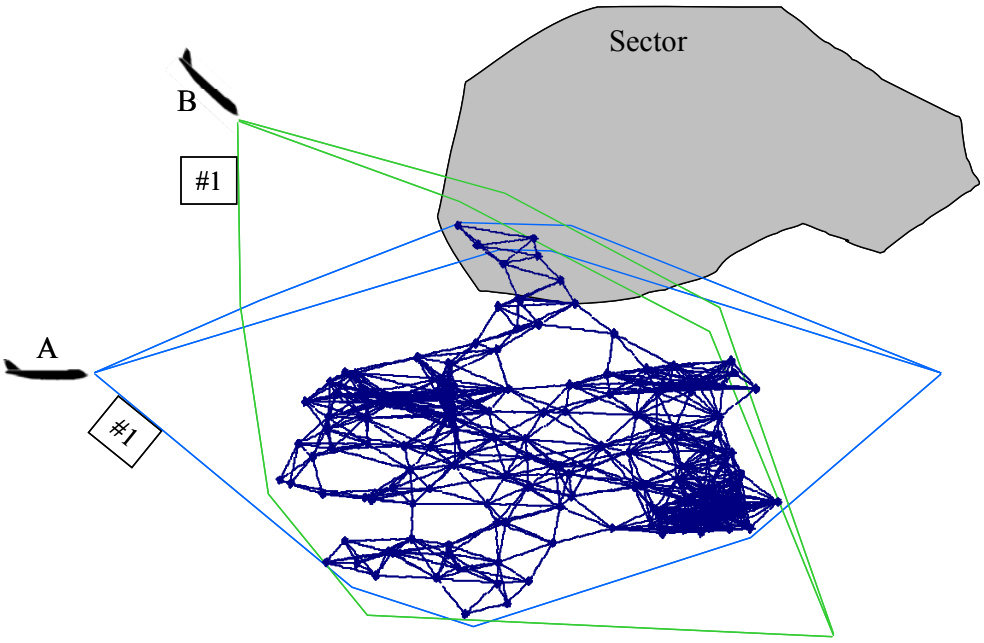

Figure 4-10: Potential Increase in Sector Count.

4.4. Evaluation of Economic Benefits Using *k*-means Cluster Analysis

We begin our economic benefit analysis by generating various probability-net refinement levels and comparing the results against the most refined probability-net consisting of all MOS reporting sites having a probability greater than 0.05. Using a *k*-means clustering heuristic, Figure 4-11 depicts two levels of refinement (k=200 and k=50). The most refined probability-net (strands omitted for picture clarity) consists of 809 MOS reporting stations using MOS data for March 23, 2005. The solid line represents a single flight plan from Chicago to Miami departing at 0523Z. We will use this individual flight plan to assess the related economic advantages of having a more detailed MOS representation. The departure and flight plan details are important since the probability-nets are dynamic with respect to time and space. As the flight passes through the probability-net(s), we can generate a *probability-footprint* that acts as a record of the strand intersections and the associated probabilities from origin to destination. A flight plan's probability-footprint will differ for each level of refinement. It is from these probability-footprints that we extract the pertinent information for our economic benefit analysis. Figure 4-12 depicts a segment of the probability-footprints for the full probability-net using all 809 pertinent MOS reporting stations and two less-refined probability-nets using 200 and 50 reporting stations.

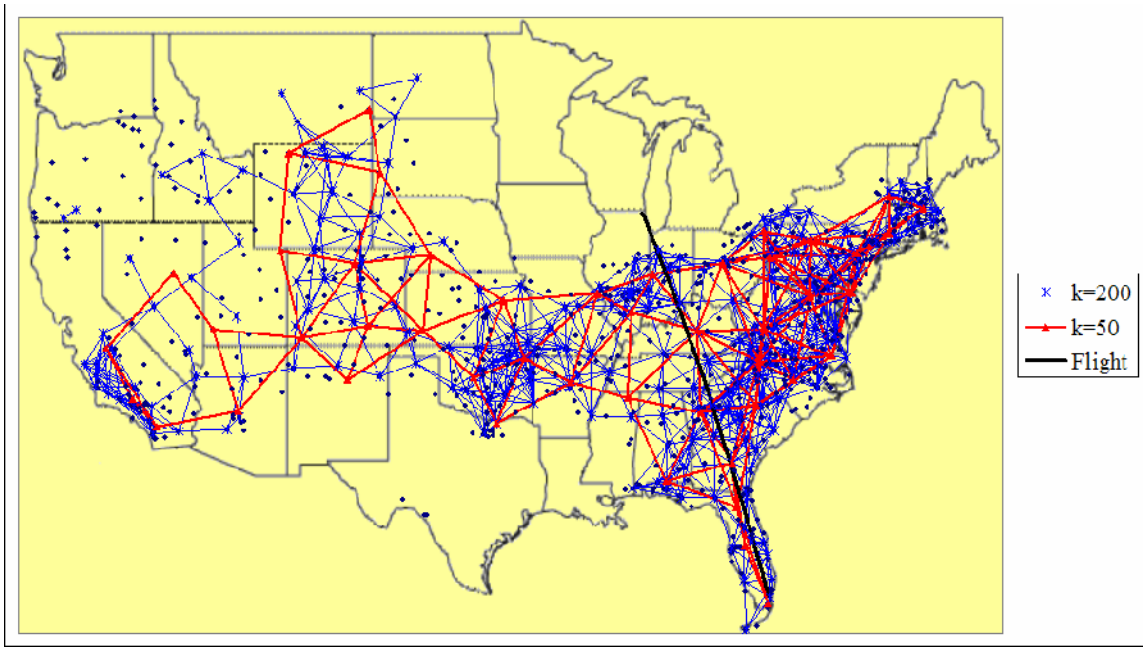

Figure 4-11: Variations in Probability-Net Refinement.

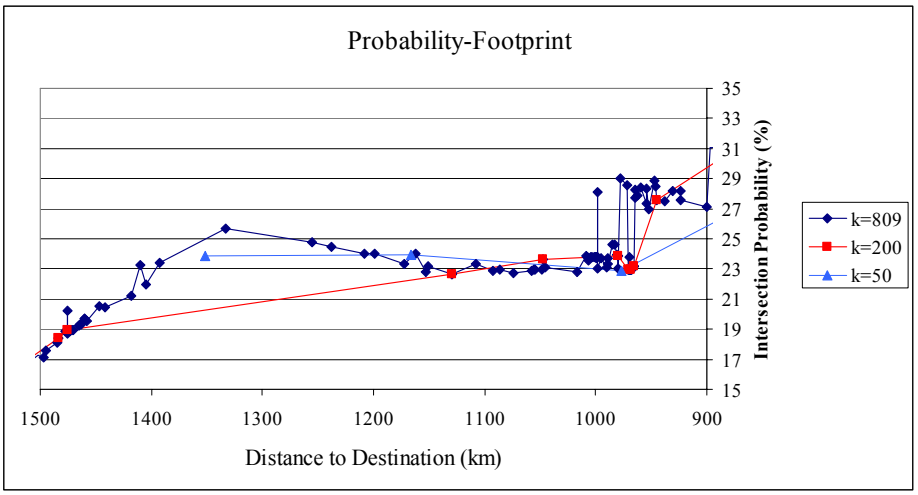

Figure 4-12: Probability-Footprints.

The economic benefit for a specific level of refinement stems from the value of information existing within the probability-footprint. A closer look at the distance interval from 1500 km to 1130 km in Figure 4-12 reveals the importance of the additional information found in the probability-footprint for the more refined structure. Figure 4-13 illustrates this fact as we assess potential flight plans. For this particular discussion, let us assume that the specified threshold strand probability is $\sigma = 0.23$ (i.e., the maximum allowed probability associated with the intersection of any strand and the flight plan). If we use a probability-net consisting of only

200 reporting stations, there is a 345 km gap between two sequential strand intersections, as indicated in Figure 4-13. Since neither point has an associated probability greater than 0.23, the minimum flight distance would be obtained by a straight line between the two waypoints illustrated by the line segment between the aircraft icon and the box labeled "*k*=200". In contrast, the probability-footprint associated with the most refined probability-net contains multiple intersections within the same 345 km interval. More importantly, some of the intersection points have associated probabilities exceeding σ, which induces an alternative flight plan (comprised of waypoints *a* and *b*) in order to prevent the higher probabilities of encountered severe weather from occurring.

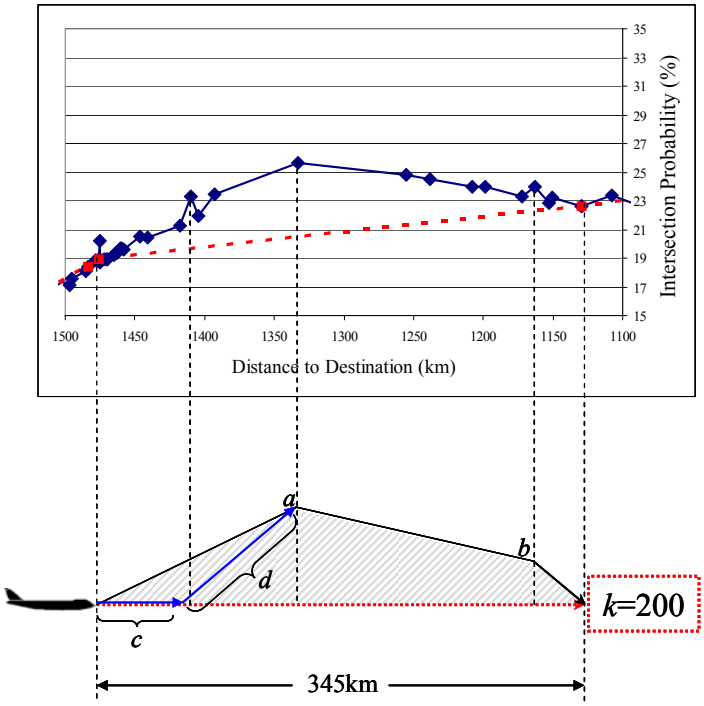

Figure 4-13: Economic Benefit Illustration.

Given that our focus is on strategic level flight planning, the related economic benefit is a function of the cost associated with the execution of each flight plan under different weather realizations. Let us designate the plan consisting of the straight-line segment as Route *A* and the alternative plan as Route *B*. In conjunction with these two routes, we define four scenarios; (1) Route *B* is executed and severe weather is not realized, (2) Route *B* is executed and severe weather is realized, (3) Route *A* is executed and severe weather is not realized, and (4) Route *A* is executed and severe weather is realized. By allocating the resources (fuel, crews, gate times,

etc.) required to support Route *B*, Scenario (1) will most likely result in an expected or on-time arrival, which translates to a potential reduction in overall operating costs. Scenario (2) may incur a slight increase in delay time as a result of further route adjustments required to circumvent the severe weather. However, these route adjustments will be minor when compared to those for Scenario (4). (We shall clarify this point with an example later in this chapter.) By allocating the same resource categories required to support Route *A*, Scenario (3) will more than likely result in an on-time arrival with lower operating costs when compared with Scenarios (1) and (2). However, it should be noted that planning a flight route through forecasted severe weather is risky business. The occurrence of Scenario (3) translates to a situation in which the flight planners beat the odds. For Scenario (4), let us assume the worst case in that the flight is en route and has traveled some distance *c* (see Figure 4-13). At this point in time, the weather situation necessitates the re-routing of the flight to waypoints *a* and *b* via the flight segment annotated by the distance *d* in Figure 4-13, thereby allowing the aircraft to circumvent the severe weather. The operating costs associated with this scenario will exceed that for the previous three scenarios based on the increased flight distance.

To further illustrate the economic benefit in relation to the four scenarios, we continue with the previous example consisting of a single flight *f* from Chicago to Miami. A principal assumption regarding our economic benefit analysis is that the aircraft executes the APCDM-generated flight plan unless the presence of severe weather dictates additional route adjustments. The exit probability for a straight-line trajectory from the origin to the destination is 0.41. Therefore, let $\sigma = 0.41$ be the threshold strand probability for the direct route (shortest path), Route *A*, and let Route *B* be the alternative route generated using a threshold strand probability $\sigma' = 0.20$ (an intermediate value). In order to calculate the expected weather delay and weather delay factors, we included two additional routes corresponding to $\sigma'' = 0.10$ and $\varepsilon = 0.01$. Figure 4-14 depicts the four routes associated with these threshold values along with their respective distances from the origin to the destination. Assuming an average ground speed of 650 km/h, we get $d_1 = 0.0,\ d' = 10.91,\ d'' = 25.54,$ and $d_2 = 47.52$ minutes, which again represent the trajectory delays based on the differences between the trajectory distances and the shortest path distance. The three-step approximation defined in (4.3) yields an expected weather delay of $t_{fA}^{EWD} = 6.14$ minutes for Route *A*, and the same distribution, but using Equation (4.2) for

the portion to the right of d' for Route B yields an expected weather delay of $t_{fB}^{EWD} = 13.73$ minutes. Using (4.4), these expected delays result in weather delay factors of $t_{fA}^{w} = 6.14$ and $t_{fB}^{w} = 2.82$ minutes, respectively. Note that these weather delay factors for the two routes provide an indication of the expected potential disruption to planned operations and connections beyond what is anticipated from the trajectory-based delay alone. For example, if we planned, scheduled resources, and executed Route A, the additional probabilistic weather delay that we could expect with this plan is much greater than that associated with having planned, scheduled resources, and executed Route B. This is compounded further when we apply the appropriate connection delay factors d_f^c in (4.5).

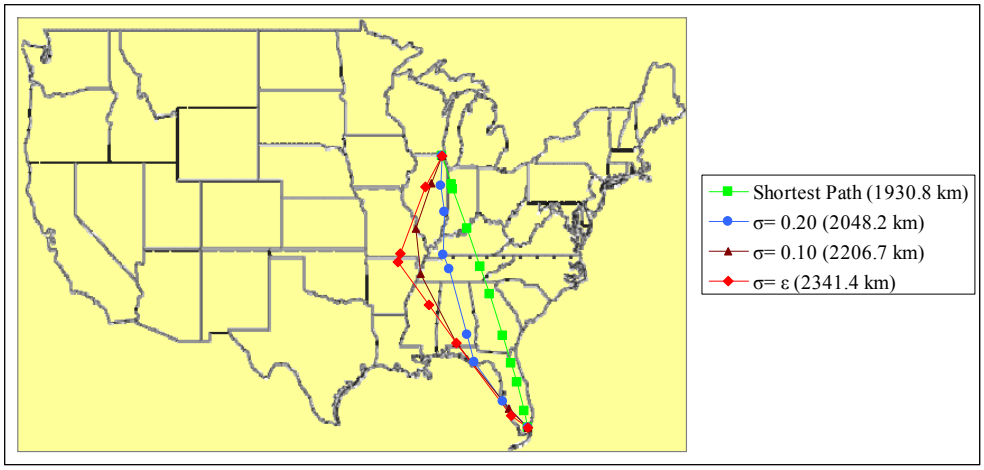

Figure 4-14: Flight Plans as a Function of σ.

4.5. Expected Weather Delay and Disruption Factors Using a Decision-Theory Technique

As an alternative technique, we present in this section a decision theory approach to determine expected weather delay and disruption factor computations. Instead of using a delay distribution for estimating expected weather delays as prescribed in Section 4.3, we assume that the planned flight will be realized with probability $(1-\sigma)$, but with probability σ, severe weather will be encountered, by virtue of which the flight will be diverted in a specified fashion with respect to the ε-threshold route. This pre-determination of an alternative route is the fundamental difference between this and the previous approach.

Using the decision-making terminology prescribed by Marshall and Oliver (1995), let D be the set consisting of all the choices from which the decision-makers must make a single

selection, let X be an uncertain event (with an associated probability distribution) for which there are at least two outcomes, and let R be the set of rewards that are a function of the decision and the outcome of the random event. For our example, D consists of the σ-threshold flight plans, X is the event that severe weather (SW) is realized or not, and the set R consists of the delay times relative to route selection and thunderstorm realization. The associated decision tree with four scenario outcomes for our illustration example of Section 4.4 is depicted in Figure 4-15, where r_1, r_2, and r_4 are the trajectory delay minutes for Scenarios (1), (2), and (4), respectively. Suppose that for these four scenarios, the decision to alter the flight route will occur at some specified distance into the flight if severe weather is realized. By assuming that Route A and Route B will be rerouted to the same point in order to circumvent the severe weather in Scenarios (2) and (4), we know that $r_4 > r_2 > r_1$ based on the geometry of the problem. From the decision tree, we can calculate expected weather delays for each route decision as follows:

$$E(\text{Route } A) = 0.41 r_4, \text{ and}$$

$$E(\text{Route } B) = 0.8 r_1 + 0.2 r_2 .$$

For our example, we assume that the decision to reroute a flight is made 200 km into the flight (since no strand intersections occurred within the first 205 km for each route), and if so, it is rerouted to the first waypoint on the ε-threshold route (see Figure 4-14). Based on this reroute criteria, the corresponding delay times are $r_1 = 10.91$, $r_2 = 45.61$, and $r_4 = 52.57$ minutes, resulting in expected weather delays of 21.55 and 17.85 minutes for Routes A and B, respectively. Therefore, by this analysis, the decision-maker would prefer Route B. Note that while these expected weather delays were calculated using an alternative approach, the results still indicate that Route B is the better selection.

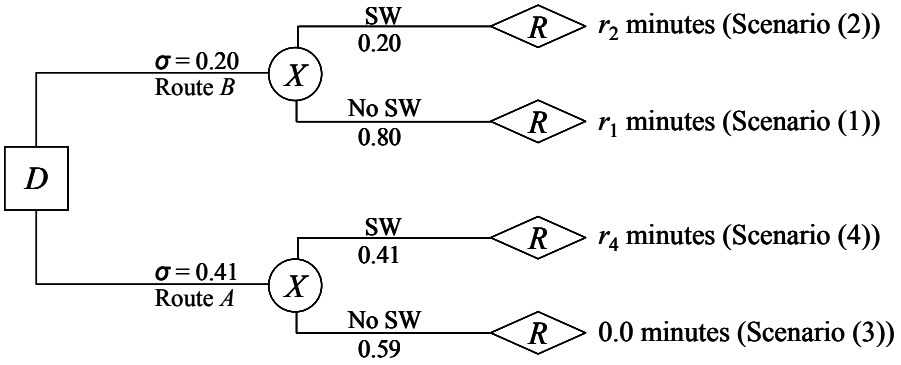

Figure 4-15: Decision Tree for Routes *A* and *B*.

The delay times r_1, r_2, and r_4 are a function of the average ground speed and the increased route distance as compared to the straight-line trajectory associated with Route *A*. By removing the trajectory-related delay from the overall delay times, we can calculate a *disruption time* that is solely a function of the weather, thereby determining the weather delay factor for each branch of the decision tree. For example, the disruption time for Scenario (1) is 0.0 minutes whereas the disruption time for Scenario (2) is $r_2 - r_1 = 34.7$ minutes. Note that the *expected disruption time* is equivalent to the previously defined *weather delay* or *disruption factor*. This weather delay or disruption factor for each of the Routes A and B equals 21.55 and 6.94 minutes, respectively. Again, the results indicate that Route *B* is the better selection when using the weather delay or disruption factor as the guiding criterion. Intuitively, flight routes generated using larger threshold probabilities would tend to have larger disruption factors than those generated with smaller threshold probabilities. Therefore, we must exercise caution in using the disruption factor by itself as a decision criterion (as indicated below).

These decisions above, however, are based upon only two routes. Given that we have planned flight trajectories and distances from the previous approach corresponding to the threshold strand probabilities $\sigma = 0.10$ and $\sigma = \varepsilon$, we can expand the decision tree as depicted in Figure 4-16. Note that there is no random event in the decision tree for the decision related to the selection of the ε -threshold route since this route circumvents any severe weather probabilities. The delays on the right-hand side were computed under the same assumption that the decision to reroute a flight is made 200 km into the flight, and if so, it is rerouted to the first waypoint on the ε-threshold route. In addition to the corresponding delay times, we also display the associated disruption times. The resulting expected weather delays and disruption factors are shown in Table 4-4. Once again, the results indicate that the best decision, based on the expected weather delay, is to select the route generated using $\sigma = 0.20$ (the previous Route *B*). However, the best decision based on the disruption factor is naturally associated with the route generated using $\sigma = \varepsilon = 0.01$, which essentially removes any chance of encountering severe weather. Therefore, a decision-maker may chose to adopt some weighted compromise between delay and disruption in making a route selection. Viewing Table 4-4, the route corresponding to $\sigma = 0.20$ appears to strike a reasonable compromise between these two factors.

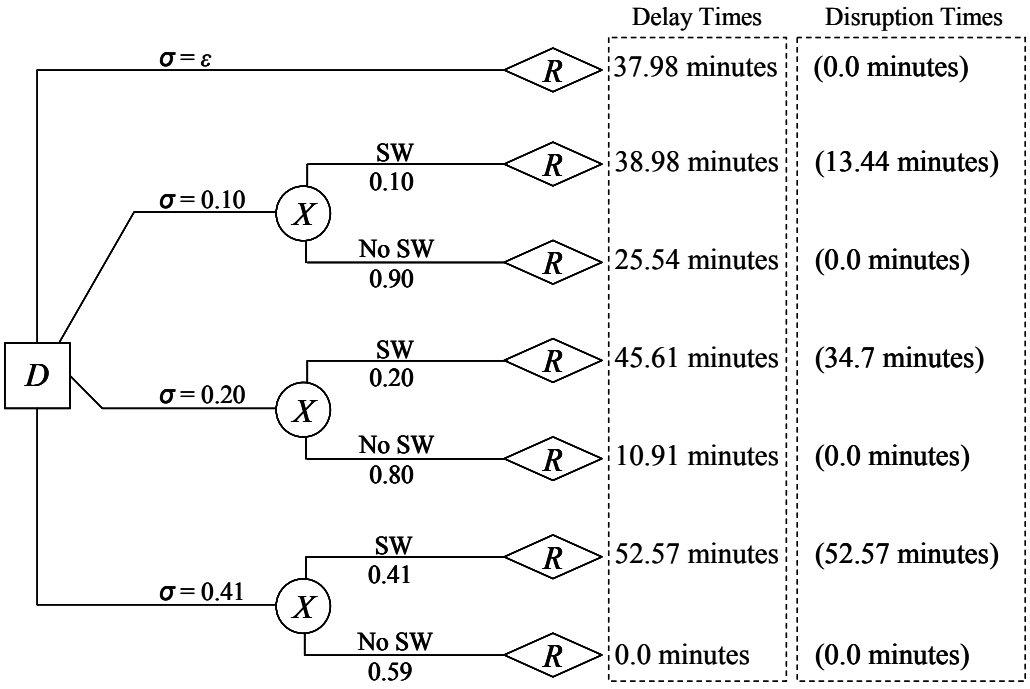

Figure 4-16: Decision Tree for Flight Plan Selection.

Table 4-4: Expected Weather Delay and Disruption Factors.

σ	Expected Delay (minutes)	Disruption Factors (minutes)
0.41	21.55	21.55
0.20	17.85	6.94
0.10	26.89	1.34
0.01	37.98	0.00

Recall that a key assumption in this example is the designation of the reroute decision point at 200 km into the flight, which stemmed from the proximity of the forecast probabilities to the various routes. Since this reroute decision point can be made earlier, we experimented further to determine the expected weather delays when (a) the decision to reroute the flight is made 100 km into the flight, and (b) the reroute decision is made 50 km into the flight. We also computed expected weather delays and disruption factors using additional values of σ. Figures 4-17 and 4-18 graphically portray the results for each reroute decision point distance. The smallest expected weather delays correspond to $\sigma = 0.25$ regardless of the location of the reroute decision point. While the smallest weather delay factor naturally corresponds to the ε-threshold route, the route corresponding to $\sigma = 0.20$ once again appears to strike a reasonable compromise between the expected weather delay and the disruption factors.

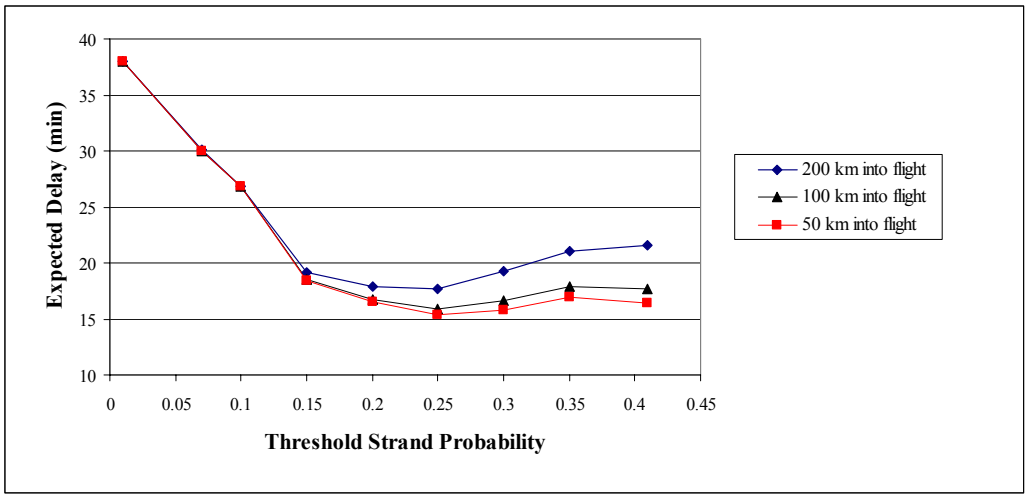

Figure 4-17: Expected Delays for Strategic Level Planning.

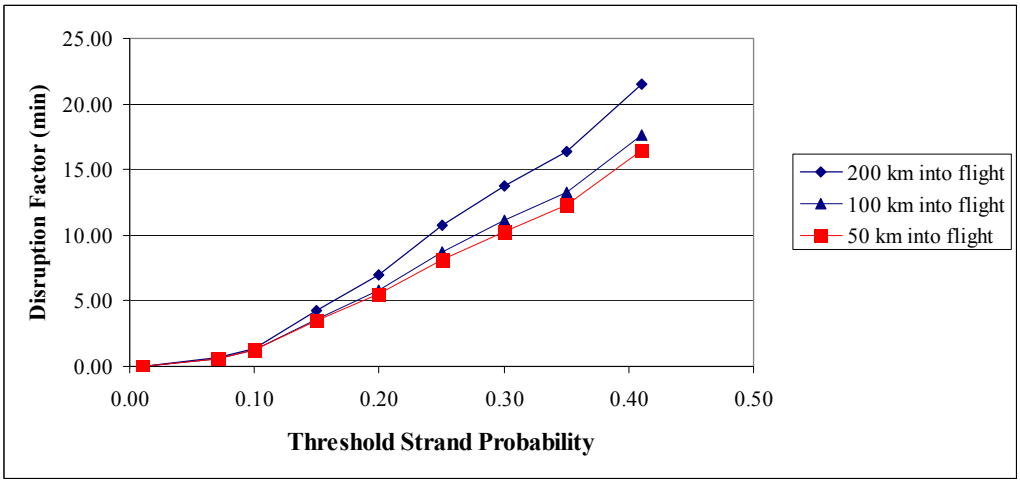

Figure 4-18: Disruption Factors for Strategic Level Planning.

Strategic level flight planning without regard to severe weather can significantly increase airline operating costs as a result of excessive delays. While there exist inherent difficulties in forecasting severe weather, it is economically beneficial to plan flight trajectories in accordance with the probabilistic incidence of severe weather rather than to ignore it and have to non-optimally readjust flight plans en route. Through a discrete representation of severe weather probabilities, the superimposition of a flight-trajectory-grid network upon our probability-net concept provides the airlines with the capability to generate flight plans that circumvent the severe weather based upon a given probability threshold. By including our proposed weather-modeling concepts along with the derived trajectories and their associated delay factors within

the framework of the APCDM model, planners can effectively account for probabilistic weather and generate a set of optimal flight plans that circumvent potentially severe weather with an acceptable threshold probability, while considering issues related to sector workloads, airspace conflicts, as well as overall equity concerns among the involved airlines.

Chapter 5

Modeling Slot Exchanges and Related Equity Concepts

The primary inputs into the APCDM are the surrogate sets P_{f0} associated with the flights $f \in F$. The various surrogate plans for a given flight are differentiated by flight trajectories (altitude and path) and departure and arrival times. The APCDM selects an optimal set of flights (one from each surrogate), which specifies the arrival time for each flight at the corresponding destination airport. Once a GDP is imposed and the arrival capacity at the associated airport is reduced, the available slots are allocated to specific flights using RBS. Hence, new arrival times are assigned to flights that are later than the originally scheduled times, which requires the re-evaluation of selected flight paths with respect to sector workloads and conflict risks. In addition, the acceptable trades are also subject to the same workload and conflict constraints. Therefore, an additional set of inputs for the APCDM is required that relates acceptable trades and their associated flight plans. In this chapter, we propose two slot-exchange approaches. In addition to the equity terms and constraints developed by Sherali et al. (2006), we propose four additional equity methods specific to characteristics of trade offers.

5.1. External Slot-Exchange Approach

5.1.1. Package-Deal Generation

Suppose that airlines submit "at-least, at-most" offers as defined by Vossen and Ball (2004). As previously stated in Chapter 2, feasible trades are represented by the presence of one or more directed cycles within a slot offer network. We define such an instance of feasible trades as a "package-deal". Note that based on the number of participating airlines, the set of available slots, and the flexibility of the individual trade offers, there can exist several viable package-deals. The flexibility of an individual trade offer is reflected by the length of the additional delay an airline is willing to accept in return for a reduction in the delay of a second particular flight. For example, if the "at-most" offer corresponds to an adjacent slot, then the offer has limited flexibility, whereas an offer that accepts any of the next four later slots has increased flexibility. Accordingly, let the package-deals be given by:

$$P_g = \left\{ \begin{array}{c} (f,p) : \text{the selection of plan } p \text{ for flight } f \text{ is part of} \\ \text{the slot exchange scheme in the package - deal } g \end{array} \right\}, \forall g = 1,...,G. \quad (5.1)$$

Note that each package-deal corresponds to a union of directed cycles that represent a collection of selected flight plans based on an agreed-upon exchange mechanism, which is also feasible to the trade restrictions.

Consider the following illustrative situation where due to weather conditions at Airport X, the FAA has reduced the airline arrival capacity by imposing a Ground Delay Program (GDP). Suppose that the execution of the RBS procedure produces the arrival slot allocations for Airlines A, B, and C as depicted in Figure 5-1, based upon their arrival times listed in the OAG. For example, flight #1 for Airline A (designated as A1) has been allocated the 0800 slot arrival time, and so forth for Airlines B and C. Under the enhancements to the GDP, Airline A owns the 0800-slot and thus, may consider offering that slot to another airline in return for a slot that reduces the delay for one of its subsequent flights. Under the "at-least, at-most" offer restriction, each airline owning two or more slots can make an offer to increase the delay of some specified flight in return for a reduction in the delay of a second particular flight. In this spirit, consider the offers from Airlines A, B, and C as shown in Figure 5-2. A key assumption used in the Package-Deal Generation algorithm is that an airline will not allow a trade to occur in which a further delay is imposed on a flight without reducing the delay of another flight. We refer to this as a *trade restriction* throughout the remainder of the dissertation.

0800	A1
0804	C1
0808	A2
0812	B1
0816	C2
0820	B2
0824	B3
0828	A3

Figure 5-1: Slot Allocations from the Imposed GDP.

In the example, Airline A has offered to increase the delay of flight #1 with an arrival time no later than the 0816 slot in return for moving flight #3 up to an arrival time no earlier than the 0816 slot, which corresponds to that flight's earliest arrival time listed in the OAG. Using the slot times as nodes and the "at-least, at-most" offers, we can represent the slot offers as a

directed network as depicted in Figure 5-3. Acceptable trades, subject to trade restrictions, are in the form of directed cycle(s) in this network. Not displayed in Figure 5-3, but integral to the generation of package-deals, is the existence of a directed self-loop at each node. This self-loop signifies the preservation of an assigned slot if no trades are accepted for that airline. In most instances, more than one set of acceptable trades exists. Therefore, a methodology is required to generate all possible trades that preserve feasibility to the trade restriction. This is accomplished through the application of the Package-Deal Generation model.

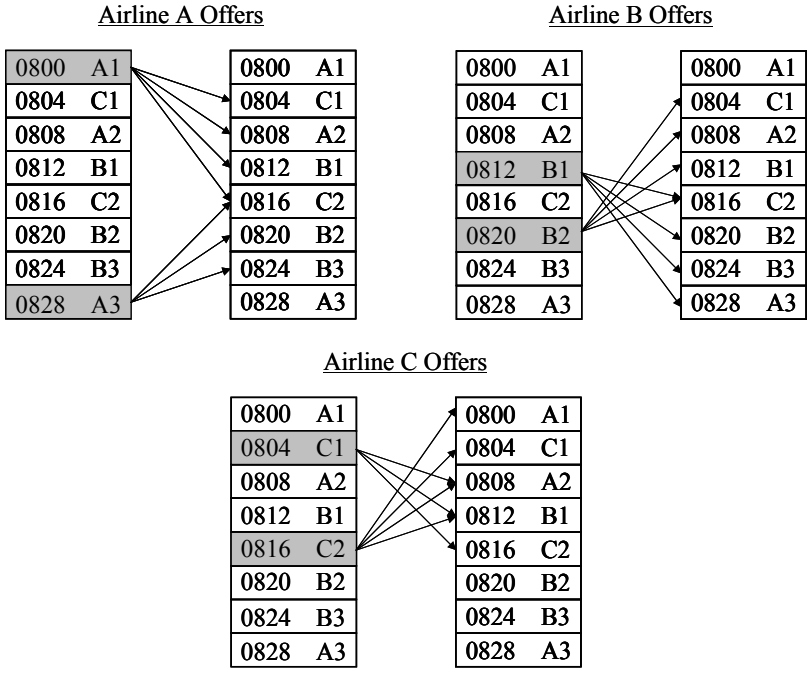

Figure 5-2: Airline Slot Offers.

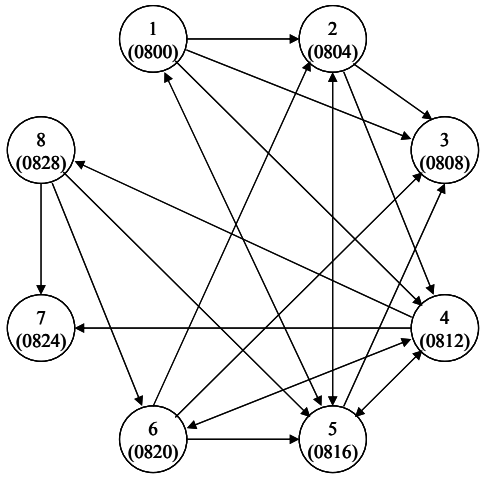

Figure 5-3: Slot Offer Network.

For notational simplicity, we designate slot time 0800 as node 1, slot time 0804 as node 2, and so on. Based upon the directed network in Figure 5-3, let $TR_{i,j}$ represent the selection of (and hence the trade represented by) the directed arc between the two slot times corresponding to nodes i and j, so that $TR_{i,j} = 1$ if the arc (i, j) is selected and is 0 otherwise. Under the offer format for each airline a, we define FID_a as the flight specified for an increase in delay, and FRD_a as the flight specified for a decrease in delay. We also, define LS_a as the set of all later slots that airline a is willing to accept, and let ES_a be the set of all earlier slots that airline a is willing and permitted to accept in return. We use the following model to generate a set of directed cycles that represent acceptable trades, where $b_{i,j}$ is a prescribed benefit parameter associated with the arc (i,j).

PDG: Maximize $$\sum_i \sum_j b_{i,j} TR_{i,j} \tag{5.2}$$

subject to $$\sum_j TR_{i,j} = 1, \qquad \forall i \tag{5.3}$$

$$\sum_i TR_{i,j} = 1, \qquad \forall j \tag{5.4}$$

$$\sum_{j \in LS_a} TR_{FID_a,j} - \sum_{k \in ES_a} TR_{FRD_a,k} \le 0, \qquad \forall a \tag{5.5}$$

$$TR_{i,j} \text{ binary}, \quad \forall (i, j). \tag{5.6}$$

Constraints (5.3) and (5.4) in the model formulation are the standard assignment constraints that drive the generation of the required directed cycles by ensuring that the out-degree and the in-degree of each node equals one. Constraint (5.5) represents the trade restriction for each airline a. The inequality allows for the condition where a flight receives a delay reduction alone. Note that our goal is to generate a variety of possible directed cycles that are feasible to the constraints. The formulation above, however, generates only one jointly compatible solution for each set of benefit parameters and specified trade restrictions. Several runs of Model PDG could be used with varying parameters and offer restrictions to generate sets of package-deals that are acceptable to the involved airlines. Such deals might, of course, also be formulated by airlines independently of using Model PDG. Table 5-1 displays the resulting directed cycles for our example over different iterative runs. Notice that the first model iteration resulted in a single directed cycle while each of the other iterations generated two directed cycles within the network.

(Nodes not listed in the cycles displayed in Table 5-1 maintained their assigned slots via the self-loops.) Each directed cycle represents a possible trade and specific unions of such cycles constitute admissible package-deals (see Table 5-2). The two cycles from the second model iteration are acceptable trades individually since each relates to an "in-house" slot exchange for a particular airline and, therefore, can be represented as separate package-deals or combined in a third package-deal.

Following the submission of trade offers from the participating airlines, we can therefore generate a number of package-deals that, in combination with other package-deals specifically proposed by the participating airlines, will serve as inputs into APCDM. The next step involves the development of the constraints that would optimally select package-deals in concert with specific flight plans that correspond to the approved slot trades, while considering sector workloads, conflict risk, and equity issues.

Table 5-1: Directed Cycles Resulting from Different Runs of Model PDG.

Model Iteration	Set of Directed Cycles
1	{(1,4,8,6,2,5,1)}
2	{(2,5,2) (4,6,4)}
3	{(1,5,1) (2,4,8,6,2)}
4	{(4,8,6,4) (1,2,5,1)}

Table 5-2: Package-Deals Corresponding to the Cycles in Table 5-1.

Package Deal	Corresponding Cycle
1	(1,4,8,6,2,5,1)
2	(2,5,2)
3	(4,6,4)
4	(2,5,2) and (4,6,4)
5	(1,5,1) and (2,4,8,6,2)
6	(4,8,6,4) and (1,2,5,1)
7	(No Trades)

5.1.2. Package-Deal Based Formulations

Recall that the principal binary variable within APCDM is x_{fp}, which takes on a value of 1 when the flight plan $p \in P_{f0}$ is selected for flight *f*, and 0 otherwise. The surrogate set P_{f0} for each flight will contain a cancellation plan, one or more plans corresponding to the assigned slot, and one or more plans corresponding to each possible traded slot in any package-deal. Note that

in this lattermost case, if more than one plan exists for some exchanged slot, then we construct a single dummy representative flight plan, say (f, p_d), for this collection. Accordingly, let

$$S_{f,p_d} = \left\{ \begin{array}{l} (f,p) : \text{plans } p \text{ of flight } f \text{ corrpespond to the} \\ \text{slot - based representative flight plan } (f, p_d) \end{array} \right\}. \tag{5.7}$$

Then, we incorporate the following constraint in APCDM:

$$\sum_{(f,p) \in S_{f,p_d}} x_{fp} = x_{f,p_d}, \quad \forall \text{ such } (f, p_d) \text{ pairs.} \tag{5.8}$$

Hence, in what follows, for the flight plans recorded in each package-deal, we will assume that for any flight *f* associated with a particular slot at the GDP airport, there is a single representative plan.

The following constraint is accommodated within APCDM:

$$\sum_{p \in P_{f0}} x_{fp} = 1, \quad \forall f. \tag{5.9}$$

Note that in case of multiple surrogate plans for a flight that pertains to a particular traded slot, P_{f0} is assumed to contain the corresponding representative plan alone; hence, (5.9) is used in concert with (5.8). Next, we represent the selection of a particular package-deal through the use of the binary variable, y_g, where

$$y_g = \begin{cases} 1 \text{ if package - deal } g \text{ is selected} \\ 0 \text{ otherwise.} \end{cases} \tag{5.10}$$

Then we accommodate the constraints

$$x_{fp} \geq y_g, \quad \forall (f,p) \in P_g, \quad \forall g = 1,...,G \tag{5.11}$$

$$x_{fp} = \sum_{g \in P^{fp}} y_g, \quad \forall (f,p) \in TR \tag{5.12}$$

where

$$TR = \{(f,p) : \text{plan } p \text{ of flight } f \text{ is part of some package - deal trade}\} \tag{5.13}$$

and where

$$P^{fp} = \{g : \text{package - deal } g \text{ contains } (f,p)\}, \quad \forall (f,p) \in TR. \tag{5.14}$$

Note that Constraint (5.11) asserts that if $y_g = 1$ (package-deal *g* is selected), then each flight plan (f,p) associated with P_g must be activated $(x_{fp} = 1, \forall (f,p) \in P_g)$. Moreover, Constraint

(5.12) ensures that if $x_{fp} = 1$ for any $(f, p) \in TR$, then exactly one package-deal that contains it must be selected (hence, in particular, the exchange prompted by $x_{fp} = 1$ cannot be "double-dipping" into more than one package-deal). Furthermore, if $x_{fp} = 0$, then $y_g = 0, \forall g \in P^{fp}$, which is also prompted by (5.11). Note that it could be that some $y_g = 0$, but yet, $x_{fp} = 1, \forall (f, p) \in P_g$, in that P_g could be a subset of the selected package-deals in such a solution.

In addition, we could further tighten the model representation by constructing a package-deal graph $G_{PD} = (N_{PD}, A_{PD})$, where the set of nodes N_{PD} represent the different package-deals $g = 1,...,G \equiv |N_{PD}|$, and for any pair of package-deals g_1 and g_2 that are not jointly compatible, we have an edge (undirected arc) (g_1, g_2) in A_{PD}. Let $\{IC_r, r = 1,...,R\}$ be a maximal clique cover for A_{PD}, where each IC_r is a maximal clique of G_{PD}, in the sense that it is a clique of G_{PD} that is not a proper subset of a larger clique, and where $\bigcup_{r=1}^{R} \{\text{subgraph induced by } IC_r\} = G_{PD}$. Then, we include the constraints

$$\sum_{g \in IC_r} y_g \leq 1, \quad \forall r = 1,...,R. \tag{5.15}$$

The difficulty associated with the compatibility issue is finding the maximal clique cover. Using our previous example, we generated seven package-deals, $g = 1,...,7$. The corresponding package-deal graph is shown in Figure 5-4. Each solid black edge represents an incompatibility between the incident nodes. The compliment of the graph, $\overline{G}_{PD}$, is illustrated with the dashed red lines. In essence, the graph $\overline{G}_{PD}$ uncovers the package-deals that are pairwise independent. Using this information, we prescribe a procedure, MCC, for generating a possible maximal clique cover.

Figure 5-5 presents a flow-chart for the procedure MCC. The procedure begins with an initialization of the incompatible graph and its compliment along with the supporting ordered sets. We begin the construction of the first maximal clique IC_1 using the first node listed in the ordered set L_1 and adding additional nodes into IC_1 that meet the required adjacency conditions. Once a maximal clique is created, it is used to update the set L_2 of nodes that are covered by the set of cliques generated thus far. Treating L_1 essentially as a circular list, the procedure MCC

continues by selecting the next node in L_1 and making a complete circular pass through it to generate another distinct maximal clique as possible. The procedure terminates when the set L_2 contains all the nodes of the graph G_{PD}.

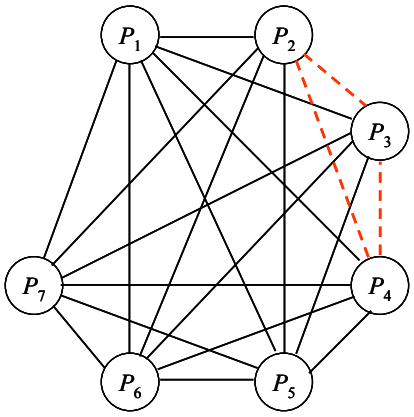

Figure 5-4: Package-Deal Graph, G_{PD}.

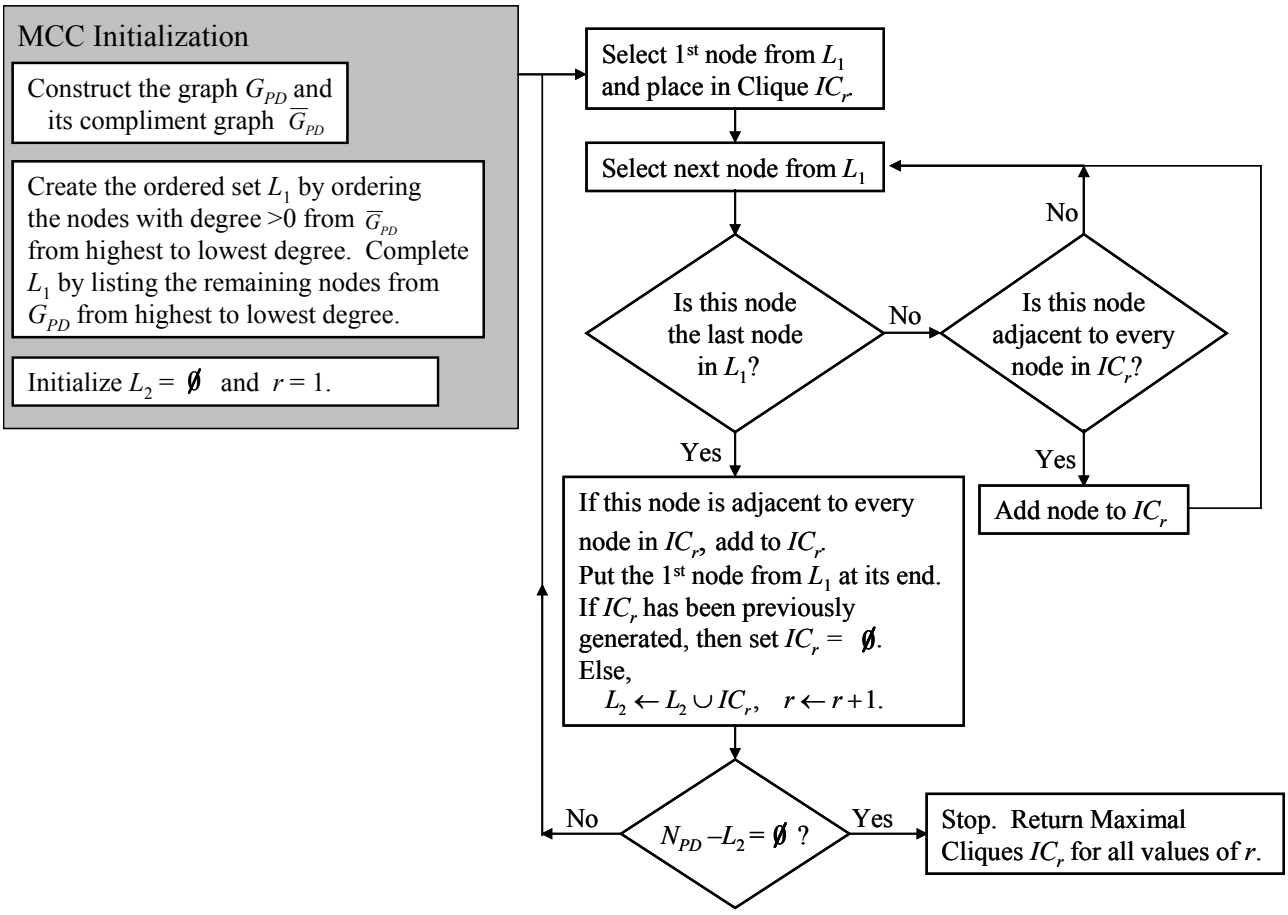

Figure 5-5: Flow-chart for Procedure MCC.

For our example depicted in Figure 5-4, the procedure MCC would begin by ordering the nodes having incident edges in the graph $\overline{G}_{PD}$ in order from highest to lowest in terms of node degree in $\overline{G}_{PD}$, and then ordering the remaining nodes from the graph G_{PD} in order from highest to lowest node degree in G_{PD}. This would produce the initial ordered set $L_1 = \{P_2, P_3, P_4, P_1, P_5, P_6, P_7\}$. The construction of the first clique, IC_1, would begin with the inclusion of node P_2 followed by the addition of all nodes that satisfy the clique adjacency criteria defined in the graph G_{PD}. Following one complete pass through the ordered set L_1, we get $IC_1 = \{P_2, P_1, P_5, P_6, P_7\}$, and the set L_2 contains all the nodes listed in this first clique. Continuing this process, the procedure MCC produces the maximal cliques and maximal clique cover specified in Table 5-3. Note that the above example contained only one clique in $\overline{G}_{PD}$. To illustrate a situation in which more than one clique exists in the compliment graph, consider the scenario in which an eighth package-deal P_8 exists that is incompatible with all other package-deals except P_5. The procedure MCC described above would then produce the ordered set $L_1 = \{P_2, P_3, P_4, P_5, P_8, P_1, P_6, P_7\}$ along with the maximal cliques and maximal clique cover as shown in Table 5-4. This completes the development of the package-deal based selection formulations (2.5b) and (5.7-5.15) that we propose for inclusion into the APCDM.

Table 5-3: Maximal Clique Cover and Individual Maximal Cliques.

r	*IC*
1	{2,1,5,6,7}
2	{3,1,5,6,7}
3	{4,1,5,6,7}

Table 5-4: Maximal Clique Cover and Individual Maximal Cliques Involving P_8.

r	*IC*
1	{2,1,5,6,7}
2	{3,1,5,6,7}
3	{4,1,5,6,7}
4	{8,1,6,7}

5.2. Internal Slot-exchange Approach

The previous approach entails an external *a priori* generation of a number of package-deals. For the flights involved with the GDP-imposed airport, each package-deal concerns a subset of these flights for which it prescribes a flight plan for each flight that is part of a specified slot exchange scheme that is feasible to the trade restrictions, as well a flight plan for each flight that maintains its slot allocated under the GDP. We now propose another approach in which package-deals are automatically generated as required within the APCDM model itself. Suppose that based on various offer schemes, we have a collection of exchange graphs $G_e = (N_e, A_e), e = 1,...,E,$ where each exchange graph G_e has a node set N_e corresponding to the related slots, and where each directed arc in A_e corresponds to a flight plan (f, p) that switches from the tail-slot to the head-slot. For example, Figure 5-3 illustrates a particular exchange graph in which, for instance, arc (1,4) corresponds to Flight A1 adopting a designated flight plan that arrives at the GDP destination airport at time 0812. Note that in case we wish to consider multiple flight plans corresponding to a given slot-trade (or arc) that might differ in their trajectories and departure times, we will maintain multiple corresponding arcs, each representing the particular plan. Observe that we do not construct self-loop arcs pertaining to plans that retain the associated assigned slot for the corresponding flight in this approach. The x_{fp}-variables pertaining to such flight plans would be directly accommodated within (2.5b), and if set equal to one, would therefore automatically imply the retention of the allocated slot. Since the selected flight plans that constitute a valid exchange scheme within any graph G_e would be represented by directed cycles, with a node being involved in at most one such cycle, we formulate the following constraints:

$$\sum_{(f,p)\in R_k^e} x_{fp} = \sum_{(f,p)\in F_k^e} x_{fp} \le 1, \quad \forall k \in N_e, \quad \forall e = 1,...,E \tag{5.16}$$

where for each $e = 1,...,E$, and $k \in N_e$, we have

$$R_k^e = \{(f,p) : x_{fp} \text{ corresponds to a "reverse" arc coming into node } k\} \tag{5.17}$$

$$F_k^e = \{(f,p) : x_{fp} \text{ corresponds to a "forward" arc going out of node } k\}. \tag{5.18}$$

Hence, (5.16) requires flows to be circulatory, and to have at most a unit flow in each circulation or cycle, with at most one cycle involving any particular node.

However, we also want to ensure that the trades prompted by the selected directed cycles satisfy the trade restrictions. Toward this end, let

$$D = \{f : \text{flight } f \text{ is offered to be delayed}\} \tag{5.19}$$

and for each $f \in D$, let

$$H_f = \{(f', p') : \text{at least one of these flight plans } p' \text{ of flight } f' \text{ belonging to the same airline must be selected in order to accept delaying flight } f\}. \tag{5.20}$$

Note that for any distinct flights f_1 and f_2 in D, we assume that $H_{f_1} \cap H_{f_2} = \emptyset$. Hence, an upward-move cannot by itself compensate for more than one downward-move. Also, let

$$D_f = \{p : \text{plan } p \text{ corresponds to the delay of } f\}, \forall f \in D. \tag{5.21}$$

Hence, in any of the exchange graphs, if for some flight $f \in D$, we have that $x_{fp} = 1$ for any $p \in D_f$, then at least one of $x_{fp'}$ for $(f', p') \in H_f$ must also be 1. This is enforced by the constraints

$$\sum_{p \in D_f} x_{fp} \leq \sum_{(f', p') \in H_f} x_{fp'}, \quad \forall f \in D. \tag{5.22}$$

While some slot exchanges may result in a significant improvement by reducing the net delay in passenger-minutes, the structure of the individual trade offers may result in a net increase in passenger-minutes of delay for one or more airlines. In some instances, this might be acceptable for the corresponding airline as long as that airline's primary concern was the acquisition of any earlier designated slot for the flight identified for an upward-move, in exchange for any designated later slot for the corresponding flight identified for the downward-move in the related offer. However, we could impose an additional restriction that for each airline, the realized net reduction in passenger-minutes of delay at the GDP-imposed airport due to upward- and downward-moves resulting from slot exchanges should be nonnegative. To model this restriction, as well as our alternative equity concepts (formulated in Section 5.3), let us define the following additional parameters and coefficients, where all delays are measured with respect to the published OAG schedule.

A^{tr}: The set of airlines involved in the trade offers.

PAX_f: The number of passengers associated with flight *f*.

D_{fp}: The delay (minutes) for plan *p* of flight *f* relative to the published OAG schedule. (Note that $D_{fp} \geq 0, \forall (f, p).$)

D_f^{GDP}: The delay (minutes) for flight *f* based on the GDP assigned slot.

The restriction on achieving a nonnegative *net reduction in passenger-minutes* (NRPM) of delay at the GDP airport for each airline can be formulated as follows:

$$NRPM_\alpha \equiv \sum_{f \in D \cap A_\alpha} \left\{ \sum_{p \in D_f} PAX_f \left[D_f^{GDP} - D_{fp} \right] x_{fp} + \sum_{(f',p') \in H_f} PAX_{f'} \left[D_{f'}^{GDP} - D_{fp'} \right] x_{fp'} \right\} \geq 0, \forall \alpha \in A^{tr}. \quad (5.23)$$

Alternatively, given each offer of downward- and upward-moves, to complement (5.22), we could require that the corresponding net reduction in passenger-minutes of delay, given by $\{\cdot\}$ in (5.23), should be nonnegative. This would permit the corresponding airline making the offer to specify additional downward-move slots for the related $f \in D$, while ensuring that any such accepted delay is adequately compensated by an associated upward-move in terms of the resulting net reduction in passenger-minutes of delay. This constraint can be formulated as follows, noting that this restriction requires each term within $\{\cdot\}$ in (5.23) to be nonnegative, as opposed to the sum of such terms over $f \in D \cap A_\alpha, \forall \alpha \in A^{tr}$.

$$\sum_{p \in D_f} PAX_f [D_f^{GDP} - D_{fp}] x_{fp} + \sum_{(f',p') \in H_f} PAX_{f'} [D_{f'}^{GDP} - D_{fp'}] x_{fp'} \geq 0, \forall f \in D. \quad (5.24)$$

Observe that since $PAX_f [D_f^{GDP} - D_{fp}] < 0, \forall p \in D_f$, and $PAX_{f'} [D_{f'}^{GDP} - D_{fp'}] > 0, \forall (f', p') \in H_f$, (5.24) implies (5.22) in the integer sense, but not necessarily in the continuous sense of a linear programming (LP) relaxation. Hence, even when we use (5.24), we retain (5.22) in order to tighten the underlying LP relaxation. In Chapter 6, we experiment with the inclusion of either (5.23) or (5.24) in the overall model formulation to provide related insights on the effect this has on the resulting solutions.

Remark 1. Note that different flights typically have different fare-class passengers, and it might be in the interest of airlines to consider this feature in accounting for the economic consequence of passenger delays. To accomplish this, instead of defining PAX_f simply as the number of passengers associated with flight *f*, we could compute this value as the total passenger revenue associated with flight *f* divided by the basic coach fare for that flight. This redefined value of

PAX_f could then be used in (5.23) and (5.24) above, as well as in the equity formulations discussed later in Section 5.3. □

Accordingly, we formulate the *slot-exchange APCDM model* (designated **SE-APCDM**) as given by (2.5a-2.5o) plus (5.16) and (5.22), and optionally, (5.23) or (5.24). Note that in (2.5b), the set P_{f0} now includes all plans that represent either slot-trades or (possibly multiple) alternatives corresponding to retaining the assigned slot at the GDP airport, for each flight *f*. Moreover, the objective function considers the overall equity achieved among the airlines in this slot-exchange bartering process, and the model also ensures that the mix of flight plans selected are compatible with sector workload and conflict risk considerations.

To illustrate the concept of using multiple exchange graphs along with the foregoing slot-exchange mechanism, consider the set of trade offers depicted in Figure 5-6. The trade offers submitted between 0800 and 0828 (above the line) are those specified in the previous example (see Figure 5-2). In addition, we have multiple "at-least, at-most" offers from Airlines A and C as depicted in the lower half of Figure 5-6. The trade offers of Figure 5-6 are represented by the two disjoint directed graphs G_1 and G_2 displayed in Figure 5-7. For the sake of illustration, we have included multiple arcs from node 11 to node 9 in G_2 to represent multiple possible surrogate flight plans for Flight A4 of Airline A, all of which have an arrival time of 0832.

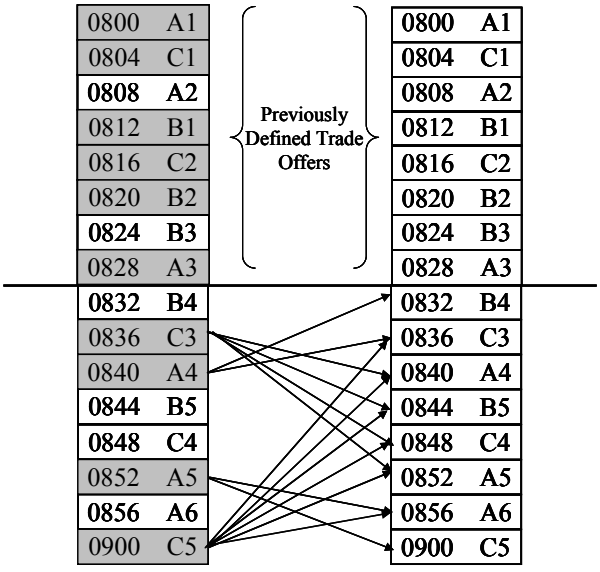

Figure 5-6: Expanded Trade Offer Example.

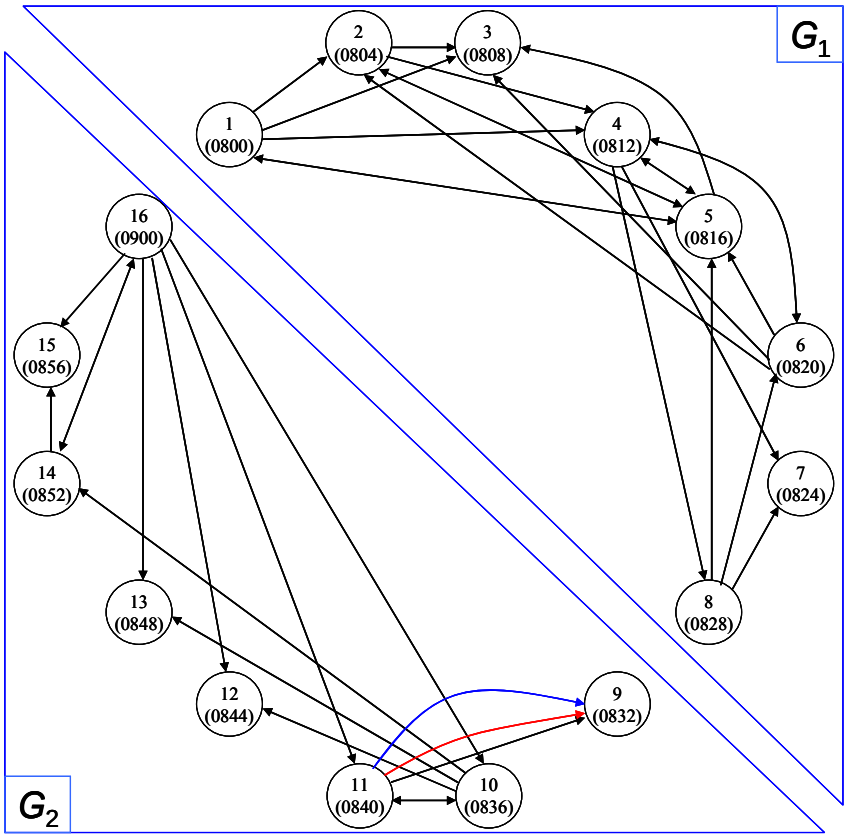

Figure 5-7: Slot Offer Network for Expanded Example.

To illustrate the generation of the circulatory flow constraint (5.16), consider node 11 from graph G_2. Recall that the primary inputs for APCDM are the surrogate flight plan sets P_{f0} associated with the flights $f \in F$, and that each arc in the slot offer network represents a specific plan for a given flight. For illustrative purposes, we have extracted node 11 and its adjacent nodes from Figure 5-7 and have depicted this relevant portion of G_2 in Figure 5-8, where we have additionally affixed a label on each incident arc that lists the specific flight name and the flight plan number corresponding to the slot arrival time associated with the node. Notice the inclusion of the multiple flight plans (designated 2, 3, and 4) for Flight A4, which pertain to Airline A having submitted three separate flight plans with a slot arrival time of 0832. Observing Figure 5-8, we have the following sets for node 11 (k = 11) in graph G_2 (e = 2) as defined in equations (5.17) and (5.18):

$$R_{11}^2 = \{(C5,2),(C3,1)\} \quad \text{and} \quad F_{11}^2 = \{(A4,1),(A4,2),(A4,3),(A4,4)\}.$$

The corresponding circulatory constraint (5.16) for k = 11 and e = 2 is thus given by

$$x_{C5,2} + x_{C3,1} = x_{A4,1} + x_{A4,2} + x_{A4,3} + x_{A4,4} \le 1.$$

To illustrate further, consider next the generation of the trade restriction constraint (5.22) for f = A5 $\in D$, where from equations (5.19) – (5.21) and figures 5-6 thru 5-8, we have

$$D = \{A1, B1, C1, C3, A5\}, \quad H_{A5} = \{(A4,1),(A4,2),(A4,3),(A4,4)\} \quad \text{and} \quad D_{A5} = \{1,2\}.$$

The associated trade restriction constraint (5.22) can then be stated as follows:

$$x_{A5,1} + x_{A5,2} \le x_{A4,1} + x_{A4,2} + x_{A4,3} + x_{A4,4}\,.$$

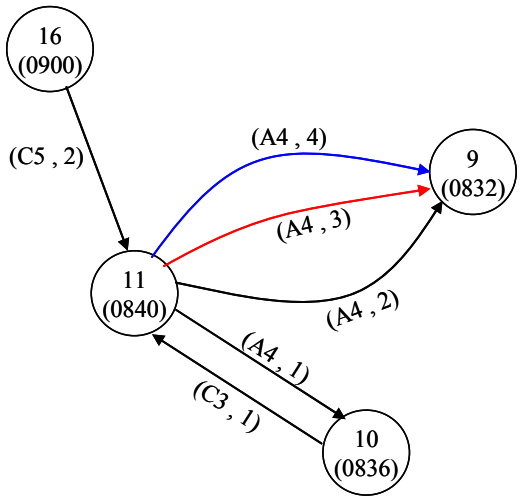

Figure 5-8: Flight and Plan Specification Labels.

For the example depicted in figures 5-6 and 5-8, we formulated the complete set of circulatory flow constraints (5.16) and the trade restriction constraints (5.22). In addition, we included the APCDM selection constraint (2.5b). For illustrative purposes, we then contrived a simple submodel comprised of just these constraints, and with an objective function to maximize the number of allowable trades, as represented by the sum of the x_{fp}-variables associated with flight plans that are involved in a trade. The solution generated by solving the resulting submodel using CPLEX 9.0 is shown in Figure 5-9. The list on the right side of Figure 5-9 highlights those slots that were traded along with the corresponding newly assigned flights.

We now proceed to present various equity issues corresponding to slot exchanges, followed by some computational experience on embedding this slot-exchange mechanism within APCDM, resulting in the selection of a set of "trade-accepted" flight plans feasible to sector workload, conflict risk, and equity considerations.

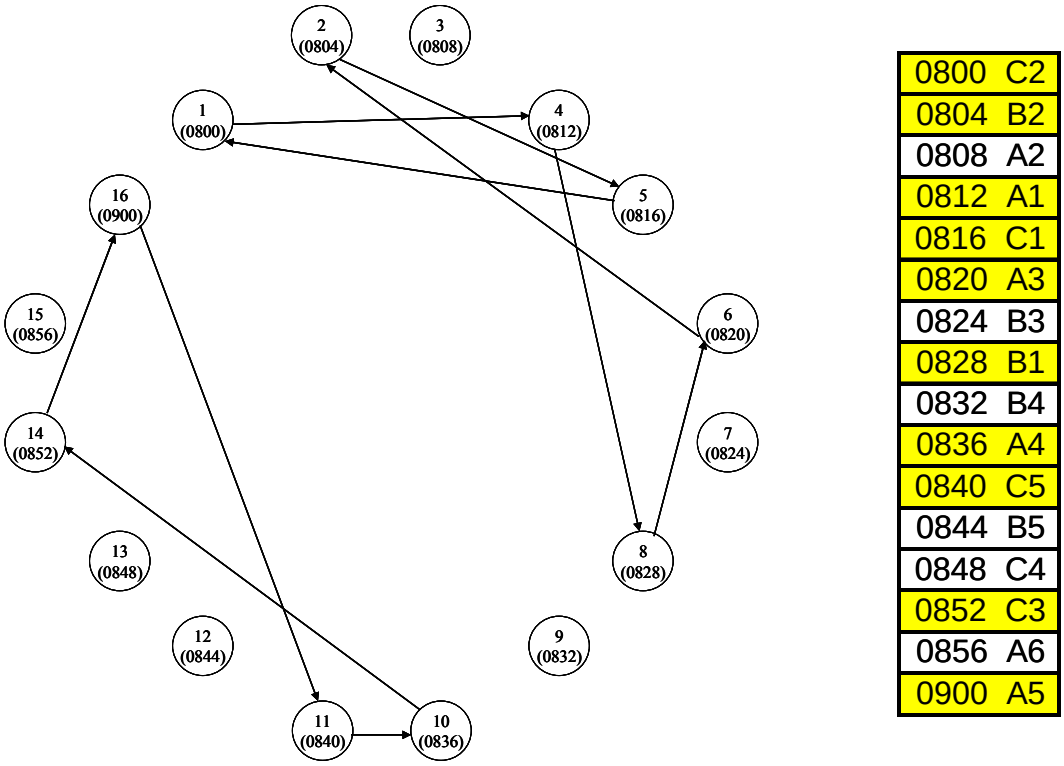

Figure 5-9: Example Results.

5.3. Equity Within Slot Exchanges

Given a set of trade offers, the ideal situation regarding slot exchanges would be represented by the solution in which every airline incurs only slight increases in delays for the flights offered for downward-moves, while receiving more significant reductions in the delays for flights offered for upward-moves. This ideal situation portrays an instance where both equity and efficiency are achieved simultaneously. Unfortunately, this situation is rarely achievable and more often than not, the antithetical situation occurs for one or more airlines involved. When addressing equity issues, Vossen et al. (2002), Tadenuma (1998), and others agree that efficiency and equity habitually conflict in that attempts to improve equity amongst the participants vying for a resource typically results in a reduction in the efficient distribution of that resource. Luss (1999) discusses the shortfalls when applying minimax objective functions to situations involving equity, and subsequently provides a lexicographic minimax solution approach, which can be applied to both single and multiple resource problems.

In our situation involving possible slot exchanges, the resource considered is the collection of available arrival slots. Vossen (2002) claims that the primary problem governing equity within resource apportionment resides in the "indivisibility" of the resource. Hence, the problem becomes one in which an equitable solution attempts to attain at least a perceived quota for every participant involved (i.e., everyone receives a fair share). Since each airline that submits a trade offer is allocated at least two slots at the arriving airport, our situation is not necessarily dependent on satisfying a quota in terms of the number of slots, but rather, also involves achieving equity within other "resource" categories such as fuel and delay costs as a result of the trade. We prescribe five equity concepts with respect to potential slot exchanges, which rely on both existing approaches as well as newly developed ideas.

Our first equity concept utilizes the collaboration efficiency paradigm that is embedded in the original APCDM model. The collaboration efficiency for each airline is based on the fuel and delay costs incurred in the overall solution prescribed by the model in comparison to the corresponding costs related to individually optimized decisions. Sherali et al. (2006) determine the total cost of executing a flight plan p of flight f as

$$c_{fp} = F_{fp} + D_{fp}, \quad \forall p \in P_f, f = 1,..., F, \tag{5.25}$$

where F_{fp} and D_{fp} are the associated fuel and delay costs, respectively. Note that while operating under a GDP, the delay is given by the (likely positive) difference between the scheduled arrival time and the actual arrival time, where the latter is either the arrival time corresponding to the allocated slot from RBS and Compression, or that pertaining to a new slot obtained via a slot exchange. Therefore, using the scheduled arrival time for each flight as an input, we can determine both the fuel and delay cost depending on the selected flight plan as prescribed in Sherali et al. (2006), and use the APCDM model's collaboration efficiency-based equity formulations. This modeling construct is summarized below and is used as a foundation for several alternative equity formulations as discussed subsequently.

Given the cost factor specified in Equation (5.25), let us define a *relative performance ratio* as follows, where $c_f^* \equiv \min_{p \in P_f} \{c_{fp}\}, \forall f$

$$d_\alpha(x) = \frac{\sum_{f \in A_\alpha} \sum_{p \in P_{f0}} W_f c_{fp} x_{fp}}{\sum_{f \in A_\alpha} W_f c_f^*}, \forall \alpha = 1,..., \overline{\alpha}. \tag{5.26}$$

Based on this ratio, we define the *collaboration efficiency* as a linear function (see Figure 5-10) for each airline α according to

$$E_\alpha(x) = \frac{D_{\max} - d_\alpha(x)}{D_{\max} - 1}, \forall \alpha = 1,..., \overline{\alpha}. \tag{5.27}$$

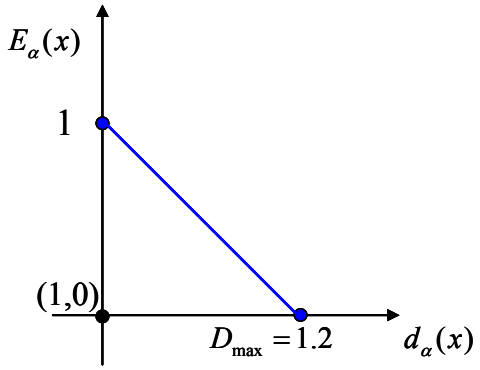

Figure 5-10: Collaboration Efficiency.

Accordingly, we then define the *collaboration equity* function as

$$E^e_\alpha(x) = E_\alpha(x) - \sum_\alpha \omega_\alpha E_\alpha(x), \tag{5.28}$$

and incorporate these efficiency and equity functions within the objective function using the terms

$$\mu^D \sum_\alpha \omega_\alpha [1 - E_\alpha(x)] + \mu^e \sum_\alpha \omega_\alpha \left| E^e_\alpha(x) \right|, \tag{5.29}$$

where, for a specified constant $E^e_{\max}$, we also restrict (as in (2.5o))

$$\omega_\alpha \left| E^e_\alpha(x) \right| \le E^e_{\max}, \forall \alpha = 1,..., \overline{\alpha}. \tag{5.30}$$

Sherali et al. (2006) have conducted sensitivity analyses of the APCDM model using either a constant value for the maximum weighted inequity, $E^e_{\max}$ (prescribed as $E^e_{\max} = 0.07/\overline{\alpha}$), or treating $E^e_{\max}$ as a variable while incorporating an additional objective term $\mu^e_{\max} E^e_{\max}$. For the purpose of considering equity with respect to slot exchanges, we will limit our approach to the case where $E^e_{\max}$ is a constant in order to simply bound the weighted collaboration inequity, $\omega_\alpha \left| E^e_\alpha(x) \right|$, for each airline α, and avoid an additional embedded minimax structure via (2.5a) and (2.5o) when $E^e_{\max}$ is a variable.

The key idea behind the development of our four alternative equity concepts is to specify different performance ratios (5.26) and their related efficiency functions (5.27), and then use the same constructs as embodied by (5.28) – (5.30) above. Toward this end, consider the following alternative definitions (a) – (d), where we focus on delays, assuming that the wind/weather optimized trajectory costs are compatible among the different surrogate plans for each flight. We define the following additional function to model these alternative equity formulations.

$D_f^{CDM}(x) \equiv \sum_{p \in P_{f0}} D_{fp} x_{fp}$: The CDM-realized delay function for flight f.

Method (a). The *relative performance ratio* in this case measures the total average delay realized per passenger (or per weighted passenger – see Remark 1), and is given by

$$d_\alpha^1(x) = \frac{\sum_{f \in A_\alpha} (PAX_f) D_f^{CDM}(x)}{\sum_{f \in A_\alpha} (PAX_f)}, \forall \alpha = 1,..., \overline{\alpha}. \tag{5.31}$$

Observe that this performance measure encompasses all the flights $f \in A_\alpha$, for each airline α, as opposed to simply those flights involved with the GDP-imposed airport(s). Accordingly, as depicted in Figure 5-11, we define *efficiency* as

$$E_\alpha^1(x) = \frac{D_{\max}^1 - d_\alpha^1(x)}{D_{\max}^1}, \forall \alpha = 1,..., \overline{\alpha}, \tag{5.32}$$

where $D_{\max}^1$ is some maximum passenger delay tolerance. We will explore different values for this tolerance based on a computational sensitivity analysis.

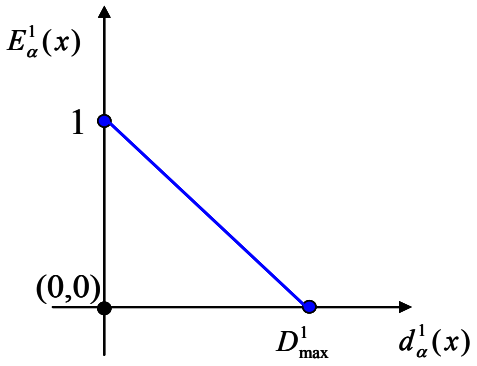

Figure 5-11: Efficiency Based on Average Delay per Passenger.

Method (b). The *relative performance ratio* in this case represents the net savings in delay per passenger due to slot exchanges, and is given by

$$d_\alpha^2(x) = \frac{\sum_{f \in A_\alpha} (PAX_f)[D_f^{GDP} - D_f^{CDM}(x)]}{\sum_{f \in A_\alpha} (PAX_f)}, \tag{5.33}$$

where for any flight not associated with the GDP-imposed airport(s), D_f^{GDP} corresponds to the delay with respect to the OAG schedule for the nominally assigned slot at that airport. (Possibly, $D_f^{GDP} = 0$.) Note from equations (5.31) and (5.33) that

$$d_\alpha^2(x) = \frac{\sum_{f \in A_\alpha} (PAX_f) D_f^{GDP}}{\sum_{f \in A_\alpha} (PAX_f)} - d_\alpha^1(x) \equiv \left(D_{\max}^2\right)_\alpha - d_\alpha^1(x), \text{say}, \forall \alpha = 1,..., \overline{\alpha}\,. \tag{5.34}$$

Let us assume that $0 < (D_{\max}^2)_\alpha < D_{\max}^1, \forall \alpha = 1,..., \overline{\alpha}$, else, this method shall revert to using Method (a). Now, when $d_\alpha^2(x) = 0$, i.e., $d_\alpha^1(x) = \left(D_{\max}^2\right)_\alpha$, we have that the CDM-realized average passenger-minutes of delay equals that corresponding to the set of nominally assigned slots. In this event, let us assume that the efficiency achieved is some $100p^*\%$, where $0 < p^* < 1$ (say, $p^* = 0.8$; we shall experiment with different values of $0.5 \le p^* < 1$, which appears reasonable). Then letting *efficiency* be defined as illustrated in Figure 5-12, using the previous relative performance ratio function $d_\alpha^1(x)$ itself in lieu of $d_\alpha^2(x)$, we get:

$$E_\alpha^2(x) = \frac{\left(D_{\max}^2\right)_\alpha - (1 - p^*) d_\alpha^1(x)}{\left(D_{\max}^2\right)_\alpha}, \forall \alpha = 1,..., \overline{\alpha}\,. \tag{5.35}$$

In contrast with Method (a), comparing figures 5-11 and 5-12, observe that the slope of the efficiency curve in Method (b) is different for each airline α, and is governed by the average GDP slot-based delay per passenger $\left(D_{\max}^2\right)_\alpha$ defined in (5.34).

Remark 2. Note that if $p^* = 1 - [(D_{\max}^2)_\alpha / D_{\max}^1]$ for any airline α, then $E_\alpha^2(x) = E_\alpha^1(x)$. Hence, given that $0 < (D_{\max}^2)_\alpha < D_{\max}^1, \forall \alpha = 1,..., \overline{\alpha}$, we could prescribe p^* as an average of the values that match the efficiency curves of methods (a) and (b), i.e., equal to

$$p_{(a)}^* = 1 - \frac{\sum_{\alpha=1}^{\overline{\alpha}} \left(D_{\max}^2\right)_\alpha}{\overline{\alpha}\, D_{\max}^1}. \tag{5.36}$$

We shall also experiment with $p^* = p^*_{(a)}$ in our computations. □

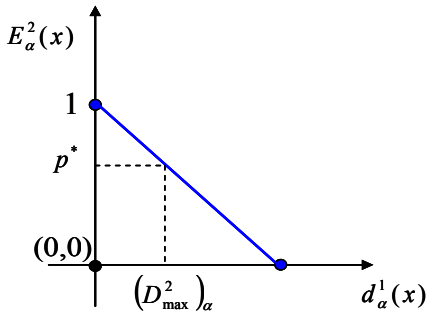

Figure 5-12: Efficiency Based on Net Delay Savings per Passenger.

Method (c). The *relative performance ratio* in this case represents the proportion of downward-moves accepted (in compensation of corresponding upward-moves), and is given by

$$d^3_\alpha(x) = \frac{\sum_{f \in D \cap A_\alpha} \sum_{p \in D_f} x_{fp}}{|D \cap A_\alpha|}, \forall \alpha \in A^{tr}, \tag{5.37}$$

where A^{tr} again is the set of airlines that have submitted trade offers. Note that in achieving equity, the focus here is on the proportion of accepted trade offers at the GDP airport(s), as opposed to the overall impact this has on the average delay per passenger across all flights $f \in A_\alpha$ as assessed by $d^1_\alpha(x)$ and $d^2_\alpha(x)$ in (5.31) and (5.34), respectively. The efficiency measure, $E^3_\alpha(x)$, in this case is also a linear function, but unlike the two previous cases, has a positive slope as shown in Figure 5-13, being simply defined as

$$E^3_\alpha(x) = d^3_\alpha(x), \forall \alpha \in A^{tr}. \tag{5.38}$$

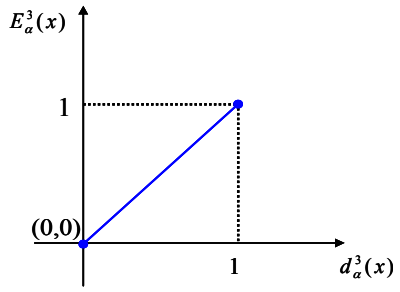

Figure 5-13: Efficiency Based on the Proportion of Downward Trades.

Method (d). The *relative performance ratio* in this case also focuses on GDP airport(s), but measures an average value realized via upward-moves per offered downward-moves, and is given by

$$d_\alpha^4(x) = \frac{\sum_{f \in D \cap A_\alpha} \sum_{(f',p') \in H_f} V_{fp'} x_{fp'}}{\left| D \cap A_\alpha \right|}, \forall \alpha \in A^{tr}, \tag{5.39}$$

where $V_{fp'} \in [0,1]$ is a predefined quantity that corresponds to a discrete, non-decreasing, single dimensional value function, which is based on a delay reduction corresponding to the number of upward-move slots attained by the flight in the particular trade (see Figure 5-14). Noting that the inequality (5.22) is likely to be satisfied as an equality in competitive situations, the definition in (5.39) is a generalization of (5.37), which, in effect, assumes a unit value of $V_{fp'}, \forall (f', p') \in H_f, \forall f \in D \cap A_\alpha$.

The critical requirement associated with this equity method is the generation of the value functions for airlines. Value functions are often used to combine multiple evaluation measures into a single measure. When a value function is based on a single measure, it is more commonly referred to as a single attribute value function (Kirkwood, 1997). Within our slot-exchange construct, an airline's value function that is associated with the slots obtained in an upward-move may be a general function of passenger load, the downstream departure frequency for the affected airport, or other critical parameters. Indeed, the measures $d_\alpha^1(x)$ and $d_\alpha^2(x)$ reflect specific value functions of this type. In the absence of airline input, we shall assume that the value functions across all flights are uniformly evaluated via the function

$$V_{fp'} \equiv 1 - e^{-\lambda \left[D_{f'}^{GDP} - D_{fp'} \right]}, \text{ where } \lambda > 0. \tag{5.40}$$

Figure 5-14 illustrates the impact on the shape of the value function with respect to increasing values of the parameter λ.

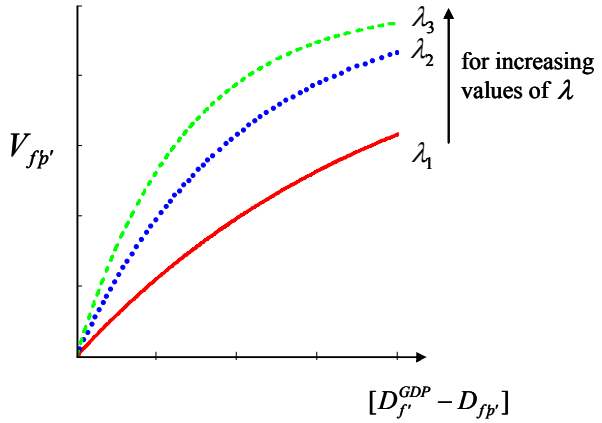

Figure 5-14: Various Value Functions.

Similar to the previous *efficiency* measure, $E^4_\alpha(x)$ is also a linear function with a positive slope as shown in Figure 5-15, and is defined as

$$E^4_\alpha(x) = d^4_\alpha(x), \forall \alpha \in A^{tr}. \tag{5.41}$$

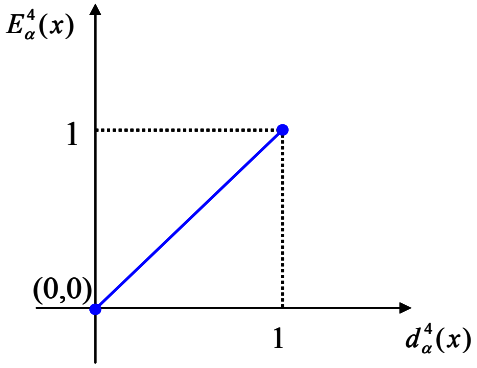

Figure 5-15: Efficiency Based on the Value per Offered Downward-Move.

Note that the value function in (5.40) is a concave function, which intuitively represents diminishing marginal returns as the delay $D_{fp'}$ reduces and the flight time approaches the OAG time. As an alternative to (5.40), we may consider a value function of the form

$$V_{fp'} \equiv 1 - e^{-\lambda\left[D^{GDP}_{f'} - D_{fp'}\right]^q}, q > 1, \text{ where } \lambda > 0, \tag{5.42}$$

which yields a convex-concave function (see Figure 5-16) that represents an increase in marginal returns for initial reductions in delay up to some point, after which diminishing marginal returns sets in for further reductions in delay.

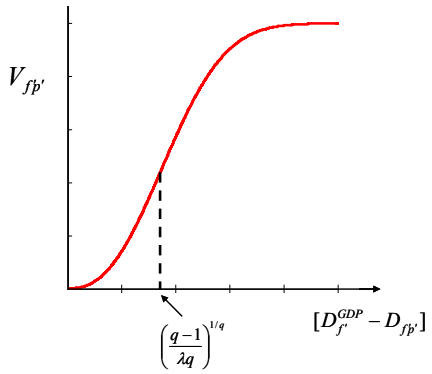

Figure 5-16: Alternative Value Function.

Proposition 1. *Consider the function* $f(x) = 1 - e^{-\lambda x^q}, q > 1,$ *where* $\lambda > 0$ *and where* $x \equiv [D_{f'}^{GDP} - D_{fp'}]$ *in* (5.42). *This function is convex-concave, with the switchover* (*inflection*) *point from convexity to concavity occurring at the point* (*of diminishing marginal returns*) *given by* $x = x_{dmr} \equiv \left(\frac{q-1}{\lambda q}\right)^{1/q}$.

Proof. From calculus, we get $f''(x) = \left(e^{-\lambda x^q}\right)\lambda q x^{q-2}\left[q - 1 - \lambda q x^q\right]$. The proof follows noting that $f''(x) = 0$ for $x = x_{dmr}$ as defined in the proposition, where $f''(x) \geq 0$ for $x \leq x_{dmr}$ and $f''(x) \leq 0$ for $x \geq x_{dmr}$. □

Remark 3. Using the alternative value function in (5.42) in conjunction with Proposition 1, we can allow the airlines to specify their own value function by simply identifying their perceived point of diminishing marginal returns (x_{dmr}) within the trade offer. Let y represent the largest reduction of delay that an airline can obtain through a slot exchange based on the flight's arrival time listed in the OAG. Since $f(x)$ as defined in Proposition 1 asymptotically approaches the value of one, we must specify a value for $f(y) < 1$. Given $x_{dmr} < y$ and the value at $f(y)$ we can then determine the parameters q and λ (see Proposition 2), which define an airline specific value function for each plan p' that represents an upward-move for a given flight f'. Figure 5-17 depicts three particular value functions for different values of x_{dmr}, while maintaining a constant value for y and selecting $f(y) = 0.95$. □

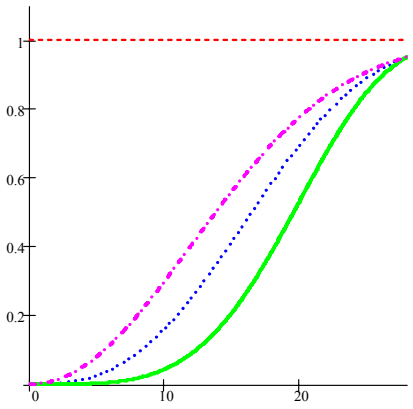

Figure 5-17: Example of Airline Specific Value Functions.

Proposition 2. *Given* $x_{dmr} < y$ *and* $f(y) = \theta$, *the corresponding parameters* q *and* λ *in* (5.42) *exist and are unique*.

Proof. From Proposition 1, we get $\lambda = \dfrac{q-1}{q x_{dmr}^{q}}$. Substituting for λ in $f(y) = \theta$ and solving for q, we get $\left(\dfrac{y}{x_{dmr}}\right)^{q} = \dfrac{-\ln(1-\theta)q}{(q-1)}$. Defining $h(q) = \left(\dfrac{y}{x_{dmr}}\right)^{q} + \dfrac{\ln(1-\theta)q}{(q-1)}, q > 1$, we then check the properties of $h(q)$ to show that a unique root exists. Because $y > x_{dmr}$, and $0 < \theta < 1$, $h(q) \to \infty$ as $q \to \infty$ and $h(q) \to -\infty$ as $q \to 1^{+}$. Therefore, a root exists. Its uniqueness follows by noting that $h'(q) = \left(\dfrac{y}{x_{dmr}}\right)^{q} \ln\left(\dfrac{y}{x_{dmr}}\right) - \dfrac{\ln(1-\theta)}{(q-1)^{2}} > 0$, since $x_{dmr} < y$, $q > 1$, and $0 < \theta < 1$. □

Remark 4. Adapting an alternative general equity formulation presented by Luss (1999), we could explore lexicographically maximizing the vector corresponding to a non-decreasing arrangement of some equity factor for each airline involved (where larger values are more preferable). To implement such a lexicographic optimization procedure, once we have maximized the minimum value for this equity factor, we could constrain all equity factors to take on at least this value, determine the set of airlines that could then achieve a strictly higher value, and subsequently maximize the minimum equity measure among the remaining airlines. This iterative process could be continued until optimality is attained, as indicated by the latter set of remaining airlines becoming null. Observe that this would require multiple runs of APCDM,

which might be suitable only for strategic planning purposes, and that might require some heuristic implementation in tactical contexts. □

Remark 5. Additional perceived equity issues arise in situations when airlines are allocated a greater portion of available slots at an airport, and thus have potentially greater flexibility regarding trade offers. However, recalling that the allotted slots are assigned using RBS and Compression, which is based on the scheduled arrival times listed in the OAG, the FAA traffic flow managers and the airlines have come to a consensus that these two enhancements to the GDP achieve an equitable initial distribution of slots (Vossen and Ball, 2001). Therefore, we will not address the initial distribution of slots as an equity-producing option. □

We now proceed to present computational results related to our proposed slot-exchange mechanism and equity concepts, and provide insights into the effects of alternative modeling constructs and parameter settings.

Chapter 6
Computational Results, Sensitivity Analyses, and Insights

In this chapter, we demonstrate the functionality of our proposed slot-exchange mechanism and related equity concepts in support of the tactical level decision-making process related to GDPs. We begin by evaluating a relatively small test set and computing the pertinent performance metrics in order to compare the SE-APCDM model solutions within, and across, each equity method as prescribed in the previous chapter. Furthermore, we impose the nonnegativity restrictions on the slot exchanges and evaluate the impact of these restrictions upon the resulting solutions. Next, we address the sensitivity of our solutions to changes in the equity cost factors for the original test set and, subsequently, a second test set characterized by an increase in slot competition. We conclude by evaluating a larger test set that closely resembles a scenario in which an airport is operating near a specified FAA-benchmarked capacity. Additionally, we evaluate and compare the computational-effort performance, under both time limits and optimality thresholds, for each equity approach in order to obtain further insights regarding potential improvements to the overall efficiency of the SE-APCDM model. All reported computations have been performed on a Dell PWS650 Workstation equipped with a 2.4 GHz Xeon processor and 1.5 Gb Random Access Memory, and running the Microsoft Windows XP operating system. The optimization problems were solved using CPLEX 9.0.

6.1. Test Data Sets

For our computational experiments, we constructed three basic scenarios as shown in Table 6-1, using real data obtained from the FAA based on the Enhanced Traffic Management System (ETMS) flight information pertaining to the Miami and Jacksonville Air Route Traffic Control Centers (ARTCC). From this data, we selected flight trajectories that traverse through a subset of the 88 sectors that comprise the two aforementioned ARTCCs. Adjustments to the flight data with respect to the arrival times were made in order to account for the slot allocations as per the assumed imposed GDP.

For the purpose of testing the slot-exchange modeling constructs, our first test set consists of 30 flights, in which 16 of the flights have been allocated arrival slots into Miami based on a hypothetical FAA-imposed GDP having a duration of one hour. Additionally, eight flights

depart from Miami within the one-hour interval. The arrival slots are at four minute increments, which satisfies Miami's reported airport arrival capacity when operating at an Instrument Flight Rules (IFR) rate shown in Figure 6-1. The solid line represents the calculated capacity while the solid dot represents the airport's reported capacity. As long as the point specified by the two-tuple (Departures per Hour, Arrivals per Hour) lies within the boundary defined by the solid line (for example, the point (40, 40) lies within this boundary, while the point (60, 60) lies outside it), we can state that the two-tuple satisfies the airport's IFR rate. For our second test set, we modified the first test set by adjusting the trade offers in order to increase slot competition between airlines. Our final test set was constructed by restricting the maximum IFR arrival and departure capacities for the airport of interest.

Table 6-1: Test Data Sets for Slot-Exchange Evaluations.

	Test Set #1	Test Set #2	Test Set #3
Number of Flights	30	30	110
Surrogates per Flight	6	6	6
Number of Airlines	5	5	6
Number of Flights Arriving Miami	16	16	40
Airlines: Flights per Airline	AAL: 10 DAL: 5 NWA: 5 UAL: 7 USA: 3	AAL: 10 DAL: 5 NWA: 5 UAL: 7 USA: 3	AAL: 24 COA: 16 DAL: 23 NWA: 14 UAL: 17 USA: 16
Time Horizon	900 minutes	900 minutes	1200 minutes
Number of Conflicts* Identified (using the Probabilistic Aircraft Encounter Module of APCDM)	Level 1: 143 Level 2: 506 Fatal: 40	Level 1: 147 Level 2: 669 Fatal: 8	Level 1: 2868 Level 2: 544 Fatal: 60

* Level 1: Based on FAA's standard separation criteria;
Level 2: Based on halving Level 1's criteria;
Fatal: Unacceptably close encounter.

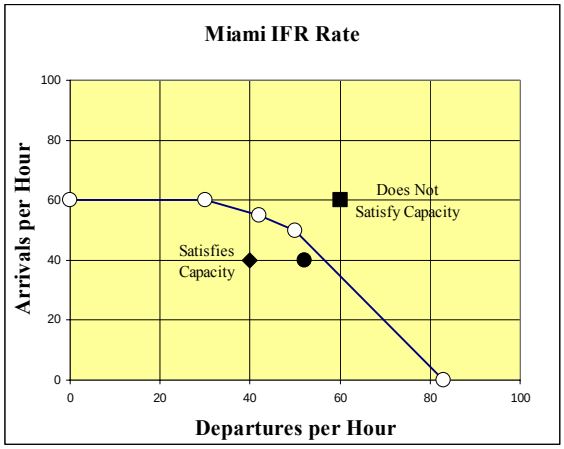

Figure 6-1: Miami IFR Rate.

Adopting the baseline threshold probabilities $p_{\text{thresh}} = \{p_1, p_2, p_{\text{fatal}}\} = \left\{1/3, 1/6, 1/18\right\}$ as recommended in Sherali et al. (2006) and 15 rectangular probabilistic realizations, the PAEM determined the number of conflicts (as shown in Table 6-1) in 71.4 cpu seconds. Given that there were no modifications made to the PAEM as part of this proposed slot-exchange approach, the relationship between the number of probabilistic realizations and the cpu time will continue to be an increasing quadratic relationship as described in Sherali et al. (2006). Regardless of which equity approach was applied within the model formulation, SE-APCDM successfully generated a feasible set of slot exchanges while considering both sector workloads and conflict resolutions. The solution characteristics and the computational times required to generate acceptable slot exchanges varied with the alternative equity approaches as discussed in the following sections.

6.2. Computational Results Using Test Set #1

The strategic level application of the APCDM model assumes various passenger load estimates, l_f, based on aircraft types, as opposed to determining actual passenger loads for each evaluated flight *f*. However, because an airline will more than likely submit a trade offer based upon the desire to reduce the delay of a flight at or near capacity, the tactical level application of the SE-APCDM model will require actual passenger loads for each flight arriving at the GDP affected airport. Therefore, the SE-APCDM model accordingly modifies the flight plan cost c_{fp} by replacing the aircraft passenger load estimate (utilized within the formula for c_{fp}) with the respective number of passengers for all flights *f* assigned to a GDP arrival slot. Table 6-2 provides the number of passengers for the flights offered for downward-moves and upward-moves, respectively, as well as the total number of passengers arriving for each airline at the GDP affected airport for the test set described in Table 6-1.

Table 6-2: Passenger Numbers for Test Set 1 at GDP Airport.

	AAL	DAL	NWA	UAL	USA
PAX in Downward-Move Offers	138	151	153	120	136
PAX in Upward-Move Offers	275	261	250	310	265
Total PAX Arriving GDP Airport	835	412	583	955	401

6.2.1. Results Using the Equity Concept in the Original APCDM Model

We first examined the generation of acceptable slot exchanges using the APCDM model's existing equity concepts as described in Sherali et al. (2003). The corresponding version of SE-APCDM produced the results shown in Table 6-3 (in 5.20 cpu seconds), which provide the time differences between the offered slots and the slots generated by the SE-APCDM based on the trade realizations for the downward-moves and upward-moves for each participating airline, designated Δ_D and Δ_U, respectively. Note that the quantities Δ_D and Δ_U displayed row-wise in Table 6-3 are computed via (5.24) as $\Delta_D \equiv \sum_{p \in D_f} [D_f^{GDP} - D_{fp}] x_{fp}$ and $\Delta_U \equiv \sum_{(f',p') \in H_f} PAX_{f'} [D_{f'}^{GDP} - D_{fp'}] x_{fp'}$ for each $f \in D$. Because each airline designates only one downward-move flight in this test set, these Δ_D and Δ_U are individual airline measures as well in this case. We also compute the net reduction in terms of passenger-minutes of delay for each airline α as given by $NRPM_\alpha$ via Equation (5.23). For example, the improvement for NWA is computed as follows: $-12 * 153 + 4 * 250 = -836$. The total improvement over all participating airlines is 4,404 passenger-minutes. Observe that AAL and UAL improve significantly at the expense of NWA. In addition, AAL is able to reduce the delay of a later flight without having to incur additional delays to the flight it offered for a downward-move. As a percentage of the total improvement, AAL and UAL improved 49.95% and 69.02%, respectively, while NWA had a net percentage improvement of -18.98%.

Table 6-3: SE-APCDM Results using APCDM Equity Approach.

Airline	Downward-Moves			Upward-Moves			
α	Offered	SE-APCDM	Δ_D (min)	Offered	SE-APCDM	Δ_U (min)	$NRPM_\alpha$
AAL	10:00	10:00	0	10:28	10:20	8	2200
NWA	10:04	10:16	-12	10:16	10:12	4	-836
UAL	10:12	10:28	-16	10:20	10:04	16	3040
USA	10:36	10:36	0	11:00	11:00	0	0
DAL	10:52	10:52	0	10:40	10:40	0	0

6.2.2. Total Average Delay-based Equity Formulation Results: Method (a)

Note that feasibility to $E_\alpha^1(x) \geq 0$ (Equation (2.5o)) requires via (5.32) that $d_\alpha^1(x) \leq D_{\max}^1$. Therefore, we began our analysis in this section with a value of $D_{\max}^1$ just large enough to assure feasibility with respect to a solution set corresponding to the selection of the

cancellation surrogate for each flight, which itself represents an upper bound on $D^1_{\max}$. We then proceeded to generate solutions based on varying values of $D^1_{\max}$ using a multiplicative scaling factor, $D^1_{\max} adjustment > 0$. Fractional values of this factor were also explored until the problem became infeasible. Figure 6-2 displays the total net reduction in passenger-minutes of delay for varying values of $D^1_{\max} adjustment$. The solution set of slot exchanges did not change for adjustment factors greater than 2.0. Likewise, for this test set, adjustment factors less than 0.25 resulted in problem infeasibility.

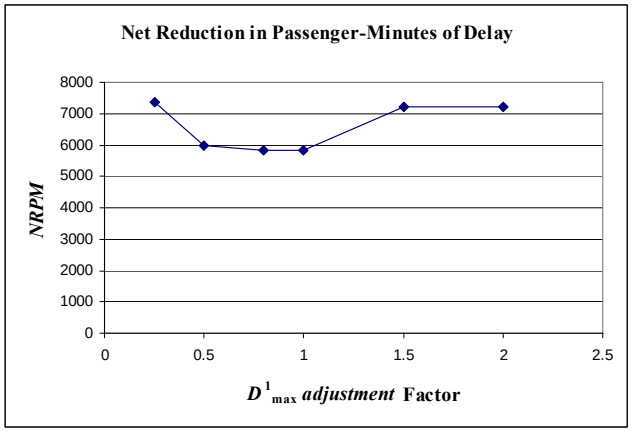

Figure 6-2: Total Net Reduction in Passenger-Minutes of Delay per $D^1_{\max}$ *adjustment* Factor.

While the total net reduction (7,364 PAX-minutes of delay) appears to be the greatest for an adjustment factor of 0.25, analysis of the improvement for each airline (see Figure 6-3) indicated that the corresponding slot-exchange solution was the least favorable for NWA. As we increased the adjustment factor from 0.25, SE-APCDM generated different slot-exchange solutions with varying results in the total reduction. Applying adjustment factors of 1.5 and greater, the slot-exchange solution did not change and resulted in a total net reduction of 7,220 PAX-minutes, which is an improvement of 2,816 PAX-Minutes when compared to the original APCDM equity approach. Note that at the upper values for the adjustment factor, it appears that the net reduction is spread more equitably among the participating airlines. Figure 6-4 provides the net reduction percentage (NRP_α) for each airline α as determined by

$$NRP_\alpha \equiv \frac{NRPM_\alpha}{\sum_{\alpha \in A^{tr}} NRPM_\alpha} \cdot 100\%, \forall \alpha \in A^{tr}. \tag{6.1}$$

While both DAL and AAL have net losses at the larger values of $D^1_{\max}adjustment$, these losses are less than those acquired by NWA and DAL when the adjustment factor is 0.25. For this test set, as we increased the value for $D^1_{\max}adjustment$, the number of slots exchanged between airlines increased until all airlines that submitted downward-move offers achieved an accepted downward-move in exchange for an upward-move. Additionally, the computational time decreased as a function of the adjustment factor as shown in Figure 6-5. In summary, it appears from this example that the larger values of $D^1_{\max}adjustment$ result in more equitable trades at a reduction in computational effort.

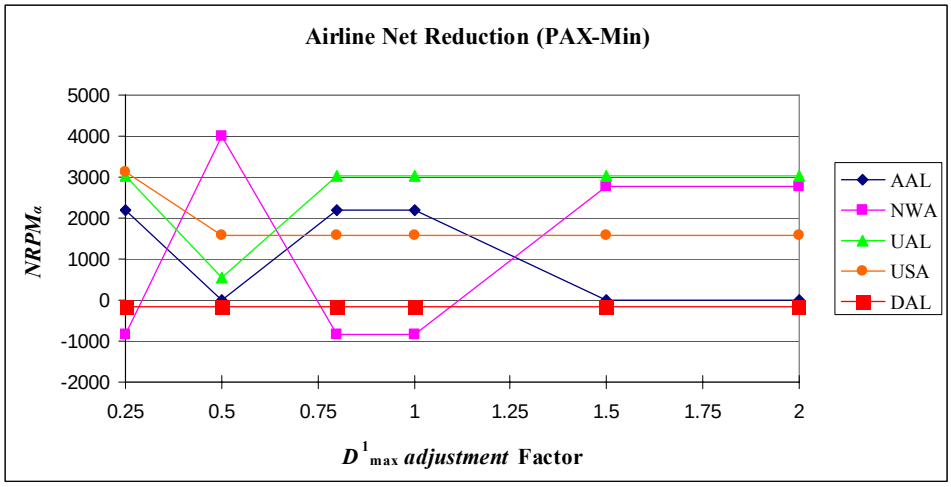

Figure 6-3: Net Reduction of Delay by Airline.

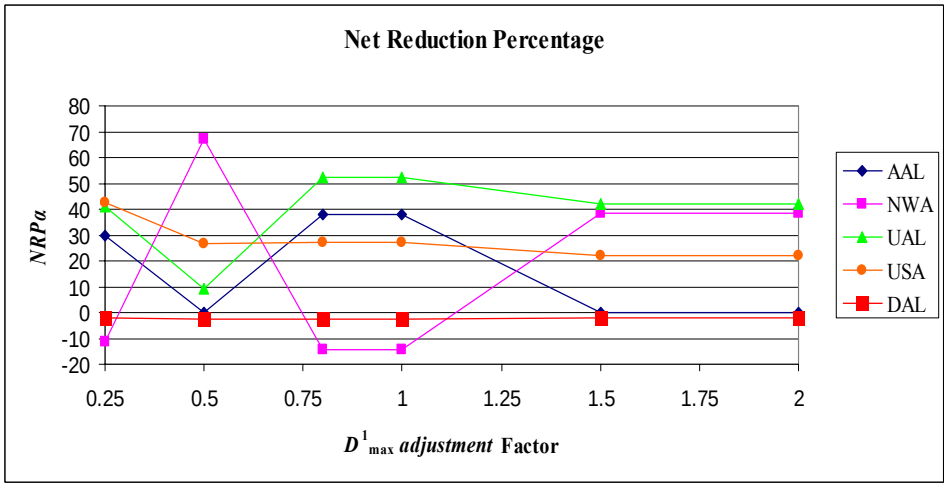

Figure 6-4: Net Reduction Percentage by Airline.

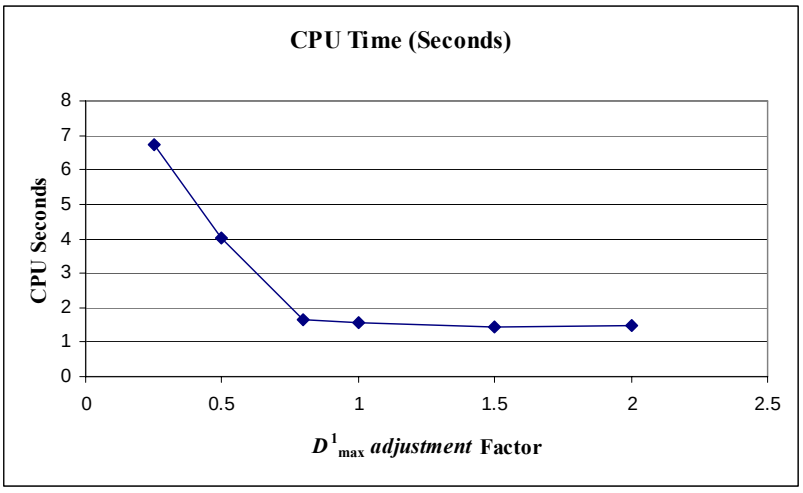

Figure 6-5: Computational Time Versus $D^1_{\max}$ *adjustment* Factor.

6.2.3. Net Delay Savings-based Equity Formulation Results: Method (b)

As described in Section 5.3, this equity formulation focuses on the net savings in delay between the allotted GDP slot time and the slot-exchange time generated by the SE-APCDM model for each flight *f*. Given the structure of this test set, the slot exchanges generated for different values of $p^* \in [0.5, 1)$ were identical. (The value $p^*_{(a)}$ given by (5.36) equals 0.666.) There were, however, variations in the set of optimal plans selected for a subset of the flights not involved in the trade offers as a result of varying p^*. (In a subsequent test set defined in Section 6.3.2, variations in p^* did result in alternative slot exchanges.) The slot-exchange results using this equity formulation are shown in Table 6-4, which equate to a total net reduction of 7,220 PAX-minutes. Note that, in terms of the total net reduction in passenger-minutes of delay, this solution is comparable to the best solution generated using the previous equity approach. However, when experimenting with a value of $p^* = 0$, the solution generated using this equity method was worse than any solution generated using the previous method. This occurs because $p^* = 0$ constrains $d^1_\alpha(x)$ to be less than or equal to the delay $(D^2_{\max})_\alpha$ corresponding to the nominally assigned slots, which severely restricts slot exchanges.

Table 6-4: SE-APCDM Results using Net Delay Savings Equity Approach.

Airline α	Downward-Moves			Upward-Moves			
	Offered	SE-APCDM	Δ_D (min)	Offered	SE-APCDM	Δ_U (min)	$NRPM_\alpha$
AAL	10:00	10:16	-16	10:28	10:20	8	-8
NWA	10:04	10:12	-8	10:16	10:00	16	2776
UAL	10:12	10:28	-16	10:20	10:04	16	3040
USA	10:36	10:40	-4	11:00	10:52	8	1576
DAL	10:52	11:00	-8	10:40	10:36	4	-164

6.2.4. Downward-Move Ratio-based Equity Formulation Results: Method (c)

In this approach, SE-APCDM attempts to equitably increase $d_\alpha^3(x)$ in order to decrease the second cost term in the objective function (2.5a). The upper-bound value for $d_\alpha^3(x)$ and its corresponding efficiency measure $E_\alpha^3(x)$ for each airline is achieved when all downward-moves are accepted. The results obtained using this equity formulation are shown in Table 6-5. The computational time required to generate the solution was 0.875 cpu-seconds. The results were equivalent to those generated using the total average delay equity formulation (Method (a)) with $D_{\max}^1 adjustment \geq 1.5$, which should be expected given that all participating airlines are involved in both downward and upward moves. This equity concept resulted in a total net reduction of 7,220 in passenger-minutes of delay at a slight reduction in computational time for this test set when compared to the solution generated from Method (a) using $D_{\max}^1 adjustment = 1.5$.

Table 6-5: SE-APCDM Results using Downward-Move Ratio Equity Approach.

Airline α	Downward-Moves			Upward-Moves			
	Offered	SE-APCDM	Δ_D (min)	Offered	SE-APCDM	Δ_U (min)	$NRPM_\alpha$
AAL	10:00	10:16	-16	10:28	10:20	8	-8
NWA	10:04	10:12	-8	10:16	10:00	16	2776
UAL	10:12	10:28	-16	10:20	10:04	16	3040
USA	10:36	10:40	-4	11:00	10:52	8	1576
DAL	10:52	11:00	-8	10:40	10:36	4	-164

6.2.5. Upward-Move Value-based Equity Formulation Results: Method (d)

The critical step for this equity approach involves the generation of the value functions for each participating airline. While each airline would undoubtedly want to generate its own value functions in an attempt to influence the resulting slot exchanges, we established a standard value function for all upward-move flights f' as a function of the resulting delay time for each

submitted path p' as defined by (5.40), where the parameter λ is used to generate and test various value functions.

Figure 6-6 displays the total net reduction in passenger-minutes of delay for varying values of the parameter λ. For this test set, as we increased λ, the net reduction in passenger-minutes of delay either decreased or remained the same as a function of the various slot exchanges. This equity approach generated a few slot-exchange solutions that had not yet been realized using the previous approaches given that the SE-APCDM model tried to generate as many upward-moves as possible while limiting the number of downward-moves. This result is expected given that the first term in the objective function (2.5a) is a function of the respective flight delays. Therefore, the SE-APCDM model generates a downward-move, which increases the delay of a specific flight, only when this can be accompanied by beneficial upward-moves. For example, when $\lambda = 0.01$, three upward-moves and two downward-moves were generated. For purposes of comparison, when using Method (c), if three upward-moves are generated, we are guaranteed that three downward-moves will be present in the solution.

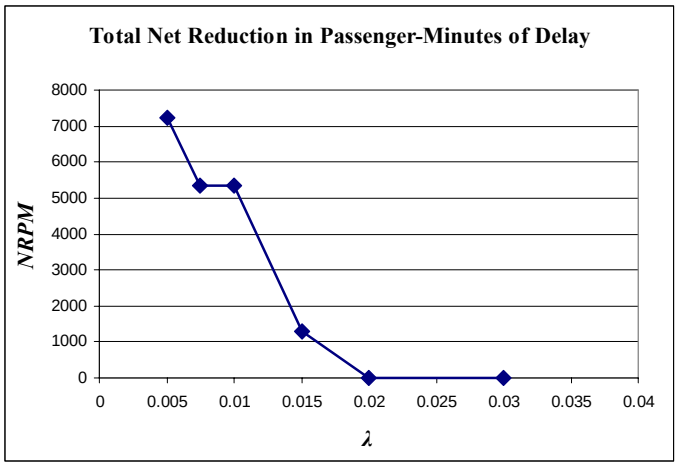

Figure 6-6: Total Improvement for the Parameter λ.

A breakdown of the net reduction in delay by airline (see Figure 6-7) indicated that for the parameter value $\lambda = 0.005$, three of the five airlines achieved a net reduction in delay at the expense of only a relatively small increase in delay for two airlines. When $\lambda \in [0.0075, 0.01]$, the total net reduction decreased; however, four of the five airlines obtained a net reduction in delay, which appears to yield a more equitable slot exchange as depicted in Figure 6-8 when compared with the solutions obtained for lower values for λ. For values of $\lambda \in [0.02, 0.4]$, the airlines maintained their original slots for this test set. As λ was increased beyond 0.5 (not

shown), the resulting slot exchanges were identical to those generated when $\lambda = 0.005$. This occurs due to the shape of the value function for large values of λ in that, there is a rapid increase in value for only minor delay reductions followed by a relatively flat line for the larger delay reductions. In essence, in the absence of any significant differences between the values relative to the potential delay reduction, the SE-APCDM model attempts to find slot exchanges that involve significant improvements in slot times. Additionally, the computational time generally increased as a function of the parameter λ as shown in Figure 6-9.

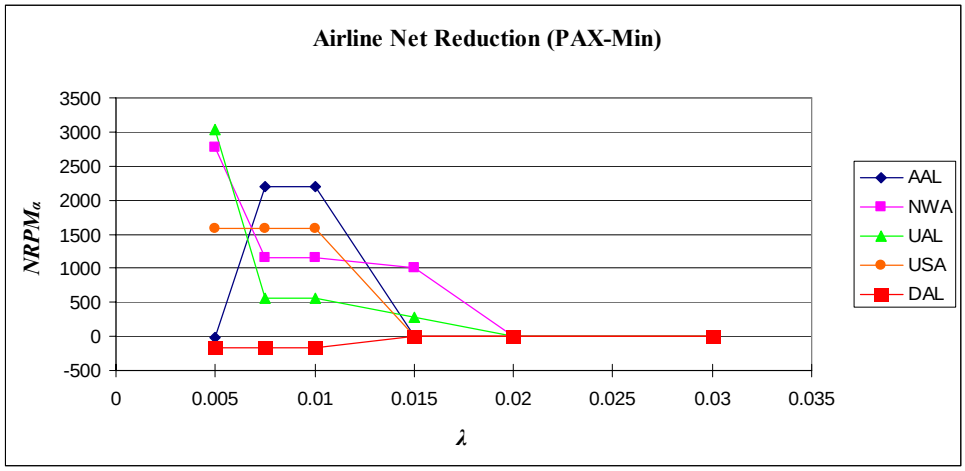

Figure 6-7: Net Reduction of Delay by Airline.

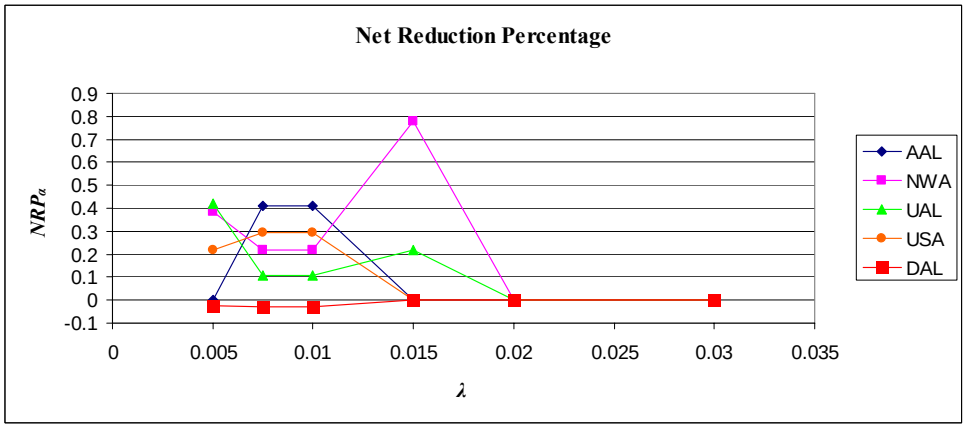

Figure 6-8: Net Reduction Percentage by Airline.

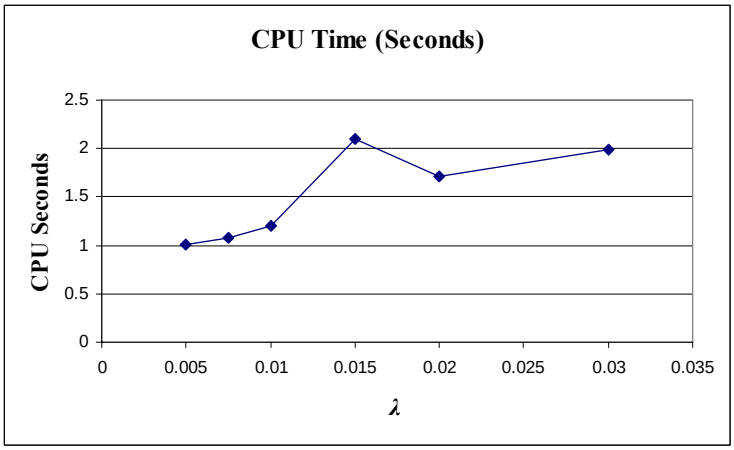

Figure 6-9: Computation Time Versus Parameter λ.

6.2.6. Comparison of the Different Equity Concepts

From the five equity approaches tested within the SE-APCDM model for this test set, the greatest total net reduction in passenger-minutes of delay was generated using Method (a) with $D^1_{\max} adjustment = 0.25$. However, the associated slot exchanges were not as equitable in terms of the net reduction percentage for each airline when compared to other possible solutions generated from the same equity approach. Figures 6-10 and 6-11 display the optimal solutions for each equity approach by airline in terms of the $NRPM_\alpha$-values for each $\alpha \in A^{tr}$, and also the net reduction percentage (NRP_α) for each airline α, respectively. It is readily apparent that, for this test set, the slot exchanges generated from methods (a) – (d) are preferable over those generated via the original APCDM approach, which exhibits a significant variability across the airlines. While the last equity approach has a total net reduction in passenger-minutes of delay less than that for methods (a) – (c), a benefit from this last approach is that four of the five participating airlines improve their delay status at a minor cost to only one airline. Therefore, depending on the primary goal of the decision-maker regarding the slot exchange, the equity methods (a) – (d) all appear to be suitable formulations for the SE-APCDM model based on this test case.

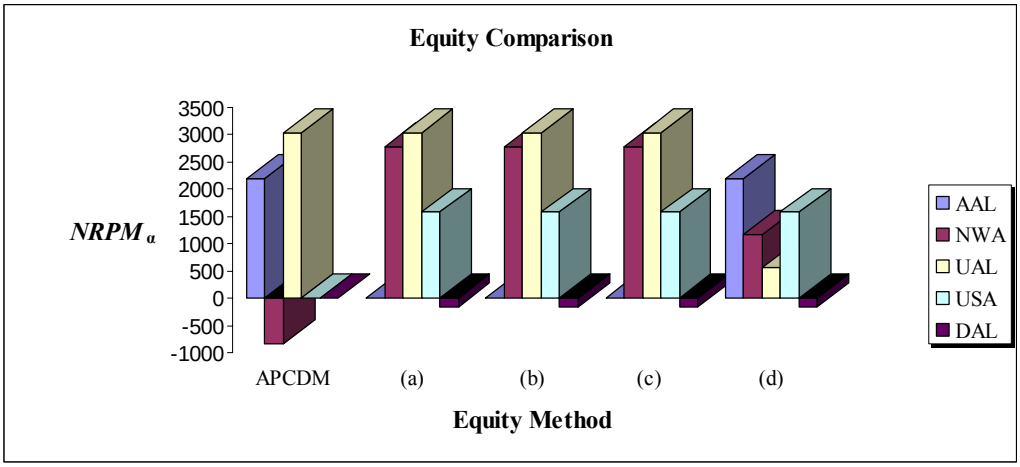

Figure 6-10: Equity Comparison in Net Reduction by Airline.

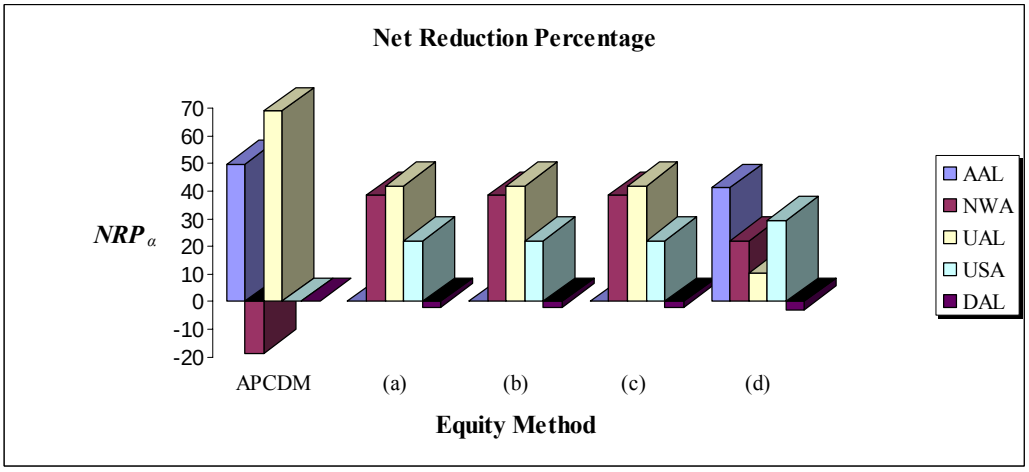

Figure 6-11: Equity Comparison in Net Reduction Percentage by Airline.

Given that the various equity formulations consider different relative performance ratio measures as specified in Section 5.3, the results depicted in Figures 6-10 and 6-11 are biased more towards Methods (a) and (b) since the focus here is on passenger-minutes as the comparison criteria. Therefore, we also compared the different methods based on the distribution of their respective collaboration efficiencies achieved over the set of airlines. These results are depicted in Figure 6-12. Note that we have normalized the collaboration efficiencies within each equity method in order to present a fair comparison across all methods. From Figure 6-12, equity Methods (a) and (c) appear to generate the most equitable solutions when using individual airline collaboration efficiencies as the comparison criteria for this test set.

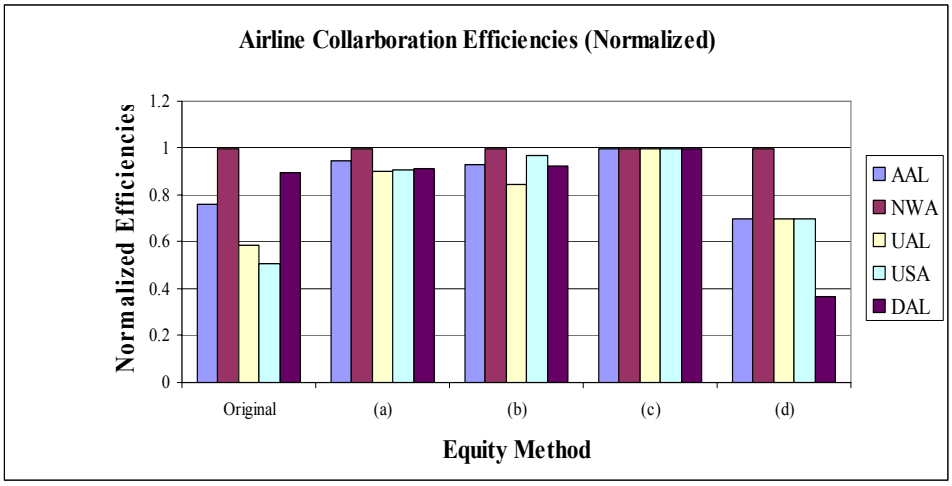

Figure 6-12: Comparison of Collaboration Efficiencies Across Respective Airlines.

6.2.7. Benchmark Runs

To gain an appreciation for the impact that the aforementioned equity approaches have on the generation of slot exchanges, we report on two additional benchmark runs using Test Set #1. For the first run, we removed all the equity terms from the original APCDM model formulation and minimized the system cost while maintaining the sector workload and airspace conflict constraints. Since the cost to execute a flight plan, c_{fp}, is a function of multiple cost factors that include delay times and the number of passengers, we expected the SE-APCDM model to produce slot exchanges that moved up flights having larger passenger loads if possible. The results from this benchmark run were consistent with our expectations and coincided with the results from equity methods (a) – (c). This equivalence, however, stems from the passenger load characteristic associated with the given trade offers. If an airline submits a trade offer based upon criteria other than passenger loads, we are not guaranteed to obtain the same results from such a run.

In the second benchmark run, we eliminated the system cost (first term in (2.5a)) and retained the various equity structures. Figure 6-13 displays the optimal solution for each equity approach in terms of the $NRPM_\alpha$ measure for each airline α. The results indicate that the exclusion of the system cost does not provide a better solution with respect to slot exchanges. Observe that Methods (a), (b), and (d) achieve perfect equity by simply retaining the allotted slots, and hence, provide no further incentive to select cost effective plans. It is important to note

that the results from the equity approaches and the benchmark runs are all scenario-dependent and a function of the trade offers from the airlines.

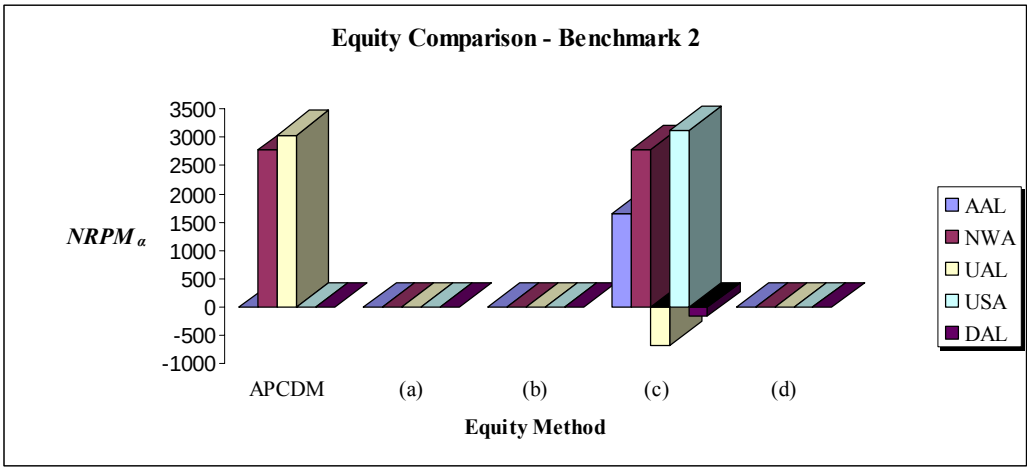

Figure 6-13: Equity Comparison in Net Reduction for Benchmark Run 2.

6.2.8. Nonnegativity Restrictions on Net Passenger-minute Delay Reductions

The structure of the individual trade offers from the initial test set resulted in a negative net reduction for two airlines as indicated in Figure 6-10 for AAL and DAL using methods (a) – (c). Using the nonnegativity constraints (5.23) (or (5.24)), we compared the impact of these additional restrictions on the solution produced using Method (a) (see Figure 6-14). Note that (5.23) and (5.24) are the same in this context because the test set consists of only one "at-least, at-most" trade offer per airline. Without this nonnegativity restriction, the total improvement from the slot exchanges was 7,220 PAX-minutes, which includes a negative improvement for DAL of −164 PAX-minutes. The addition of the nonnegativity constraint reduced the total improvement to 3,924 PAX-minutes. Note that, based on the formulation of its relative performance ratio (5.37), Method (c) considers only the number of accepted moves without concern for whether or not it produces additional delays (i.e., negative values for *NRPM*). Therefore, it is important to use (5.23) in concert with Method (c). Given that the addition of the nonnegativity formulation in (5.23) makes practical sense with respect to both the structure of trade offers and particular equity methods, we will retain this constraint in all future runs, except as noted for specific purposes.

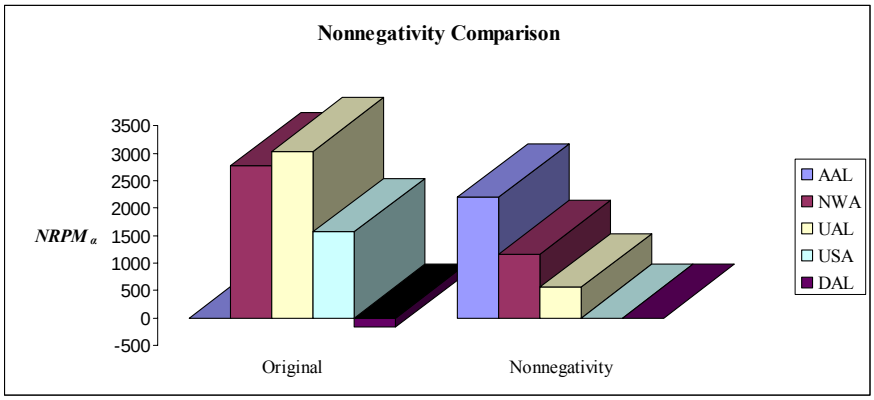

Figure 6-14: Nonnegativity Comparison.

6.3. Sensitivity Analysis of the Equity Weight Factors

Throughout our analysis of the various equity approaches, we have retained the original APCDM model relative weights $(\mu^D, \mu^e, \mu^e_{\max})$ for the equity terms in (2.5a) in which each weight is a function of μ_0. By restricting our analysis to the case where $E^e_{\max}$ is a constant, $\mu^e_{\max}$ is inconsequential, while $\mu^D = \mu^e = \mu_0 \sum_{f=1}^{F} c^*_f$, where $\mu_0 = 0.1$ as prescribed in Sherali et al. (2006).

6.3.1. Sensitivity Analysis with Respect to the Parameter μ_0

We begin by replicating within the present slot-exchange construct the sensitivity analysis conducted in Sherali et al. (2006) by defining the *Average CDM Improvement* as

$$0.5\left[\left\{\sum_{\alpha=1}^{\bar{\alpha}} \omega_\alpha E_\alpha(x)\right\}_{\mu_0=\bar{\mu}_0} - \left\{\sum_{\alpha=1}^{\bar{\alpha}} \omega_\alpha E_\alpha(x)\right\}_{\mu_0=0}\right] + 0.5\left[\{x^e\}_{\mu_0=0} - \{x^e\}_{\mu_0=\bar{\mu}_0}\right], \tag{6.2}$$

where $\{\cdot\}_{\mu_0=\bar{\mu}_0}$ is the value of the corresponding quantity $\{\cdot\}$ for the solution generated when $\mu_0 = \bar{\mu}_0$. Equity methods (a) and (d) under (5.23) were not sensitive to the variations of the parameter μ_0 as we increased the value of μ_0 from zero to 0.3. Only Method (c) displayed some sensitivity to initial changes in μ_0 around the value of 0.05, but (6.2) remained unaffected as μ_0 increased further. Figure 6-15 depicts the results of this sensitivity analysis for Method (c), where (6.2) is expressed as a corresponding percentage of $0.5\left\{\sum_{\alpha=1}^{\bar{\alpha}} \omega_\alpha E_\alpha(x)\right\}_{\mu_0=0} + 0.5\{x^e\}_{\mu_0=0}$.

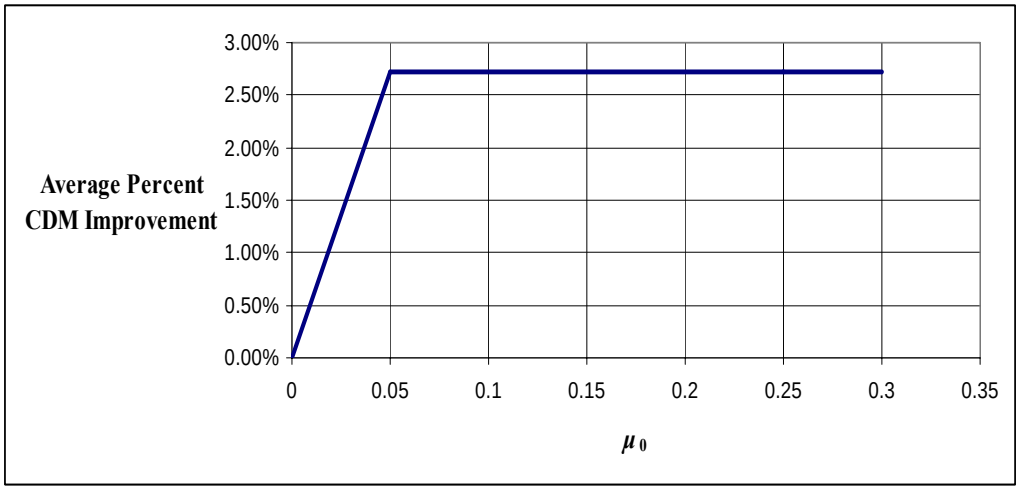

Figure 6-15: Sensitivity Analysis for Method (c) with Respect to μ_0.

Given the apparent insensitivity of the relevant slot-exchange equity terms with respect to the parameter μ_0 for this test set, we adopt the same prescription for the value of μ_0 as in the original APCDM model when defining $\mu^D = \mu_0 \sum_{f=1}^{F} c_f^*$.

6.3.2. Sensitivity Analysis under Increased Slot Competition (Test Set #2)

In Test Set #1, the airlines do not all compete for identical earlier slots as specified by their respective upward-move offers. To explore the effect of increased competition for slots, we generated an alternative test set (Test Set #2) in which the airlines all compete for the same earlier slots. Figure 6-16 depicts this second test set. The directed arcs represent potential downward-moves while the dotted box encompasses the earlier slots that the airlines are attempting to acquire through the slot-exchange procedure. To remove additional clutter from the slot-exchange network in Figure 6-16, we have omitted the directed arcs that exist within the dotted box (e.g., AAL has directed arcs from 0800 to the 0804, 0808, 0812, and 0816 slots). Notice that given the specified downward-move limits for this test set and the trade restriction stipulation, AAL will be involved in a slot exchange if and only if DAL acquires the 0836 slot. Otherwise, AAL will maintain its original time slots. In addition to the changes in the trade offers, we reduced the time interval between the OAG listed arrival time and the GDP arrival time associated with each path p for flight f.

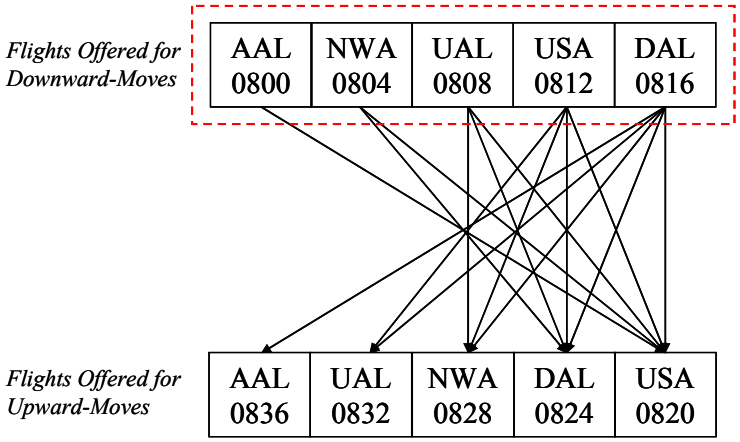

Figure 6-16: Identical Slot Competition Test Set.

The equity comparison under (5.23) for this alternative test set is displayed in Figure 6-17. It is readily apparent from Figure 6-17 that for each equity method, at least four of the five participating airlines achieve net reductions with respect to passenger delays. While the numerical results again are scenario-dependent, we anticipated such an improvement over the original test set since the number of potential slot exchanges increased due to the increased density of the slot-exchange network in the vicinity of the desirable earlier slots. More importantly, when applying Method (a), the resulting solutions were, in fact, sensitive to variations in the cost parameter μ_0 as depicted in Figure 6-18. As we initially increased the value of the cost parameter μ_0 from $\mu_0 = 0$ to $\mu_0 = 0.15$, we obtained a CDM improvement. Values of the cost parameter greater than 0.15 resulted in only minor improvements in the APCDM model's performance with respect to the CDM improvement criterion.

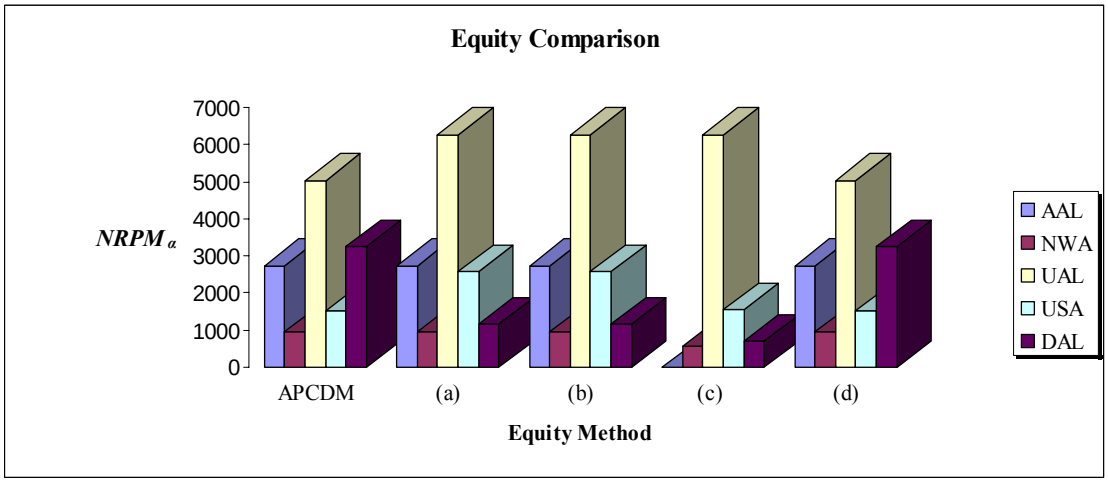

Figure 6-17: Identical Slot Competition Equity Comparison.

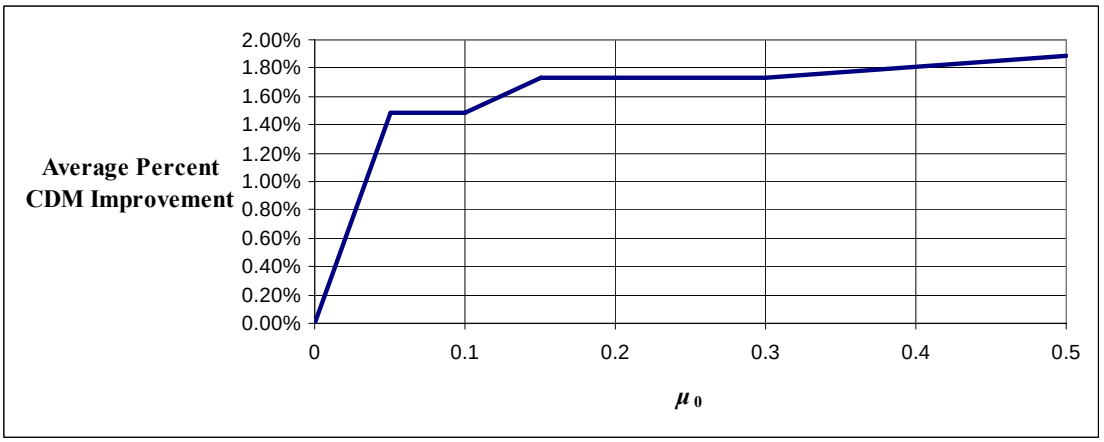

Figure 6-18: Sensitivity Analysis for Method (a) Under Identical Slot Competition.

In addition to the insights gained with respect to the sensitivity of Method (a) to the cost parameter μ_0, we gleaned further insights into Method (b) with this alternative test set by varying p^* in (5.35) with the nonnegativity restriction (5.23) omitted. As we increased the value of p^* from 0.8 to 0.85, the total net reduction in delay improved from 13,696 PAX-minutes to 13,808 PAX-minutes. However, as depicted in Figure 6-19, this improvement in the net reduction in PAX-minutes of delay came at the expense of DAL, which experiences a net increase in delay of 932 PAX-minutes as a result of the slot exchange generated using $p^* = 0.85$. When comparing individual airline normalized collaboration efficiencies (see Figure 6-20), it is apparent that the increase of p^* from 0.80 to 0.85 results in a greater spread among the individual collaboration efficiencies. More importantly, this increase in the value of p^* results in an increase of 56.2% in the second term of (5.29). Therefore, while we gain additional improvements in passenger-minutes of delay for values of $0.85 \le p^* < 1$, a more equitable slot exchange for the participating airlines is achieved for values of $0.5 \le p^* \le 0.8$ (where the slope of the efficiency curves become steeper for reduced values of p^*). For this alternative test set, $p^*_{(a)} = 0.7104$ (see Figure 6-21), which produces the same slot-exchange solution as the optimal solution for Method (a). This result is expected given that $p^*_{(a)}$ in (5.36) is the average value that matches the efficiency curves of Methods (a) and (b).

Note in Figure 6-21 that the sum of the collaboration efficiency and equity terms in the objective function, as defined in (5.29), decreases as we increase p^* up to $p^* = 0.85$. Since the

slot-exchange solutions for $p^* \in [0.5, 0.8]$ are identical (hence, $d_\alpha^1(x)$ remains constant), the slope of the efficiency curve for each airline in (5.35) increases (becomes less negative) as we increase the value of p^*, which in turn reduces the variation between the individual airline collaboration efficiencies. However, when $p^* = 0.85$, a new slot-exchange solution is generated that further reduces the value of the overall objective function (2.5a) while slightly increasing the sum of the terms in (5.29). As we continue to increase the value of p^* beyond 0.85, the sum of the collaboration efficiency and equity terms in (5.29) decreases again due to the behavior of the efficiency curve slope in relation to p^*.

Finally, we note that when we impose the nonnegativity constraint (5.23) along with Method (b) for this particular experiment, the slot-exchange solution generated with $p^* \geq 0.85$ is prohibited, in favor of a more equitable solution as discussed above.

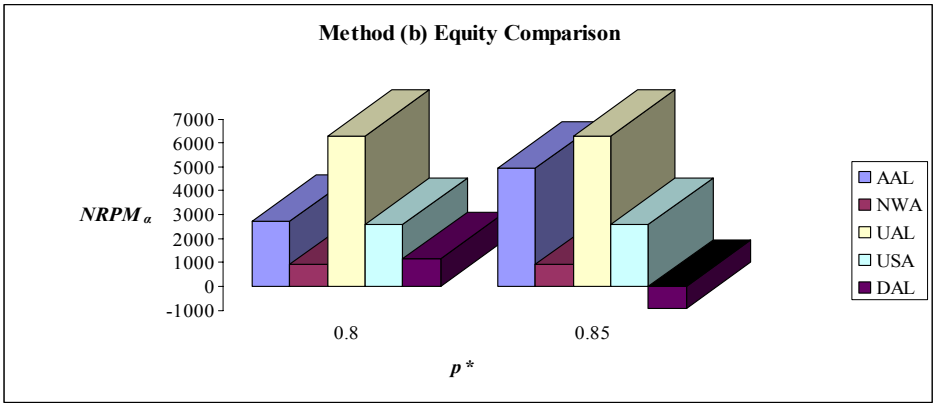

Figure 6-19: Method (b) Equity Comparison for Variations of *p.**

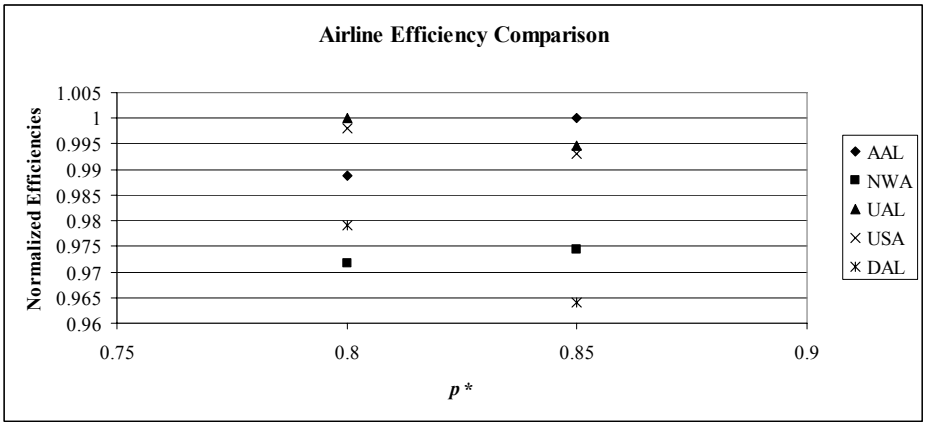

Figure 6-20: Airline Efficiency Comparison for Method (b).

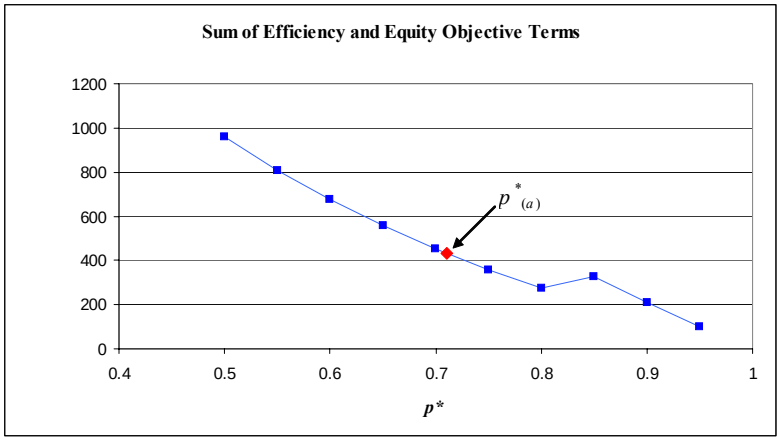

Figure 6-21: Variations in the Sum of Collaboration Efficiency and Equity Terms.

6.4. Computational Results Using Test Set #3

The FAA (2004) Benchmark Results for the Miami International Airport (MIA) details the airport's reported capacity under optimal, marginal, and Instrument Flight Rules (IFR) operating rates. The SE-APCDM model proved effective in generating slot exchanges for the previous test cases in which the arrival and departure rates were well below the published IFR operating rates, therefore, this third test set (see Table 6-1) was generated to evaluate the effectiveness of the SE-APCDM model given a hypothetically FAA-imposed GDP having a duration of one hour for MIA, while operating near the IFR maximum capacity rates (40 arrivals and 52 departures per hour). In addition to the 40 arrivals and 52 departures, we included 18 flights that transit the Miami and Jacksonville ARTCCs. To evaluate the flexibility of the SE-APCDM model, we included multiple "at-least, at-most" trade offers from two (AAL and NWA) of the six airlines (see Table 6-6). The existence of multiple trades most prominently affects the equity formulations for Methods (c) and (d), given that the denominators in (5.37) and (5.39) are no longer equal to one for the airlines submitting multiple offers.

Table 6-6: Trade Offers and Passenger Counts.

Downward-Move Flight	Allotted Time	# PAX	Upward-Move Flight	Allotted Time	# PAX
AAL1	600	98	AAL3	616.5	160
AAL8	642	111	AAL10	652.5	200
COA2	630	118	COA3	636	170
DAL1	606	122	DAL2	610.5	179
NWA1	601.5	142	NWA3	621	230
NWA4	645	155	NWA5	651	320
UAL1	607.5	95	UAL2	609	215
USA1	612	112	USA2	618	217

The SE-APCDM (using (5.23)) again mediated several slot exchanges under various equity formulations for this test case of MIA operating at maximum IFR capacity. Figure 6-22 displays the optimal solutions generated for each equity approach by airlines in terms of the $NRPM_{\alpha}$-values for each $\alpha \in A^{tr}$. The first significant observation is that Equity Method (c) did not prescribe any slot exchanges, even though there do exist plausible slot exchanges as identified by the original APCDM equity formulation as well as by Methods (a), (b), and (d). A second significant observation is the exclusion of a slot exchange for COA given that the structure of the trade offers provides at least the opportunity of a slot exchange between the two COA flights themselves, even if an exchange does not occur involving another airline. After further analysis, we discovered that these two observations result from a fatal conflict identified by the model. In other words, all the submitted flight plans associated with any potential upward-move for flight COA3 place the aircraft within the fatal conflict range of another more preferably selected flight plan, i.e., they penetrate this aircraft's separation shell specified by 500 feet in the in-trail and cross-track dimensions, and 100 feet in altitude dimension (Sherali et al., 2003). Therefore, the upward-move flight plans for COA3 are explicitly prohibited as prescribed in (2.5g), and this flight retains its allotted GDP slot. *This also underscores the importance of examining potential slot exchanges in combination with the joint viability of all accepted flight plans*.

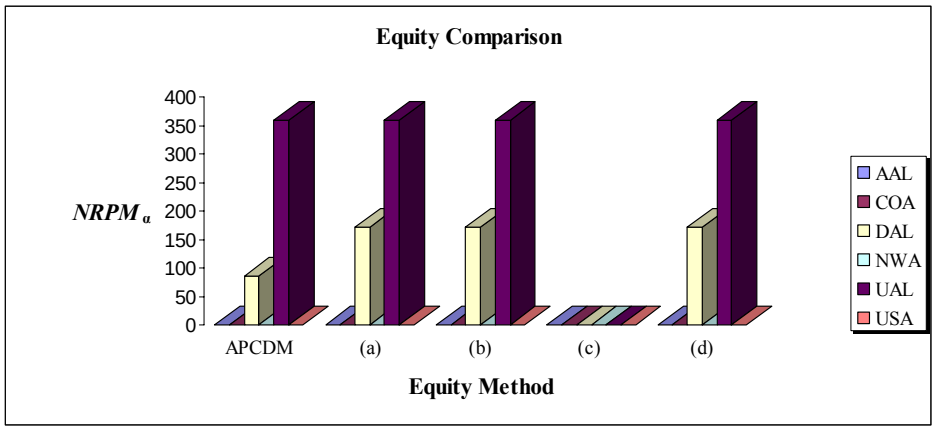

Figure 6-22: Equity Comparison in Net Reduction by Airline.

Due to the imposed trade restriction in (5.22), the retention of COA3's allotted GDP slot eliminates any potential downward-moves for COA2 and, thus, the collaboration efficiency for Method (c) in (5.38) for COA equals zero. Hence, using the cost parameter $\mu_0 = 0.1$, the optimal solution from SE-APCDM for Method (c) produced no slot exchanges as shown in Figure 6-22.

However, when we removed (5.23) and increased μ_0 beyond 0.165, downward-moves were generated for all flights (compensated by corresponding upward-moves). While this result initially seemed beneficial for all airlines, a further analysis indicated that it came at a considerable expense for another airline not involved in the slot-exchange scheme. As mentioned in the preceding paragraph, COA was unable to obtain a slot exchange due to a fatal conflict associated with the upward-move flight plans. By increasing the cost parameter μ_0, we essentially forced a slot exchange to occur for COA, which was only possible if the flight that COA had a fatal conflict with was cancelled (this cancellation was a viable offer made by the associated airline). Since that flight in question was also allocated an arrival slot into MIA, this situation is not favorable and should not be considered as a viable solution. Note that the other equity methods, which explicitly consider the delay costs for all airlines, precluded this cancellation from occurring.

6.5. Computational Effort Analysis

In order for the SE-APCDM model to be a successful decision support tool for the FAA at the tactical level, it must provide results well within the decision timeline. Note from Figure 6-22 that the slot exchanges generated under (5.23) using the original APCDM equity formulation performed almost as well as Methods (a), (b), and (d) did in terms of net reduction in passenger-minutes of delay. These results under the original APCDM equity formulation, however, required a computational effort in excess of 7 hours, which is unacceptable given the nature of GDPs. As indicated in Table 6-7, when we limited the processing time to 20 minutes, the equity methods (a) – (d) performed significantly better than the original APCDM equity formulation with respect to the optimality gap between the generated mixed-integer programming solution and the corresponding linear programming solution at termination. Hence, the equity methods (a) – (d) provide a structure that is evidently relatively easier to optimize, at least to near-optimality (i.e. within 3% of optimality).

Table 6-7: Equity Method Performance under Time Limits.

Equity Method	IP/LP Gap
Original	21.70%
A	0.80%
B	0.30%
C	0.58%
D	2.99%

Whereas the results for Test Set #3 suggest that methods (a) – (d) perform better under cpu time limits, we further compared the computational effort required for each of the aforementioned equity approaches given an optimality threshold by modifying the three test cases of Table 6-1 with respect to flights or cost parameters to generate several alternative representative test sets as indicated in Table 6-8. For example, we generated Slot-exchange Computational Test Set #2 (denoted SCT-2) by increasing the fuel cost parameter from $1.20 per gallon used in Test Set #1 to $2.14 per gallon, and so forth as indicated in the notes of Table 6-8. For each alternative test set, we terminated the model run and recorded the computational effort required in cpu seconds once we obtained a solution within 5% of optimality. It is readily apparent that the computational effort required for methods (a) – (d) is less than the computational effort required under the original APCDM model equity formulation. In particular, we obtained near-optimal solutions quickly for methods (a) – (d) for the larger alternative test sets (SCT-9,…, SCT-13) in contrast to the original APCDM model equity formulation, which we failed to produce solutions meeting the 5% optimality criterion due to the memory limitations of the computer. On the other hand, as indicated before, Methods (a), (b), and (d) tend to produce slot-exchange solutions similar to those resulting from using the original APCDM equity formulation.

Table 6-8: Computational Effort for Alternative Test Sets Using Different Equity Formulations.

		Equity Approach (cpu seconds)				
Label	Test Set	Method (a)	Method (b)	Method (c)	Method (d)	Original APCDM
SCT - 1	1	0.78	0.79	0.86	0.78	2.375
SCT - 2	1 (1)	0.80	0.75	0.80	0.73	5.70
SCT - 3	1 (2)	0.81	0.86	0.95	0.83	5.72
SCT - 4	1 (3)	0.75	0.81	0.94	0.75	2.41
SCT - 5	2	0.66	0.64	0.97	1.25	2.14
SCT - 6	2 (1)	0.50	0.52	0.94	0.94	1.64
SCT - 7	2 (2)	0.63	0.69	0.83	1.06	1.77
SCT - 8	2 (3)	0.64	0.66	0.86	1.19	1.58
SCT - 9	3	32.01	32.90	12.39	37.78	*
SCT - 10	3 (1)	29.40	24.87	10.44	55.25	*
SCT - 11	3 (2)	32.22	28.81	8.66	11.52	*
SCT - 12	3 (3)	40.95	46.88	12.92	28.92	*
SCT - 13	3 (4)	236.11	66.91	66.10	185.97	*

Notes:

(1) - increased fuel cost from 1.20 $/gal to 2.14 $/gal
(2) - increased delay penalty from 0.2 to 0.4
(3) - decreased maximum sector capacity by 30%
(4) - modified Test Set #3 to 40 arrivals, 40 departures, and no transit flights
* Exceeded the computer's memory capacity

As discussed in Section 6.2.8, the optimal solutions produced under (5.23) prevent negative values for the net reduction in passenger-minutes of delay for airlines. However, the inclusion of (5.23) may also significantly reduce the total *NRPM* for the GDP airport by eliminating high payoff slot exchanges (i.e., slot exchanges that have only a minor increase in delay for the designated downward-move flight in return for a large reduction in delay for the corresponding upward-move flight). For Test Set #3, the removal of (5.23) generated the results shown in Figure 6-23 for Method (a), which represents a 76.8% increase in the total *NRPM* (from 531 passenger-minutes under the nonnegativity constraints to 2296 passenger-minutes without (5.23)). Method (b), without (5.23), produced the same results as Method (a), while the removal of (5.23) for Method (d) produced a total *NRPM* of 1270 passenger-minutes. The potential increase in the total *NRPM* without (5.23) as depicted in Figure 6-23, however, comes at a "computational price". For instance, the computational effort required for Method (a) increased from 32.01 cpu-seconds to 87.39 cpu-seconds. Similar increases in the computational effort were observed for Methods (b) and (d) as well. The ability of the SE-APCDM model to generate optimal slot exchanges with or without (5.23) provides another level of flexibility to the decision makers for mediating any trade offer scenario.

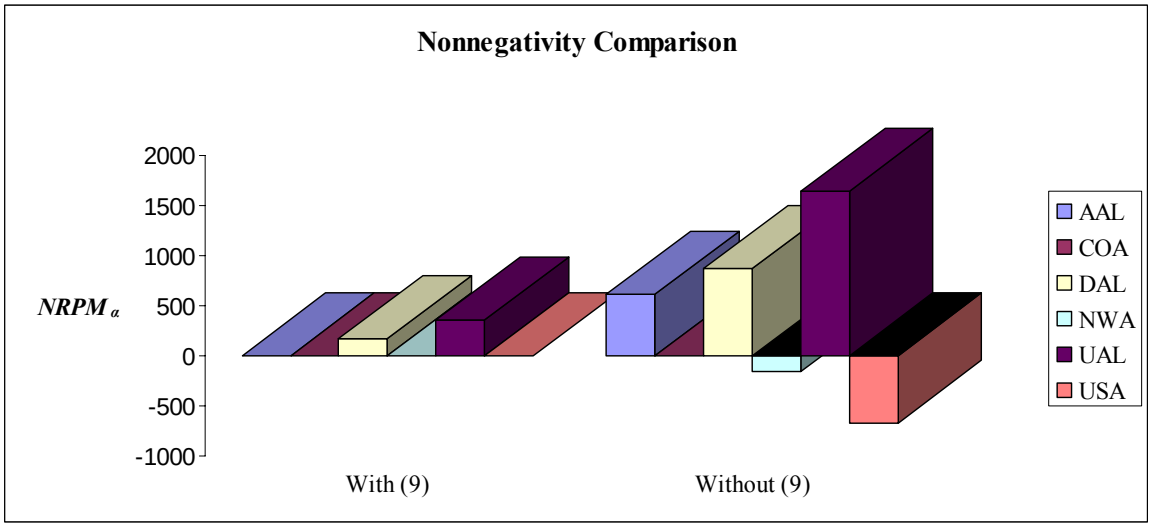

Figure 6-23: Nonnegativity Comparison for Test Set #3.

Using real data obtained from the FAA based on ETMS, we have demonstrated the ability to generate viable slot exchanges under a GDP scenario in support of the FAA's CDM initiative. Additionally, we have provided and evaluated four alternative equity approaches that

will allow the FAA to mediate slot-trading opportunities fairly while maintaining flexibility in the evaluation criteria. As a safeguard for the participating airlines, we have included nonnegativity constraints to ensure that slot exchanges will not result in an increase in the net reduction in passenger-minutes of delay. Computationally, in summary, our proposed APCDM model concepts provide effective decision-making support to the FAA that can be implemented in a timely fashion at the tactical level.

Chapter 7

Summary, Conclusions, and Recommendations for Future Research

7.1. Summary and Conclusions

The weather, above all other external factors, wreaks the greatest havoc within the airline industry. According to the Bureau of Transportation Statistics, 24.83% of all flight delays in 2005 were weather-induced (DOT, 2006), amounting to billions of US dollars in delay-related costs. With respect to strategic and tactical level flight planning, the ideal scenario would be one in which the airlines and the Federal Aviation Administration (FAA) could acquire perfect knowledge on the dynamic characteristics of the severe weather patterns that habitually degrade aviation operations. This perfect knowledge would subsequently reduce many of the complications associated with generating weather-based flight routes and, thus, reduce the delay-related costs inherent with Ground Delay Programs and unexpected reroutes. Given the unstable nature of weather and the accuracy of current forecasting models, this scenario is yet to be realized and we are left with the task of strategic level flight planning shrouded in weather uncertainty.

Even though there are no absolutes when it comes to severe weather forecasting, a complete disregard for weather forecasts in conducting strategic level flight planning is an impractical option. Accordingly, we have presented and evaluated two significant modeling concepts within the context of a large-scale Airspace Planning and Collaborative Decision-Making Model in order to enhance its current functionality in support of both strategic and tactical level flight assessments under severe weather uncertainties. Within this dissertation, we have provided evidence that by incorporating severe weather probabilities into flight plan generation at the strategic level, we can significantly reduce the expected delay cost of a flight. Furthermore, by integrating the proposed slot-exchange mechanisms and accompanying equity formulations within the APCDM model, we have demonstrated that passenger delay costs associated with GDPs can be appreciably reduced as well.

The strategic level concept developed is a new severe weather-modeling paradigm, which incorporates Model Output Statistics (MOS) forecasted severe weather probability data from the National Weather Service's Meteorological Development Lab. The probability data associated with specific MOS reporting sites serves as the foundation for the construction of our discretized

severe weather probability-nets that are subsequently used to determine the probability that a flight trajectory could encounter severe weather. More importantly, by superimposing a flight-trajectory-grid network onto the probability-nets, we developed an approach to generate flight plans that can circumvent severe weather phenomena with specified probability levels based on determining constrained, time-dependent shortest paths between the respective origin and destination airports. By generating alternative flight plans pertaining to specified threshold strand probabilities, we prescribed a methodology for computing appropriate expected weather delay and related disruption factors for inclusion within the APCDM model. We also derived a technique for conducting a cost benefit analysis using a *k*-means clustering mechanism in concert with our delay assessment methodology in order to evaluate delay costs and system disruptions associated with different levels of probability-net refinement.

The notion of "slot ownership", formalized via the FAA's Collaborative Decision-Making initiative under the enhancements to the GDP, has spawned new research efforts pertaining to slot-trading opportunities that could provide additional benefits in terms of flight efficiencies and desirable airline schedules. Therefore, our tactical level concept focuses on reducing the costs associated with GDPs. Given that airlines submit trade offers of the "at-least, at-most" type, we have produced a modeling capability that automatically incorporates the acceptance of a combination of such trades in terms of related slot exchanges, while simultaneously considering the impact of the resultant overall mix of flight plans on sector workloads, safety with respect to conflict risk, and equity among the involved airlines. In keeping with the spirit of the FAA's collaborative decision-making initiative, we have also proposed alternative formulations of the concept of achieving equity with respect to the generated slot exchanges. Computational results based on test cases derived from FAA's Enhanced Traffic Management System (ETMS) data provide insights into the effect of different equity measures and the extent of flexibility inherent in the offered trade opportunities. The four proposed slot-exchange-based equity formulations, in conjunction with the developed slot-exchange mechanisms, demonstrated a potential for significant net savings in computational effort ranging from 25% to 86% over the original APCDM model equity formulation. The results also indicated that the designed slot-exchange model, SE-APCDM, offers a viable tool that can be used by the FAA for both tactical air traffic management purposes, as well as

strategic applications to study the impact of different types of trade restrictions, collaboration policies, and equity concepts, among others as discussed by Sherali et al. (2003, 2006).

7.2. Recommendations for Future Research

The primary reason for incorporating severe weather data from the Model Output Statistics (MOS) resides on the point-by-point structure of the forecasts, which was essential to the development of our probability-net concept. With over 1,500 reporting sites providing quantitative forecast probabilities, the computational results reported herein for constructing the probability-nets and assessing flight trajectories clearly demonstrates that our algorithm can be applied in a timely fashion to support strategic level decision-making. Unfortunately, some of the severe weather data, such as thunderstorm probabilities, are provided at only six hours intervals. Therefore, we recommend the development and use of weather forecast sources that can provide the essential point-by-point probability data for relatively smaller time intervals.

For prototypical reasons, the flight plan generation implemented in this dissertation imports flight waypoints into Microsoft Excel and subsequently plots these points onto a chart with the U.S. map incorporated in the background. Further refinement of the C++ code in conjunction with advanced graphical output capabilities would serve to greatly enhance the capabilities of our proposed flight-plan-generation tool.

On November 17, 2005, FlightAware (2006) released a Live Flight Tracking web-site that provides real-time en route flight data (minute-by-minute locations, altitude, and airspeed) and historical flight records for 120 days. It is currently the most popular tracking service available on the internet. In addition to the flight tracking capability, the web-site also provides airport information and relevant statistics. The information is free and available for both private and commercial air traffic use. Given that the historical flight data for each flight contains a flight log, the realized flight trajectory could be evaluated using the forecasted severe weather probabilities provided by MOS to derive alternative statistically-based weather delay factors based on comparing planned and achieved flight routes. We recommend the development of such a technique and its benchmarking against our proposed methodology for future research.

Finally, regarding our slot-exchange mechanisms, we recommend further experimentation in order to evaluate the efficiency and effectiveness of our proposed approach under longer GDP periods and under scenarios involving multi-airport GDPs. It is also useful to

explore avenues for including Slot Credit Substitutions (SCS) within the equity formulations. The premise behind SCS is that an airline submits a flight (along with its assigned slot under a GDP) for cancellation, conditioned on the ability to move a later flight to an earlier slot time. Given that a submitted SCS can alter the flight times of one or more flights as a function of newly acquired slot times, these new flight plans must be evaluated with respect to sector workloads, conflict risk, and equity among the involved airlines. Our modeling framework provides the mechanism for incorporating such considerations, and it would be useful to conduct specific case-studies to assess the economic value of Slot Credit Substitutions. Another interesting area of future research is to examine side-payments as part of the trade-offer and equity structure, as suggested by Vossen (2002).

References

Abramson, B., Brown, J., Edwards, W., Murphy, A., and Winkler, R. L. (1996), Hailfinder: A Bayesian System for Forecasting Severe Weather, *International Journal of Forecasting*, 12, 57-71.

Alonso, A. (1997), Optimización Combinatorial Estocástica Aplicada al Control del Tráfico Aéreo, Ph.D. Thesis Dissertation, Unversidad Complutense de Madrid.

Alonso, A., Escudero, L., and Ortuno, M. T. (2000), A Stochastic 0-1 Program Based Approach for the Air Traffic Flow Management Problem, *European Journal of Operational Research*, 120, 47-62.

Antolik, M. S. (2005), Model Output Statistics (MOS) – Objective Interpretation of NWP Model Output, Meteorological Development Laboratory, Statistical Modeling Branch, NOAA/National Weather Service, Silver Spring, Md.

Aviation Weather Center. (2003), About Area Forecasts, internet website, http://aviationweather.gov/products/fa/info.shtml.

Aviation Weather Center. (2005), Aviation Digital Data Service (ADDS), internet website, http://adds.aviationweather.noaa.gov/java.

Aviation Weather Center. (2005), Collaborative Convection Forecast Product: Product Description Document, internet website, http://www.aviationweather.gov/products/ccfp.

Ball, M., Hoffman, R., Knorr, D., Wetherly, J., and Wambsganss, M. (2000), Assessing the Benefits of Collaborative Decision Making in Air Traffic Management, Proc. 3rd USA/Europe Air Traffic Management R&D Seminar, Napoli, Italy.

Ball, M., Hoffman, R., and Vossen, T. (2002), An Analysis of Resource Rationing Methods for Collaborative Decision Making, Working Paper, Robert H. Smith School of Business, University of Maryland, College Park, Md.

Bertsimas, D. J. and Stock, S. (1998), The Multi-Airport Flow Management Problem with En Route Capacities, *Operations Research* 46(3), 406-422.

Boeing. (2006), Commercial Airplanes, Technical Characteristics – Boeing 737-700, internet website, http://www.boeing.com/commercial/737family/pf/pf_700tech.html.

Chang, K., Howard, K., Oiesen, R., Shisler, L., Tanino, M., and Wambsganss, M. C. (2001), Enhancements to the FAA Ground-Delay Program Under Collaborative Decision Making, *Interfaces*, 31(1), 57-76.

Cofino, A. S., Cano, R., Sordo, C., and Gutierrez, J. M. (2002), Bayesian Networks for Probabilistic Weather Prediction, European Conference on Artificial Intelligence, Lyons, France.

Crawley, J. (2001), "U.S. Lays Out 10-Year Plan to Reduce Flight Delays," in Reuters News Service.

Dembo, R. S. (1991), Scenario optimization, *Annals of Operations Research* 30, 63-80.

Department of Transportation. (2006), Bureau of Transportation Statistics, Aviation Delays, internet website, http://www.transtats.bts.gov.

Encyclopedia Britannica. (2004), Weather Forecasting, Encyclopedia Britannica Online, internet website, http://search.eb.com/eb/article?eu=109123.

Environmental Modeling Center. (2004), National Centers for Environmental Prediction: EMC Model Documentation, internet website, http://wwwt.emc.ncep.noaa.gov/modelinfo.

European Centre for Medium-Range Weather Forecasts. (2002), The Early History of Numerical Weather Prediction, internet website, http://www.ecmwf.int/products/forecasts.

Evans, J. E. (2001), Tactical Weather Decision Support to Complement "Strategic" Traffic Flow Management for Convective Weather, 4th USA/EUROPE ATM R&D Seminar, Santa Fe, New Mexico.

Federal Aviation Administration. (2006), FAA Operations and Performance Data, internet website, http://www.apo.data.faa.gov.

Federal Aviation Administration. (2005), National Severe Weather Playbook, internet website, http://www.fly.faa.gov/playbook.html.

Federal Aviation Administration. (2004), Weather Information Sources Used By Briefers /Pilots, internet website, http://www.faa.gov/ats/afss/pieafs/briefh.htm.

Federal Aviation Administration. (2004), Benchmark Results: Miami, internet website http://www.faa.gov/events/benchmarks/DOWNLOAD/pdf/MIA_2004.pdf.

Federal Register. (2001), Volume 66, Number 113, pp. 31731-31748.

FlightAware. (2006), Live Flight Tracking and Statistical Analysis, internet website, http://flightaware.com.

Hall, T., Brooks, H. E., and Doswell III, C. A. (1999), Precipitation Forecasting Using a Neural Network, *Weather and Forecasting* 14(3), 338-345.

Hallion, R. P. (2004), Remembering the Legacy: Highlights of the First 100 Years of Aviation, *The Bridge: Linking Engineering and Society*, National Academy of Engineering of the National Academies 34(1), 5-11.

Hicks, T., Crawford, T., and Wilson, M. (2004), A Fuzzy Logic System for Automated Short Term Aviation Weather Forecasts, 3rd Conference on Artificial Intelligence Applications to Environmental Sciences.

Hsieh, W. W. and Tang, B. (1998), Applying Neural Network Models to Prediction and Data Analysis in Meteorology and Oceanography, *Bulletin of the American Meteorological Society* 79(9), 1855-1870.

Kirkwood, C. W. (1997), *Strategic Decision Making: Multiobjective Decision Analysis with Spreadsheets*, Duxbury Press, Albany, New York.

Luss, H. (1999), On Equitable Resource Allocation Problems: A Lexicographical Minimax Approach, *Operations Research* 47(3), 461–478.

Marzban, C. and Stumpf, G. J. (1996), A Neural Network for Tornado Prediction Based on Doppler Radar-Derived Attributes, *Journal of Applied Meteorology* 35, 617-626.

Maner, W. and Joyce, S. (1997), Weather Lore + Fuzzy Logic = Weather Forecasts, CLIPS Virtual Conference, internet website, http://www.pws.com/compsci/clips.html.

Marshall, K. T. and Oliver, R. M. (1995), *Decision Making and Forecasting: With Emphasis on Model Building and Policy Analysis*, McGraw-Hill, Inc., New York.

Matos, P., Chen, B., and Ormerod, R. (1996), Optimization Models for Re-routing Air Traffic Flows, Warwick Business School Research Papers, No. 240, University of Warwick, Coventry.

McCann, D. W. (1992), A Neural Network Short-Term Forecast of Significant Thunderstorms, *Weather and Forecasting* 7(3), 525-535.

McQueen, J., Du, J., Zhou, B., DiMego, G., Juang, H., Ferrier, B., Manikin, G., Rogers, E., Black, T., and Toth, Z. (2004), Overview of the NOAA/NWS/NCEP Short Range Ensemble Forecast (SREF) System, NOAA/NWS/NCEP/Environmental Modeling Center.

Meteorological Development Lab. (2004), Current GFS and Eta MOS Stations and WMO Headers, internet website, http://www.nws.noaa.gov/mdl/synop/stadrg.htm.

Metron Aviation. (2004), Commercial Market Base: Enhanced Substitution Module, internet website, http://www.metronaviation.com/esm.php.

National Centers for Environmental Prediction. (2004), Ensemble Prediction Systems, internet website, http://www.hpc.ncep.noaa.gov/ensembletraining.

National Oceanic and Atmospheric Administration. (2005), FY 2006 Budget Summary, internet website, http://www.publicaffairs.noaa.gov/budget2006/pdf/bluebook2006.pdf

National Weather Service. (2003), NCEP Central Operations: The National Centers, internet website, http://www.nco.ncep.noaa.gov/about.shtml.

National Weather Service. (2005), Meteorological Development Lab (MDL), internet website, http://www.nws.noaa.gov/mdl/.

Nilim, A., El Ghaoui, L., Hansen, M., and Duong V. (2001), Trajectory-based Air Traffic Management (TB-ATM) under weather uncertainty, 4th USA/EUROPE ATM R&D Seminar, Santa Fe, New Mexico.

Pole, A., West, M., and Harrison, J. (1994), *Applied Bayesian Forecasting and Time Series Analysis*, Texts in Statistical Science, Chapman and Hall, New York.

Riordan, D. and Hansen, B. K. (2002), A Fuzzy Case-Based System for Weather Prediction, *Engineering Intelligent Systems* 3, 139-146.

Rockafellar, R. T. and Wets, R. J. (1991), Scenario and Policy Aggregation in Optimization under Uncertainty, *Mathematics of Operations Research* 16, 119-147.

Rosenberger, J. M., Johnson, E. L., and Nemhauser, G. L., Rerouting Aircraft for Airline Recover, Transportation Science, Vol. 37, No. 4, November 2003, pp. 408-421.

Severe Weather Forecasting Center. (2000), The Method Behind the Madness II, internet website, http://www.neatideas.com/weather/tech.htm.

Sherali, H. D., Smith, J. C., Trani, A. A., and Sale, S. (2000), National airspace sector occupancy and conflict analysis models for evaluating scenarios under the free-flight paradigm, *Transportation Science* 34(4), 321-336.

Sherali, H. D., Hobeika, A. G., and Kangwalklai, S. (2003), Time-Dependent, Label-Constrained Shortest Path Problems with Applications, *Transportation Science* 37(3), 278-293.

Sherali, H. D., Staats, R. W., and Trani, A. A. (2003), An Airspace Planning and Collaborative Decision-Making Model: Part I – Probabilistic Conflicts, Workload, and Equity Considerations, *Transportation Science* 37(4), 434-456.

Sherali, H. D., Staats, R. W., and Trani, A. A. (2006), An Airspace Planning and Collaborative Decision Making Model: Part II – Cost Model, Data Considerations, and Computations, *Transportation Science* 40, to appear.

Shoemaker, D. (2003), Soaring Forecasts: Digging for Data at NWS Web Sites, *The Front, National Weather Service* 2(3), 1-5.

Short Range Ensemble Forecasting. (2004), General Weather Forecasting, internet website, http://wwwt.emc.ncep.noaa.gov/mmb/SREF/SREF.html.

Sowell, T. (1998), Fuzzy Logic for "Just Plain Folks", Chapter 1: Fuzzy Logic – a Powerful New Way to Analyze and Control Complex Systems, internet website, http://www.fuzzy-logic.com.

Tadenuma, K. (1998), Efficiency First or Equity First? Two Principles and Rationality of Social Choice, internet website, http://www.econ.hit-u.ac.jp/~kenkyu/jpn/pub/DP/tn-DP-1998-01.pdf.

Thengvall, B. G., Bard, J. F., and Yu, G. (2003), A Bundle Algorithm Approach for the Aircraft Schedule Recovery Problem During Hub Closures, *Transportation Science* 37(4), 392-407.

Treby, A. (2002), Optimal Weather Routing Using Ensemble Weather Forecasts, 37th Annual ORSNZ Conference, University of Auckland, Auckland, New Zealand.

University Corporation for Atmospheric Research, UCAR. (1998), Eta Model Characteristics: Background Information, internet website, http://www.comet.ucar.edu/nwplessons/etalesson2/characteristicsbackground.htm

Vossen, T. (2002), Fair Allocation Methods in Air Traffic Management, Ph.D. Dissertation, University of Maryland, College Park, MD.

Vossen, T. and Ball, M. (2001), Optimization and Mediated Bartering Models for Ground Delay Programs, Working Paper, Robert H. Smith School of Business, University of Maryland, College Park, MD.

Vossen, T. and Ball, M. (2004), Slot Trading Opportunities in Collaborative Ground Delay Programs, Working Paper, Robert H. Smith School of Business, University of Maryland, College Park, MD.

Vossen, T., Ball, M., Hoffman, R., and Wambsganss, M. (2002), A General Approach to Equity in Traffic Flow Management and its Application to Mitigating Exemption Bias in Ground Delay Programs, internet website, http://www.nextor.org/or.htm.

Wikipedia, the free encyclopedia. (2006), Great-circle Distance, internet website http://en.wikipedia.org/wiki/Great_circle_distance#The_formula.

Vita

Lieutenant Colonel Michael V. McCrea is a Ph.D. Candidate in Industrial and Systems Engineering, assigned to the United States Army Student Detachment, with duty at the Virginia Polytechnic Institute and State University, Blacksburg, Virginia. His dissertation research is in support of the Federal Aviation Administration (FAA)'s Collaborative Decision-Making initiative designed to modernize the US National Airspace System.

Lieutenant Colonel McCrea received a Regular Army commission and a Bachelor of Science Degree in Aerospace Engineering from the United States Military Academy at West Point in May 1987. After graduation, he was assigned to the 3rd Battalion, 2nd Air Defense Artillery Regiment at Fort Lewis, Washington, where he served as a Chaparral Missile System Platoon Leader, Battery Executive Officer, and Battalion Adjutant until January 1991. From October 1991 to October 1992, Lieutenant Colonel McCrea successfully served as a Vulcan/Stinger Battery Commander for the 5th Battalion, 5th Air Defense Artillery Regiment, 2nd Infantry Division, in the Republic of Korea. Following his command assignment, he was assigned to the Air Defense Artillery School at Fort Bliss, Texas, where he served as a Small Group Instructor for the Officer Basic and Advanced Courses.

Lieutenant Colonel McCrea received his Master of Science Degree in Operations Research from the Naval Postgraduate School in Monterey, California, in March 1997, and received the Chief of Staff of the Army's Excellence in Operations Research Award. Following graduation, he returned to West Point and served as an Instructor and Assistant Professor in the Department of Mathematical Sciences until June 2000. In July 2001, Lieutenant Colonel McCrea was assigned to the Combined Forces Command and the United States Forces Command in the Republic of Korea where he served as the Chief Ground Analyst, Operations Analysis Branch until June 2003.

His military awards and decorations include the Defense Meritorious Service Medal, the Meritorious Service Medal, the Army Commendation Medal, the Korean Defense Service Medal, the Parachutist Badge, and the German Armed Forces Physical Fitness Badge.

Civilian Education

1997 Master of Science in Operations Research, Naval Postgraduate School, Monterey, CA.
1987 Bachelor of Science in Aerospace Engineering, United States Military Academy, West Point, NY.

Military Education

2001 Command and General Staff Officer's Course, U.S. Army Command and General Staff College, Fort Leavenworth, KS.
2001 Joint Planner's Course, U.S. Army Command and General Staff College, Fort Leavenworth, KS.
1994 Combined Armed Services Staff School, U.S. Army Command and General Staff College, Fort Leavenworth, KS.
1991 Air Defense Artillery Officer Advanced Course, Fort Bliss, TX.
1987 Air Defense Artillery Officer Basic Course, Fort Bliss, TX.

Membership in Professional Organizations

Institute for Operations Research and the Management Sciences (INFORMS)
Military Operations Research Society (MORS)
Air Defense Artillery Association

M.S. Thesis

"Peroxone Treatment of Explosive Contaminated Groundwater Analysis and Evaluation", Naval Postgraduate School, March 1997.

Academic Experience

Assistant Professor, Department of Mathematical Sciences, (USMA): Taught courses in Probability and Statistics, 1999 - 2000

Instructor, Department of Mathematical Sciences, (USMA): Taught courses in Calculus I and Discrete Mathematics, 1997-1999.

Presentations

Implementation of Slot Exchanges within an Airspace Planning and Collaborative Decision-Making Model, November 2005, the Institute for Operations Research and the Management Sciences (INFORMS) Annual Meeting, San Francisco, CA.

Implementation of Slot Exchanges and Weather-Based Rerouting within the Airspace Planning and Collaborative Decision-Making Model (APCDM), August 2005, National Center of Excellence in Aviation Operations Research (NEXTOR) – CDM Project Review, College Park, MD.

Using Analytical Tools in Support of a Multi-National Planning Exercise, June 2002, 70th Military Operations Research Society (MORS) Symposium, Fort Leavenworth, KS.

Joint Analytical Study: Phase II, April 2002, Defense Analysis Seminar, Korean Institute for Defense Analysis, Seoul, Korea.